Global land eligibility for green hydrogen production: a cost-potential curve analysis

A thesis submitted
to the TUM School of Life Sciences
Master's Program Sustainable Resource Management
in partial fulfillment of the requirements for the degree of
Master of Science

By
Tal Barak
Matriculation number 03736497

Supervisors:
Dr.-Ing. Serafin von Roon
M.Sc. Tapio Schmidt-Achert
M.Sc. Miguel Martinez Perez
Forschungsstelle für Energiewirtschaft e.V. (FfE e.V.)

Dr.-Ing. Philipp Kuhn
Chair of Renewable and Sustainable Energy Systems
TUM School of Engineering and Design
Technical University of Munich

November 2023

Abstract

Green hydrogen is becoming pivotal to the ongoing global energy transition, prompting numerous countries to strategize for its future supply. Its generation via electrolysis involves large spatial requirements for its underlying renewable energy source and adequate water supply, posing a challenge for countries limited by these resources to meet their future hydrogen demand domestically. These developments compel a global assessment of hydrogen potentials and the identification of favorable production locations capable of supporting both their domestic market and international export. This thesis addresses this imperative by developing and applying a comprehensive global land eligibility analysis, followed by estimating hydrogen potentials on a 50km² spatial resolution grid. Furthermore, this thesis uses a novel approach, evaluating global land eligibility constraints not only spatially but also in terms of hydrogen production potentials and their associated costs. The analysis revealed that economically viable hydrogen potentials are predominantly hindered by water scarcity, most notably in Africa. Additional major restrictors include protected areas, agricultural land, and the terrain slope. The eligible global land for hydrogen is estimated to have a production potential of 5,193 megatons per year, attainable within a maximal levelized cost of 12 €/kg as of 2020, surpassing projected worldwide demand significantly. Global hydrogen potentials are highly concentrated in very few countries, with Australia contributing 20% to the global potential and Kazakhstan, Brazil, Argentina, the United States, and Russia each accounting for 6% to 7%. The results of this thesis are shared in an interactive dashboard that facilitates flexible analysis across various geographic scopes.

Keywords: Green hydrogen, cost-potentials, land eligibility analysis, global analysis, LCOH

Acknowledgments

I would like to express my gratitude to my supervisors at the FfE, Tapio Schmidt-Achert and Miguel Martinez Perez, and my supervisor at the TUM, Dr. Philipp Kuhn, for their ongoing support and guidance throughout the thesis journey. A special thanks go to my friends and family for their continuous encouragement and moral support. In particular, I would like to thank my flatmate and dear friend, Jakub Rzemieniewski, for not only providing domestic support and academic advice, but also comedic relief during this challenging period.

I dedicate this thesis to the memory of my grandfather, Prof. Joshua Pelleg, who dedicated his life to science and academia. May he rest with additional peace as I graduate from my studies.

Contents

List of figures

List of tables

List of Acronyms and Abbreviations

AC	Assessment criteria
AC	Alternating current
AHP	Analytic hierarchy process
ALK	Alkaline
CAPEX	Investment specific costs
CRP	Country risk premiums
CSP	Concentrated solar power
DC	Direct current
EC	Exclusion criteria or exclusion criterion
EEA	European Economic Area
EJ	Exajoule
FfE	Forschungsstelle für Energiewirtschaft (Research Institute for Energy)
FO	Frequency of occurrence
G20	Group of 20
GFSAD	Global Food Security-Support Analysis Data
GIS	Geographic information systems
GSA	Global Solar Atlas
GWA	Global Wind Atlas
HHV	High heating value
HYPAT	H_2 Potential Atlas
IEA	International Energy Agency
IFC PS6	International Finance Corporation's Performance Standard 6
IPCC	Intergovernmental Panel on Climate Change
IRENA	International Renewable Energy Agency
IUCN	International Union for Conservation of Nature
km²	Square kilometer
LCCS	Land Cover Classification System
LCOE	Levelized cost of electricity
LCOH	Levelized cost of hydrogen
LE	Land eligibility
LHV	Low heating value

LL	Lower limit
MCS	Most compatible scenario
MENA	Middle East and North Africa
MERRA-2	Modern-Era Retrospective Analysis for Research and Application, Version 2
Mt	Megaton
MW	Megawatt
MWh	Megawatt hour
N/A	Not applicable
NP	Number of publications
OPEX	Operational costs
PD	Power density
PEM	Proton exchange membrane
PtX	Power-to-X
PV	Photovoltaics
RE	Renewable energy
RES	Renewable energy source
SO	Solid oxide
SQL	Structured query language
SR	Spatial resolution
SRID	Spatial reference identifier
SWARA	Stepwise weight assessment ratio analysis
TC	Transportation costs
TPES	Total primary energy supply
TUM	Technical University of Munich
TWh	Terawatt hours
UL	Upper limit
UN FAO	United Nations Food and Agriculture Organization
WACC	Weighted average cost of capital
WDPA	World Database on Protected Areas
WRI	World Resource Institute

1 Introduction

1.1 Motivation

Green hydrogen is gaining unprecedented momentum in the global energy transition arena and is set to play a vital role in political and economic strategies for net-zero emissions. Not only is it a carbon-free fuel, but it also has the potential to decarbonize hard-to-abate sectors (Capurso et al., 2022, pp. 1–2). The share of hydrogen from the global energy mix is expected to increase significantly. In 2022, it made only 2.5% of the global energy consumption (IEA, 2023, p. 5), and it is estimated to reach 14%, from which 94% will be green hydrogen by 2050 in the scenario where the 1.5°C climate goal is met (IRENA, 2023, p. 36). A similar trend is expected in Europe, where hydrogen's share from the European energy mix is projected to rise from 2% in 2018 to 13-14% by 2050 (European Commission, 2020, p. 1).

More and more nationalities are establishing their hydrogen future strategies (World Energy Council, 2021), including Germany, a key advocate of hydrogen in future clean energy systems (German Federal Ministry for Economic Affairs and Energy, 2020). With its increasing importance in energy economies, countries aspire to secure their future hydrogen supply. In Germany and many other European countries, future hydrogen production is unlikely to meet demand. As result, hydrogen imports will be needed to close the demand gap (Breitschopf et al., 2022, p. 5). For instance, the European Union is estimated to domestically produce 10 megatons (Mt) of green hydrogen and import another 10 Mt by 2030 (European Commission, 2022). These developments provoke the need for a global hydrogen potentials assessment and the identification of suitable locations in which it can be produced and imported from.

While the potential of green hydrogen to advance the net-zero future scenario is promising, its production relies on already scarce resources such as land and water (Tonelli et al., 2023, p. 1). If hydrogen is to fulfill its expectations, it is crucial not only to evaluate its technical potential but also to ensure its production can support a sustainable development framework that will foster a just energy transition (Breitschopf et al., 2022; Dillman & Heinonen, 2022; Müller et al., 2023). In response to these challenges, various academic and private establishments aspire to shed light on the hydrogen sector and its economy. One of them is the Research Institute for Energy (Forschungsstelle für Energiewirtschaft, FfE) in Munich, which developed a model that simulates the European energy system and the role of hydrogen in it (FfE, 2022). This thesis is written in collaboration with the FfE and with the purpose of contributing to the understanding of the future hydrogen landscape by estimating its worldwide production potentials and costs.

1.2 Green Hydrogen Overview

Hydrogen can be produced in several methods. However, climate-neutral hydrogen is powered by renewable energy (RE) and is referred to as green hydrogen. Solar and wind power are considered prominent renewable energy sources (RES) for hydrogen production. Green hydrogen is generated via electrolysis, in which water is split into oxygen and hydrogen by electricity. There are different electrolysis technologies, but the dominant ones are proton exchange membrane (PEM), solid oxide (SO), and alkaline (ALK) electrolyzers (Ishaq et al., 2022, p. 26248). Furthermore, electrolysis can rely on desalinated water (Yates et al., 2020, p. 5).

A significant advantage of green hydrogen is its potential to remedy the intermittent nature of RES (Almutairi, 2022; Ao Xuan et al., 2022; Ishaq et al., 2022). While traditional electrical energy storage mediums like batteries are reaching their viable limits, green hydrogen can serve as a carbon-neutral energy carrier (Müller et al., 2023, p. 2). However, one of the most significant setbacks to green hydrogen today is its costly production method in comparison to non-carbon-free methods (IRENA, 2022; Kovač et al., 2021; Y. Wu, Deng, et al., 2021). Nonetheless, technological developments, scalability, and the ongoing reduction in RE costs are gradually leading green hydrogen to reach economic viability, which is expected to happen within the next decade (IRENA, 2022, p. 6)

With its increasing importance to future energy markets, there is a growing interest both in the scientific community and outside of it to evaluate whether the future supply of global green hydrogen can meet its demand with economic feasibility. A common approach to characterize the costs of hydrogen production is with a techno-economic assessment, which is typically applied to electricity production plants. This analysis considers operational costs, investment costs, output, and payback period of a plant over its lifetime. As result, it derives the levelized cost of electricity (LCOE) (Ince et al., 2021, p. 11; Shen et al., 2020, p. 1), and in the context of hydrogen, the levelized cost of hydrogen (LCOH).

A primary factor driving the costs and potentials of green hydrogen is the regional conditions of its underlying RES (Franzmann et al., 2023, p. 2). Thus, regions with favorable RES conditions are more attractive for hydrogen production. At the same time, the potential of attractive locations might be limited due to various constraints such as topographic conditions or other types of land use (IRENA, 2022, p. 6). Furthermore, the production of hydrogen contributes to increased pressure on already limited land and water resources (Tonelli et al., 2023, p. 2). Considering this,

identifying suitable regions for large-scale hydrogen production requires not only the assessment of RES conditions of potential locations, production relays on already scarce resources such.

As the productivity of green hydrogen production is highly sensitive to its underlying RES quality, on a large regional scale, hydrogen potentials cannot be represented by a single value but rather a continuous function which is driven by renewable energy capacity (IRENA, 2022, p. 6). This function can be illustrated with a cost-potential curve, that is expressed with the LCOH. As the LCOH is a function of hydrogen production potentials, consequently, it is also a function of the available area for its production. In this thesis, these two underlying variables are estimated with the purpose of generating a global cost-potential curve for green hydrogen.

The following section presents relevant literature on global hydrogen costs and potentials, as well as land eligibility for hydrogen production as a prerequisite for these estimates. From this point on in this work, hydrogen and green hydrogen are used interchangeably and always refer to the latter.

2 State of knowledge and Research Gap

In this section, the state of knowledge is discussed from three perspectives. First, the cumulative knowledge of global estimations of hydrogen costs and potentials is described. Second, the same topic is presented in the context of the FfE framework, as this work builds upon that. Third, the state of knowledge is discussed concerning land eligibility for hydrogen production. Finally, the goal and objectives of this thesis are expressed with the research questions guiding this work.

2.1 Global Costs and Potentials of Green Hydrogen

This section provides an overview of publications that contribute to the overall understanding of global hydrogen costs and potentials.

While studies that estimate domestic hydrogen potentials are more prevalent, global-scale analyses are less common. In the few studies that deal with a large geographic scope, a frequently used methodology is dividing the studied area into a fixed-sized grid and optimizing hydrogen costs on a cell basis. However, the components and boundaries of the optimized hydrogen production system vary among studies (Franzmann et al., 2023, p. 2). In research for this work, nine publications that estimate green hydrogen potentials on a global or large regional scale were identified and are summarized in Table 1.

Table 1: Overview of publications estimating green hydrogen costs and potentials on a large regional scale

Publication | Project	Type	Potential year	Scope	RES for electrolysis				Weather data[1]		Off-grid system	TC	LE
				Onshore wind	PV	Hybrid	Other[2]	Source	Year			
Braun et al. (2022) | MENA-Fuels	Gray literature	2020 2030 2040	MENA	x	x		Offshore wind, CSP	MERRA-2	2002	x		x
Breitschopf et al. (2022) & Pieton et al. (2023) | HYPAT[3]	Gray literature	2030 2050	Global[4]	x	x		Offshore wind, CSP	EAR5	2010		x	x
Fasihi and Breyer (2020)	Peer-reviewed	2020 2030 2040 2050	Global	x	x	x		NASA	2005	x		
Franzmann et al. (2023)	Peer-reviewed	2020 2030 2040 2050	Global (28 countries)	x	x	x		MERRA-2 GWA	2019			x
Institute of Energy and Climate Research (2023) | H2Atlas-Africa[5]	Gray literature	2020 2050	West, South, and East Africa	x	x		Hydropower	No data	No data	x		x
Heuser et al. (2020)	Gray literature	2050	Global (selected regions)	x	x			MERRA-2 GWA GSA		x	x	x
IRENA (2022)	Gray literature	2030 2050	Global	x	x	x	Offshore wind	EAR5	2018	x		x
Lux et al. (2021)	Peer-reviewed	2030 2050	MENA (10 countries)	x	x		Offshore wind, CSP, Rooftop PV	EAR5	2010	x		x
Pfennig et al. (2023) | Fraunhofer IEE | Global PtX Atlas	Peer-reviewed	2050	Global w/o EEA (98 countries)[6]	x	x	x		EAR5	2008-2012	x	x	x
Martínez Pérez (2022) | FfE	Master thesis	2020	Global	x	x	x		MERRA-2	2012	x		x

[1] All publications used weather data with an hourly spatial resolution.
[2] Concentrated solar power (CSP)
[3] H_2 Potential Atlas (HYPAT)
[4] Estimations are performed for 10 countries, and the results will be scaled up (in future work) to 70 countries, covering 90% of the global RE potential (Pieton et al., 2023).
[5] No detailed documentation was identified for this project. Attributes for this entry were based on the project's webpage (Institute of Energy and Climate Research, 2023).
[6] Pfennig et al. (2023) selected 600 sites for which they performed optimization and later upscaled the results on a global scale, excluding the European Economic Area (EEA).

While there is literature that focuses on the cost aspect exclusively (Agora Energiewende and AFRY Management Consulting, 2021; Brändle et al., 2021), Table 1 includes publications that estimated both costs and potentials. This overview builds upon some of the already identified publications by Pieton et al. (2023). Considering the wide interest in this topic, publications were not limited to peer-reviewed articles but other types as well. Furthermore, certain studies (Braun et al., 2022; Lux et al., 2021; Pfennig et al., 2023) did not focus on hydrogen potentials exclusively but also on other Power-to-X (PtX) products. The overview also includes attributes that were applied in this study, which are based on input from previous FfE work (Martínez Pérez, 2022). Nonetheless, this input is described in depth in the following section.

As mentioned previously, the RES powering the hydrogen production is the determinant factor driving its cost. In the reviewed publications, open space photovoltaic (PV) and onshore wind were the predominant RES for electrolysis, as well as their hybrid configuration, i.e., electrolysis powered by both RES. In addition to the differences in system definitions among studies, there are also differences in the input weather data, which is the basis for a grided cost optimization model. By using spatially and temporally resolved past meteorological patterns, RE potentials are forecasted, and subsequently, the derivable hydrogen costs and potentials. Most often, these estimates are projected for future scenarios, and sometimes for more than one year, also referred to as potential years in this work. In some cases, scenarios differ not only on their timeline but on other aspects as well. For example, IRENA (2022) analyzed a pessimistic and optimistic scenario that demonstrated the impact of future technological developments on hydrogen costs. Only a few studies included transportation costs (TC) in their analysis, and even fewer evaluated infrastructure-related export costs (Franzmann et al., 2023; Pieton et al., 2023). All publications but one (Fasihi & Breyer, 2020) applied a land eligibility (LE) analysis for hydrogen production; however, this will be discussed in greater detail in the following sections.

In terms of geographic scopes, IRENA (2022) and Fasihi and Breyer (2020) were the only publications that optimized costs and potentials with worldwide coverage. While Pieton et al. (2023) and Pfennig et al. (2023) had an almost complete global analysis, they performed the optimization for a sample of locations and then upscaled the results almost globally. Furthermore, the medium of results also played a role here. Most publications reported their results in the form of articles or reports, which inevitably requires some level of aggregation to convey insights concisely. In the report from IRENA (2022), for instance, while a fully global analysis was conducted, the results were presented individually for the Group of 20 (G20) countries and an additional six other high-potential countries, whereas the rest of the world was aggregated into

geographic regions. Pfennig et al. (2023) and Institute of Energy and Climate Research (2023), on the other hand, published interactive dashboards that enable a country-level analysis for each country in their scope.

This thesis joins the efforts to quantify hydrogen costs and potentials. One of the contributions of this work is its complete coverage of the world and the relatively high spatial resolution of the output results. Furthermore, this thesis opted for an interactive platform to share the results in order to allow the analysis on different aggregation levels and for different geographic regions. By doing so, it has the ability to provide insights for decision-makers around the world. The scope and level of detail in this thesis were enabled by preceding research within the FfE framework, which is detailed in the following section.

2.2 FfE Framework

In this section, the state of knowledge is discussed in the context of an existing FfE study (Martínez Pérez, 2022), which is the foundation for this thesis. Martínez Pérez (2022, p. 38) used a linear optimization model to minimize the yearly costs of green hydrogen. The decision variables were the component sizes of the underlying production system. The study focused exclusively on hydrogen costs, leaving production potentials out of its scope. This thesis complements the aforementioned study by computing the latter metric. To set the context for this work, an overview of the optimization model by Martínez Pérez (2022) is presented below.

Similar to the publications presented in Table 1, Martínez Pérez (2022) optimized green hydrogen costs using a grided approach based on MERRA-2 cells for the weather year of 2012. MERRA-2 stands for Modern-Era Retrospective analysis for Research and Applications, Version 2, and is provided by NASA Global Modeling and Assimilation Office (2022). The MERRA-2 data has an hourly temporal resolution and a spatial resolution of approximately 50 km in the latitudinal direction. The analysis considered only inland cells, with the exception of the Antarctic and North Pole, resulting in 51,677 cells.

The modeled system is a simplified off-grid electrolysis-based hydrogen production system, and its components are illustrated in Figure 1. The model used a PEM electrolyzer powered by open space PV, onshore wind, or a hybrid configuration of both. From here on, PV refers to open space PV unless specified otherwise. Additionally, the model included a stationary battery system and hydrogen storage in tabular accumulator form. The model did not include components such as a compressor, desalination system, heater, or electricity transmission system.

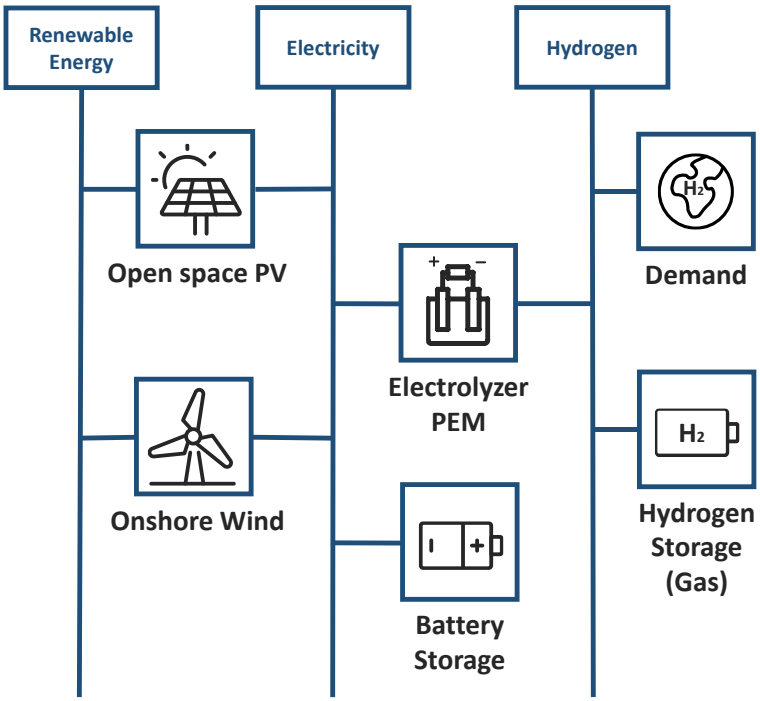

Figure 1: Simplified electrolysis-based hydrogen production system, source: Martínez Pérez (2022)

The cost optimization was based on techno-economic assumptions, where investment-specific costs (CAPEX), operational costs (OPEX), and the weighted average cost of capital (WACC) for the different components of the production system were derived from the year 2020. The exact economic parameters used in the optimization model are available in Martínez Pérez (2022, p. 49). The costs associated with water usage for electrolysis were not included in the model. However, such costs, including those related to desalination, are estimated to be relatively negligible (Yates et al., 2020, p. 5). Additionally, the model did not account for transportation costs and import costs from the production site to the consumption site. Nonetheless, these are expected to be evaluated in future developments of the model. Furthermore, country risk premiums (CRP) were considered in the cost optimization to account for additional investment risk associated with a specific country. The CRP data was provided by Damodaran (2023) and is continuously updated. The specific values used for the optimization model are presented in Martínez Pérez (2022, p. 115).

Finally, the optimization output provided for each cell the minimal LCOH (€/kg) and the required installed capacity of each system component (i.e., PV and onshore wind) in megawatt (MW) to satisfy a demand of 1 kg hydrogen per hour. In each cell, the optimization was performed for three system configuration scenarios: PV only, onshore wind only, and a hybrid system powered by both RES. The optimization was carried out for a small system that can be upscaled according

to the confinement of the available area in a cell. Figure 2 presents the results of minimal LCOH levels by cell. Highly attractive LCOH levels were identified in Australia, southern Chile, the United States, the North Sea region in Europe, Greenland, the small area in the east of Brazil, and Saudi Arabia (Martínez Pérez, 2022, p. 78).

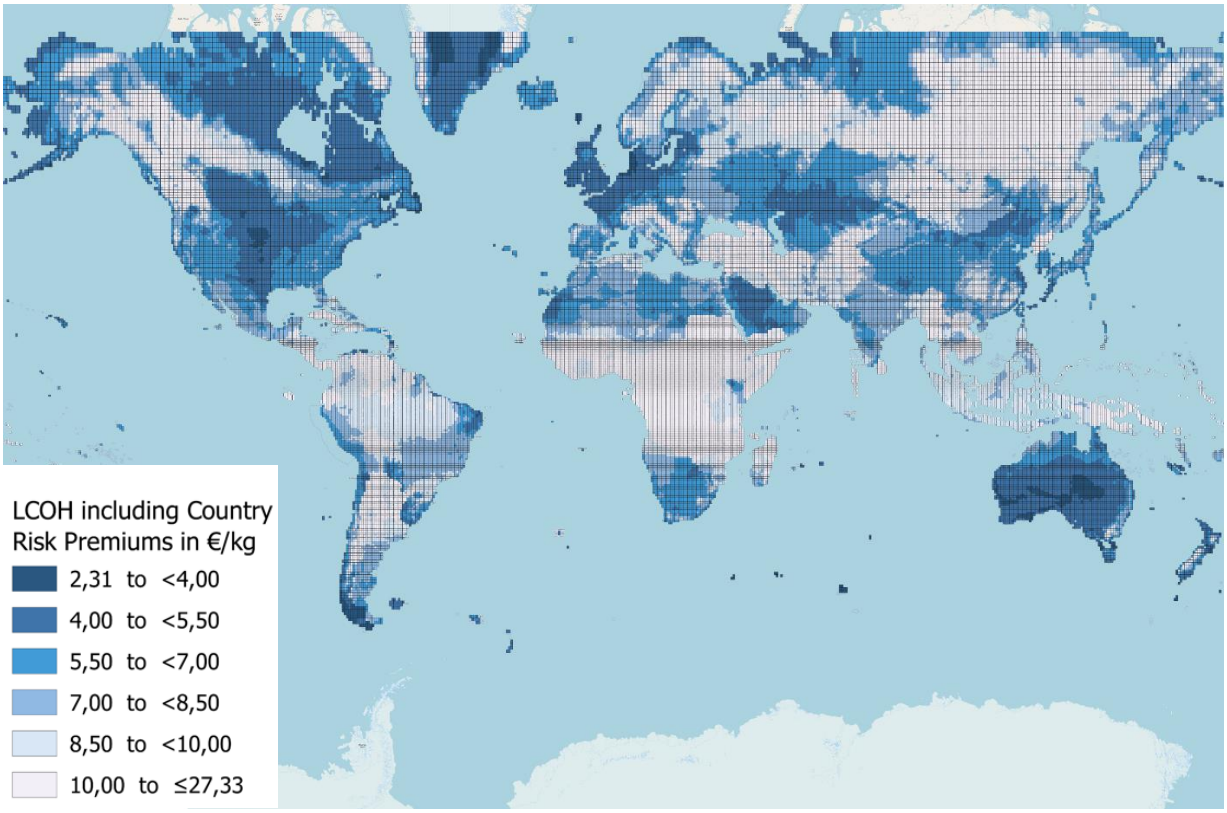

Figure 2: Global map of LCOH (€/kg) including CRP, source: Martínez Pérez (2022)

Regarding the system configuration, 75% of systems were hybrid, while PV only and onshore wind only made 22% and 3%, respectively. Figure 3 illustrates the proportion between the two RES installed capacities of the optimized system using the share of PV from the total system installed capacity. The figure demonstrates that PV was generally more dominant (Martínez Pérez, 2022, p. 91). For further details and results, see Martínez Pérez (2022).

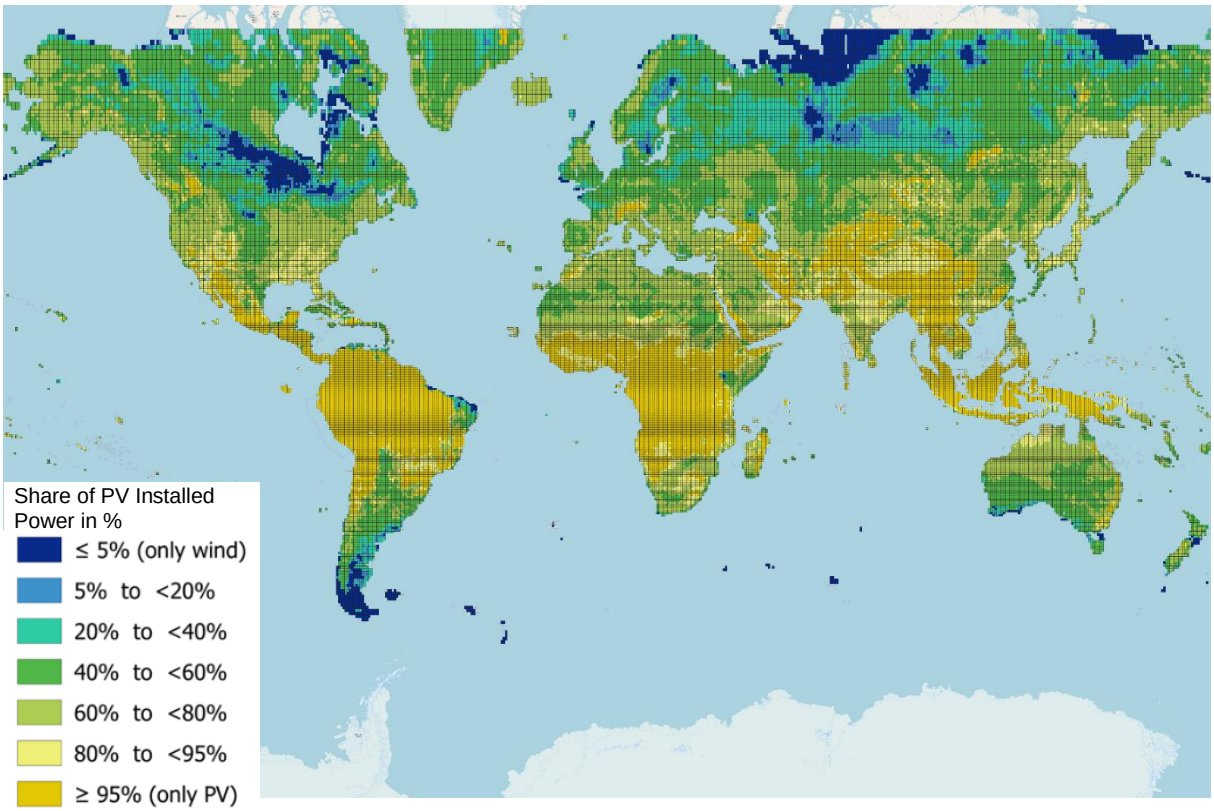

Figure 3: Global map of optimized share of PV installed capacity, source: Martínez Pérez (2022)

As noted previously, the results from Martínez Pérez (2022) were only meant to illustrate the costs of hydrogen without the production potentials associated with these costs. Furthermore, the model did not consider any limitations to land use, i.e., land that is unsuitable for hydrogen production. Considering this, while certain locations might exhibit promising economic potential, in reality, land use restrictions could hinder the realization of this potential. This thesis addresses this limitation by defining the eligible land for hydrogen production and deriving hydrogen costs and potentials. Moreover, it is worth mentioning that typically in literature, the available land for hydrogen production is defined first, and only then are costs and potentials estimated for the eligible land. In this context, the reversed order of actions of this work and Martínez Pérez (2022) provides a certain advantage that is explained in the following section.

2.3 Land Eligibility Analysis

A preliminary requirement for estimating green hydrogen costs and potentials is determining the available and suitable areas for its production. In the discipline of RE land use, such evaluation can be achieved by a land eligibility (LE) analysis (Ryberg et al., 2017). This section discusses

the state of knowledge of LE literature in the broader context of RES and on a more narrow aspect of green hydrogen. Furthermore, emphasis is given to large-scale geographic analyses.

To better understand LE analysis, it is useful to familiarize with land use suitability analysis. Land use suitability analysis is applied in various disciplines and can be broadly defined as a tool to identify "the most appropriate spatial pattern for future land uses according to specify requirements, preferences, or predictors of some activity" (Malczewski, 2004, p. 4). Ryberg et al. (2017, p. 2) defined the LE of a particular RE technology as "the binary conclusion dictating whether the technology in question is allowed to be placed at a particular location." Geographic information systems (GIS) are widely used in this practice. In a GIS-based LE analysis, an area of interest is subdivided into basic units, which are then classified according to their suitability for a particular activity (Malczewski, 2004, p. 4). Considering the complexity involved in spatial planning for RE and hydrogen production infrastructure, utilizing GIS is essential (Müller et al., 2023; Spyridonidou & Vagiona, 2020, 2023). While GIS-based methods are most commonly used in RE site selection, there are other methodologies, such as fuzzy logic membership functions or analytic hierarchy process (AHP) (Spyridonidou & Vagiona, 2020, 2023).

An important distinction must be made in land suitability analysis between the site selection problem and the site search problem. The first deals with ranking a set of potential sites and identifying an optimal alternative, while the latter deals with establishing boundaries of sites and has no pre-determined set of candidates (Malczewski, 2004, pp. 4–5). In the context of RE, site selection or assessment methodologies can be generally divided into four stages. The first is the exclusion stage, in which land that does not meet a set of minimal criteria, or exclusion criteria (EC), is removed from further consideration (Spyridonidou & Vagiona, 2020, p. 2952). These criteria usually take the form of a threshold or an acceptable range (Ryberg et al., 2017, p. 2). In the second stage, assessment criteria (AC) are selected to determine potential sites' suitability level. Once AC are defined, the set of potential sites are assessed in the third stage with respect to these criteria. In the fourth stage, the assessment results are optimized to identify the optimal site (Messaoudi et al., 2019, p. 31810; Spyridonidou & Vagiona, 2020, p. 4, 2023, p. 2952). Similarly to the distinction made by Malczewski (2004, p. 5), the first stage is equivalent to the site search problem, resulting in the boundaries for potential sites, while the following three stages can be attributed to the site selection problem. This thesis tackles the site search problem exclusively, and accordingly, the last three stages described above are outside of its scope. From this point forward in this work, the first stage, i.e., the exclusion stage, is referred to as LE or LE analysis.

LE analyses are usually conducted on a regional scale, and their constraints typically depend on the geographic region and RE technology in question (Ryberg et al., 2017, p. 2). Considering this, the global application of an LE analysis for green hydrogen that is powered by more than one RES poses a significant challenge. Spyridonidou and Vagiona (2023, p. 2974) echoed this challenge in their review of solar energy site planning. They noted that on a narrower geographic analysis, the definition of LE constraints could rely on local land use regulations and policies. However, in international literature, such legislative frameworks were generally missing but nonetheless much needed. Cremonese et al. (2023, p. 19423) reinforced this finding in their study, concluding that international standards for future hydrogen-related projects will be critical. It is worth mentioning that the definition of LE in this work was not based on regulatory information and, therefore, should not be considered as such. Nonetheless, it contributes to the global hydrogen LE discussion.

While the importance of LE for RES is increasing in the scientific community, there are still various knowledge gaps in this topic, particularly in the context of spatially large-scale analyses (Ryberg et al., 2017, p. 3). Ryberg et al. (2017) reviewed LE relevant literature of various RES and identified significant inconsistencies in three key aspects: criteria definitions, LE methodologies, and data usage. Research for this work found that these inconsistencies were very common in the green hydrogen LE literature as well. Nonetheless, this topic is discussed in depth in later sections of this work. In order to remedy the aforementioned inconsistencies, Ryberg et al. (2017) developed a methodological LE framework for RES, as well as a Python-based model (GitHub, 2023) to practically apply it. Several studies in the field of hydrogen costs and potentials (Franzmann et al., 2023; Heuser et al., 2020; Welder et al., 2018) made use of this tool. However, it was found to be less suitable for this work due to the specific desired results structure and the preferable software deployment environment.

The work of Ryberg et al. (2017) is further developed in publications such as Ryberg et al. (2018), which evaluated RES land eligibility sensitivity to various constraints in Europe, or Ryberg et al. (2020) that conducted a similar evaluation in the context of onshore wind. Spyridonidou and Vagiona also shed light on the LE discipline with two systematic reviews highlighting prominent criteria for site-selection procedures, one for wind energy projects (2020) and one for solar energy projects (2023). Rediske et al. (2019) reviewed PV siting literature similarly and indicated determinant site selection factors. Nevertheless, a systematic review in the field of green hydrogen LE, such as those above, was not identified.

In green hydrogen LE and site selection relevant literature, studies with a local scale, such as country or province analyses, were more prevalent, while studies with a global or large regional scale were scarce. Furthermore, many local studies, such as Ali et al. (2022) and Almutairi (2022), tended to focus predominantly on both the site selection problem and the site search problem, while global studies, such as IRENA (2022) and Franzmann et al. (2023) usually applied a GIS-based LE as the preliminary step for evaluating hydrogen costs and potentials. One global study that emphasized land-use implications of green hydrogen was Tonelli et al. (2023), which evaluated the additional land and water scarcity induced by large-scale hydrogen production.

The LE criteria definitions for hydrogen production were mostly based on preliminary literature reviews, some more extensive than others. However, the number of references used to define each criterion was usually between one and three. In addition to literature sources, several studies with a local scope (S. S. H. Dehshiri & Dehshiri, 2022; S. J. H. Dehshiri & Zanjirchi, 2022; Wang et al., 2019) based their site selection procedures on interviews with experts. While this approach could be insightful if conducted with an international panel of experts, it would require an extensive qualitative analysis that is out of the scope of this thesis. Furthermore, although the term LE insinuates that it evaluates the physical suitability of land only, it may include criteria that evaluate socio-political components as well. This approach is rooted in a holistic sustainable development evaluation (Breitschopf et al., 2022), which will be further explained in later sections.

LE analysis is primarily used to determine possible locations for production sites. However, it can also be further investigated to provide additional insights for future land use planning. Ryberg et al. (2018) pointed out that the latter use case of LE has not received sufficient consideration in large-scale analyses. In response, they mapped the land constraints to various RES in Europe according to criteria groups, as well as the overlapping of these groups. For instance, they showed that 77% of the area in Europe was restricted due to physical EC, while 63% was restricted due to socio-political EC, and 22% was restricted by the intersection of both EC groups. The goal of Ryberg et al. (2018) was to assist researchers to better understand the implications of the EC applied in their LE work. Similar to Ryberg et al. (2018), most LE analyses examining restrictions to hydrogen production measure the level of restrictions according to the size of restricted land. However, one study was identified using another approach. Okunlola et al. (2022) estimated green hydrogen potentials in Canada, and in order to quantify the impact of various EC, they first estimated hydrogen potentials with a baseline scenario. Then, they measured the reduction of

hydrogen potentials by applying additional EC. Franzmann et al. (2023) also used a hydrogen-potentials-based approach to demonstrate the impact of certain constraints on a global scale. For example, they illustrated global hydrogen cost-potential curves in 2050 according to water stress levels.

This thesis aims to mitigate the global hydrogen LE literature gap by conducting a systematic literature review similar to the reviews mentioned above in the field of RES and with an emphasis on a global scale LE analysis. Furthermore, this work provides additional insights into the LE hydrogen field by analyzing restrictions factors of land eligibility not only from a spatial perspective but also from a hydrogen potential perspective that considers the economic value of these potentials. This analysis contributes to a better understanding of the economic implications of LE restrictions beyond spatial measurements.

2.4 Research Goals and Objectives

This thesis aims to define the global land eligibility for green hydrogen production, estimate its costs and potentials, and derive the global cost-potential curve of green hydrogen. Furthermore, the thesis seeks to provide a nuanced understanding of how different land exclusion criteria and the indicators used to measure their impact influence the identification of suitable areas for green hydrogen production. Finally, this work strives to elucidate the geographic distribution of green hydrogen potentials by sharing the results in an interactive manner that allows a flexible geographic analysis. The following research questions guide the thesis:

1. How to define a global LE analysis for green hydrogen production? What are the appropriate land exclusion criteria and their indicators?
2. Which LE criteria are most restrictive to hydrogen production and where in terms of land availability and hydrogen potentials, and what insights could be learned from the differences between these two measures?
3. What is the global hydrogen production potential, and how is it geographically distributed?

The rest of this work is structured in three parts, each focusing on one of the research questions.

3 Materials and Methods

This section describes the materials and methods used in this thesis. The workflow in this thesis was divided into three steps, where the results of each step feed into the following one.

3.1 Systematic Literature Review

The main objective of this literature review was to identify the most important criteria for a green hydrogen LE analysis, as well as identify the most suitable indicators, threshold values, and data sets for these criteria. In particular, for the purpose of a global analysis. Additionally, the review aimed to point out other valuable insights or knowledge gaps in the field of hydrogen LE analysis and site selection. The choice of a systematic literature review as a method was based on studies (Rediske et al., 2019; Ryberg et al., 2017; Spyridonidou & Vagiona, 2020, 2023) that used an equivalent approach to answer similar research questions in the field of LE for various RES.

The main steps of the literature review followed the guidelines of Čablová et al. (2017), as well as the reviews mentioned above. After reviewing several search engines for this review, SCOPUS was found to be the most suitable for the needs of the literature search and, therefore, was the only search engine that was used. Nonetheless, since the topic in question is prevalent in gray literature, such as reports and projects with webpage documentation, further records were identified through other sources. Moreover, some additional records were identified in the reference list of papers identified in the initial search.

In line with the objective of this review, the literature search aimed to identify publications that can contribute to the knowledge of green hydrogen LE analysis, particularly with regard to GIS-based LE and its relevant criteria. Nonetheless, the search was not limited to GIS site selection methods. Early research for this work pointed out that such contributions could be found in studies that deal with estimating hydrogen production potentials and site selection procedures. Furthermore, as it was observed that global studies are scarce, regional and local studies were taken into consideration as well. The search terms were chosen based on the prevalent author keywords that were used in publications in the relevant field. The search results were filtered to those that were published in the last five years (the current year and the four preceding years) and in English[7]. This process resulted in the following search string:

[7] As one relevant publication in German (Braun et al., 2022) was identified through other sources, an exception was made to include it.

"(AUTHKEY (hydrogen AND ("cost potential" OR "LCOH" OR "global analysis" OR "Global optimization" OR "GIS" OR "Geographic information system" OR "levelized cost of hydrogen" OR "cost of hydrogen" OR "cost optimization" OR "hydrogen export" OR "production potential" OR "spatial analysis" OR "levelized cost" OR "land eligibility" OR "site selection" OR "multi-criteria decision-making")) AND LANGUAGE (English)) AND (LIMIT-TO (PUBYEAR , 2023) OR LIMIT-TO (PUBYEAR , 2022) OR LIMIT-TO (PUBYEAR , 2021) OR LIMIT-TO (PUBYEAR , 2020) OR LIMIT-TO (PUBYEAR , 2019))"

The search was conducted in June 2023 and resulted in 226 publications. An additional nine publications were identified in other Sources. The search results were filtered to include publications that discussed green hydrogen, which is powered by open-space PV and/or onshore wind turbines. Moreover, only studies that mentioned criteria to evaluate suitable land and/or sites for hydrogen production were included. Finally, 27 studies were selected for this systematic review. The search process is depicted in the PRISMA study flow diagram (Figure 4). The creation of the diagram followed the work of Čablová et al. (2017, p. 78) and Rediske et al. (2019, p. 1691). From this point forward, unless specified otherwise, figures in this work were created by the author.

Finally, the results were summarized in a tabular form that highlighted the most important criteria to consider for the purpose of green hydrogen LE. Once the criteria were identified, a comparative assessment of their definitions among the reviewed studies provided a basis for defining the LE criteria in this work. The results of the systematic literature review served as the input for the following step in this work, i.e., the application of a green hydrogen LE analysis on a global scale, which is described methodically in the following section.

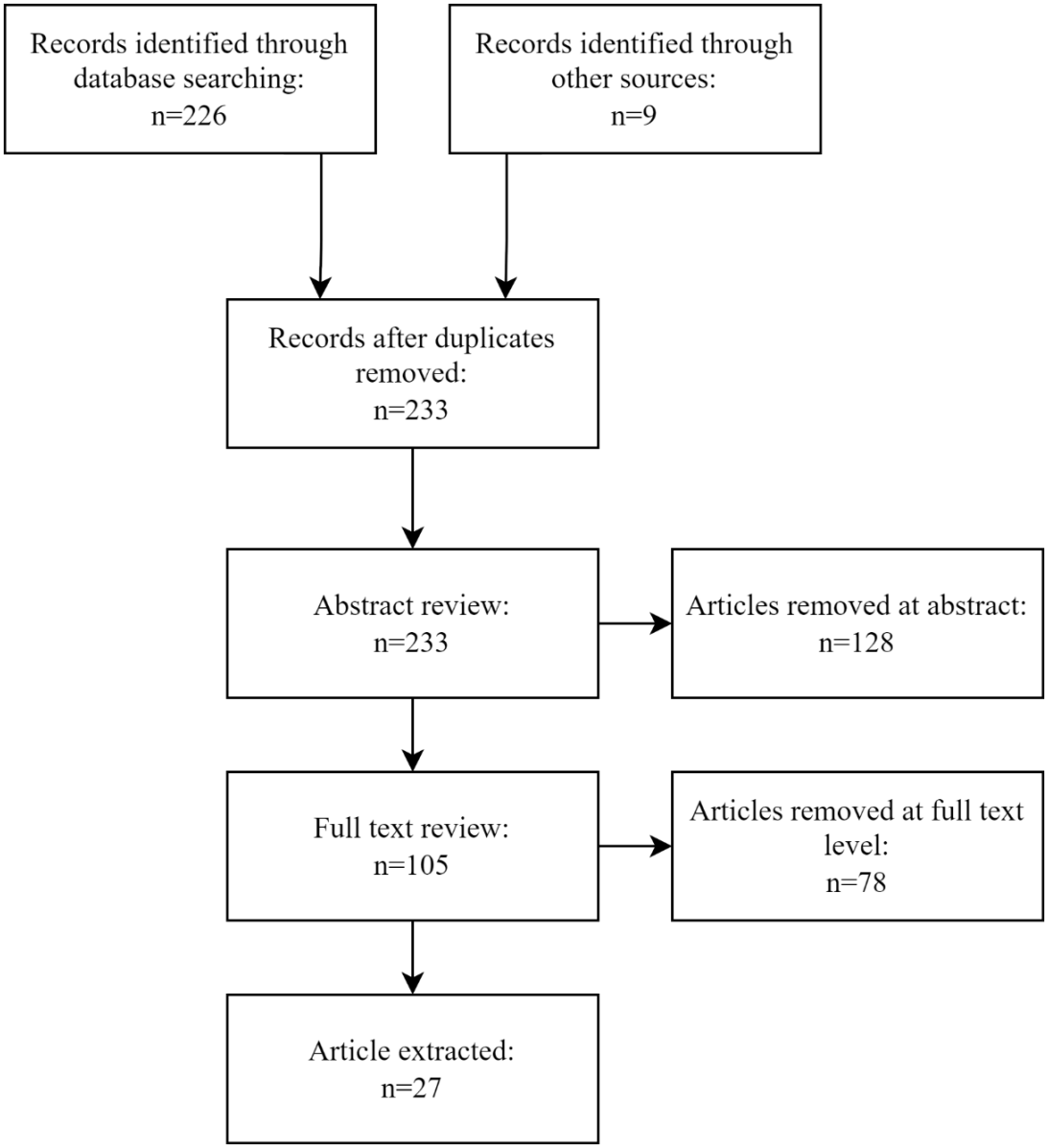

Figure 4: PRISMA study flow diagram

3.2 Land Eligibility Analysis

As previously mentioned, LE analysis aims to produce a "binary conclusion dictating whether the technology in question is allowed to be placed at a particular location" (Ryberg et al., 2017, p. 2), which is typically subdivided into a set of basic units to be classified (Malczewski, 2004, p. 4). In the context of this work, the "particular location" was the whole world, and the basic units were MERRA-2 cells, based on input data provided by Martínez Pérez (2022), see 2.2 for further details.

The provided input dataset included 51,677 cells with a spatial resolution of about 50 km² where cells around the equator are larger, and cells approaching the poles are smaller. The dataset considered only inland cells, with the exception of the Antarctic and North Pole (Martínez Pérez, 2022, p. 36). A polygon geometry was provided for each cell using the 4326 spatial reference identifier (SRID). Furthermore, the dataset included the country assigned to each cell. As the distribution of cells did not align with the borders of countries, cells that spread over more than one country were assigned to the dominant country in that cell, i.e., the country which had the largest share of land (Martínez Pérez, 2022, p. 57).

The land eligibility in each cell was determined by the set of criteria that were defined in this work, and each criterion was assessed using a relevant dataset. The exact description and further details regarding the set of criteria and their corresponding datasets are discussed later in this work in 4.1.2, where the criteria are summarized in Table 11. The provided input data (Martínez Pérez, 2022) and the LE criteria underlying data sets were all uploaded into the FfE database, a PostgreSQL database, which is an open-source object-relational database system. The application of the LE analysis was scripted in structured query language (SQL) with a PostgreSQL syntax. The script applied various functionalities of PostGIS, a PostgreSQL extension that enables the processing of geographic data (PostGIS, 2023).

Considering the global scope of this work, large datasets needed to be processed, which oftentimes required a lengthy running time. To tackle this issue, PostGIS functionalities, such as spatial indexing and clustering, were used, which improved performance significantly. Furthermore, performance was improved by compromising data accuracy to a certain extent. For example, running time was accelerated by applying the ST_Simplify function of PostGIS (2023). The function simplifies the shape of geometries and thus expedites their processing, but at the same time, it reduces data accuracy. Nonetheless, in a global scale analysis, such inaccuracies are relatively negligible. Furthermore, opting for datasets with lower spatial resolution advanced running time as well. Lastly and most importantly, the powerful server provided by the FfE enabled the processing of large datasets. Considering this, it is important to note that replicating the methods used in this work for large-scale analyses requires a powerful machine, which is not the standard local machine.

To demonstrate the LE application process, Figure 5 exemplifies a theoretical exclusion scenario of a single MERRA-2 cell. The figure demonstrates how an area can be excluded by a single criterion, e.g., a protected area, or by several criteria that may intersect, such as the intersection between forests and slope in this example. The remaining areas which do not fall within the

exclusion boundaries are considered eligible for hydrogen production. The final outcome of the script provided two geometries in each cell, one for eligible land and one for excluded land.

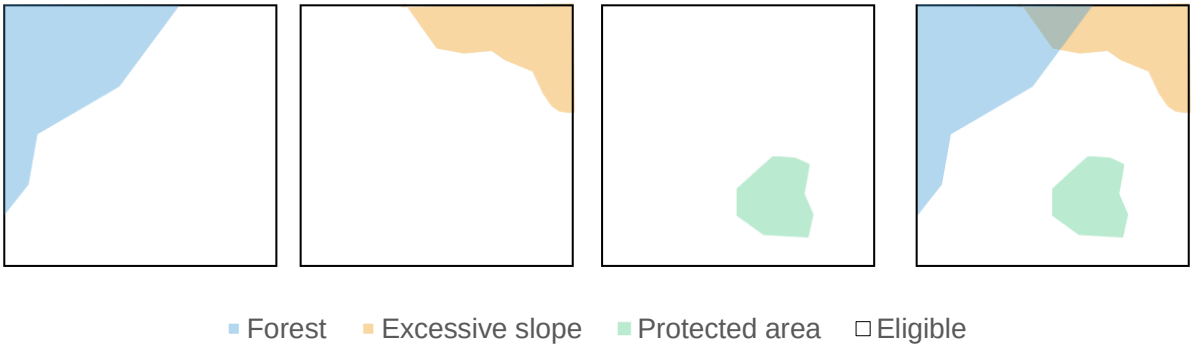

Figure 5: Illustration of LE application in a MERRA-2 cell

As exemplified in Figure 5, the LE analysis for each criterion was first applied individually, and lastly, all criteria were combined. This approach was taken as this work analyzed the individual impact of each criterion on green hydrogen land eligibility to target the most restricting criteria. It is important to mention that this work did not investigate the intersection of criteria, e.g., analyzing which criteria overlapped and which areas were excluded by multiple criteria. While analyzing the LE from this perspective could be insightful, it would significantly increase the level of complexity. Therefore, it was decided to exclude it from the scope of this thesis.

The datasets used in this analysis came in two formats of spatial data: raster and polygons. Raster data is a matrix of fixed-size pixels, where each pixel stores a value (PostGIS, 2023). For instance, elevation data is typically stored as raster data. On the other hand, polygons represent the boundary of a specific area and do not have a fixed rectangular shape like raster data. For example, the boundaries of protected areas could be represented with polygons. Accordingly, two types of scripts were created to process each data type.

Furthermore, scripts were also designed for two exclusion scenarios: a scenario where the exclusion definition was uniform for PV and onshore wind and a scenario where the definition differed between the two RES technologies. The output of LE for each cell and criterion was saved into the FfE database in the form of a table named merra2_ec. The structure of the table and samples of scripts for each underlying data type and exclusion scenario are available in Appendix 7.1.1.1.

Once all the exclusion geometries for each cell and EC were produced, they were unified to generate the final eligible and excluded geometries for hydrogen production in each cell. The unification of a specific set of EC in this work is referred to as an LE scenario. This work produced more than one LE scenario to further evaluate the impact of certain criteria. Therefore, a script was required to enable the creation of multiple scenarios efficiently. First, a table was created to assign each LE scenario with its relevant set of EC. The table structure is available in Appendix 7.1.1.2. Then, the set of EC under each LE scenario was unified by a script, and the results were saved into the database object merra2_le. The script and output data structure are available in Appendix 7.1.1.3.

Once the eligible area per LE scenario and cell were determined, the final step was carried out. That is the estimation of hydrogen potentials and, subsequently, the derivation of the cost-potential curve. The methodology of the last step is described in the following section.

3.3 Costs and Potentials

Once the available land was extracted for each MERRA-2 cell, hydrogen costs and potentials were estimated by combining the land eligibility data with the LCOH data generated by the FfE optimization model (Martínez Pérez, 2022).

As previously described in 2.2, the optimization model (Martínez Pérez, 2022) provided for each cell the optimal LCOH (€/kg) and the required installed capacity of each system component in megawatt (MW) to satisfy a demand of 1 kg hydrogen per hour. The optimization was performed for the three system configuration scenarios and was carried out for a small system, which can be later upscaled according to the confinement of eligible land in a cell.

For determining the upscaling limits, the system-required installed capacity was converted into the system land requirements, expressed in km². For this conversion, the power density (PD) for each technology was used. The PD is the nameplate power capacity, or installed capacity (MW), per surface unit (Enevoldsen & Jacobson, 2021, p. 41). As wind turbines typically produce alternating current (AC) (Action Renewables, 2019), their power density is assumed to be expressed in AC. For PV; however, PD can expressed in either AC or direct current (DC) (Bolinger & Bolinger, 2022). As the optimization model (Martínez Pérez, 2022) output provided the installed capacity in AC, the PD was expressed in the same unit. The conversion of the system's required installed capacity to its required land is presented in the equation below:

$$RL_{ij} = \frac{RIC_{ij}}{PD_i}$$

Where:

- RL_{ij} is the required land for RES technology i in cell j
- RIC_i is the required installed capacity for RES technology i in cell j
- and PD_i is the power density for RES technology i

In order to define the PD values for each RES technology, relevant literature was reviewed. Among the global hydrogen potential studies, three used a similar approach. The studies and their used PD values are presented in Table 2. The source column provides the reference on which the PD values were based in the respective publication.

Table 2: Power density values in global hydrogen studies

Publication	PV	Onshore wind	Unit in source	Source
Fasihi and Breyer (2020)	74	8.4	MW/km²	Bogdanov & Breyer (2016)[8]
IRENA (2022)	45	5	MW_{ac}/km²	PV: Ong et al. (2013) and Bolinger and Bolinger (2022) Onshore wind: G. C. Wu et al. (2015) and Enevoldsen and Jacobson (2021)
Pfennig et al. (2023)	40	15	MW_{ac}/km²	None[9]

In the context of PV, while IRENA (2022) and Pfennig et al. (2023) showed similar values, Fasihi and Breyer (2020) used a significantly higher value. In reviewing Bogdanov and Breyer (2016), the reference used by Fasihi and Breyer (2020), no reference nor a method was identified for the selection of the PD values. Furthermore, the PV value used by Bogdanov and Breyer (2016, p. 182) was intended for optimally tilted and single-axis tracking PV systems, which are characterized by high PD (Bolinger & Bolinger, 2022), while the FfE optimization model (Martínez Pérez, 2022) used a fixed tilt PV. Ong et al. (2013, p. 4), the reference cited by IRENA (2022), analyzed 72% of utility-scale PV and CSP capacity in the United States and found that the capacity-weighted average land use for fixed-tilt PV was 45 MW_{ac}/km² and 43 MW_{ac}/km² for a small PV plant (>1 MW, <20 MW) and a large PV plant (>20 MW) respectively (Ong et

[8] It was not identified whether the study expressed power densities with was expressed in MWac/km² or MWdc/km²
[9] While Pfennig et al. (2023, p. 6) did not mention the power densities were expressed in AC, this was assumed as their model results were expressed in AC.

al., 2013, p. 18). Bolinger and Bolinger (2022, p. 590) pointed out that the study by Ong et al. (2013) was conducted a decade ago and that the PV sector saw major technological improvements that significantly improved PDs. To reevaluate these values, they analyzed 736 PV plants in the United States, focusing on the period between 2011 and 2019. They found that median benchmarks for PDs were 45 MW_{ac}/km^2 for tracking plants and 69 MW_{ac}/km^2 for fixed tilt plants. IRENA (2022) used the lower value; however, no information was found regarding the type of PV technology that was used in their model.

With the discussion above somewhat inconclusive, another assessment was conducted to validate the PD values. A sample of 20 PV sites was selected from the list of the biggest PV power stations in the world, available at Wikipedia (2023). The sample considered only stations with a commission date from 2014 and on, and that included data regarding the area size of stations and their power capacity in MW_{ac} or MW_{dc}, ideally with both values. In stations where both values were available, the AC:DC factor was calculated, and these factors were then averaged. In stations where only MW_{ac} was available, the MW_{dc} was calculated by dividing the MW_{ac} by the average AC:DC factor. Finally, the PD for each station was calculated by dividing the station's area by its power capacity. Therefore, two PD values were assigned to each station based on its MW_{ac} and MW_{dc}. The calculations are expressed in the equations below:

$$F_{AC/DC_i} = \frac{MW_{ac_i}}{MW_{dc_i}}$$

$$MW_{dc_i} = \frac{MW_{ac_i}}{Average\ F_{AC/DC}}$$

$$PD_{ac_i} = \frac{MW_{ac_i}}{km^2{}_i}$$

$$PD_{dc_i} = \frac{MW_{dc_i}}{km^2{}_i}$$

Where:

- F_{AC/DC_i} is the AC:DC factor of station i
- MW_{ac_i} is the AC power capacity of station i
- MW_{dc_i} is the DC power capacity of station i
- $Average\ F_{AC/DC}$ is the average of all F_{AC/DC_i} (considering only stations where both AC and DC values were available)
- PD_{ac_i} is the AC power density expressed of station i

- PD_{dc_i} is the DC power density of station i
- $km^2{}_i$ is the area size of station i

Two validations were made, the first averaging the PD_{ac} for all stations where the MW_{ac} was available (13 stations). The averaged power density of the stations resulted in 40.26 MW_{ac}/km^2. In the second validation, the average PD_{dc} of all 20 stations was multiplied by the average AC:DC factor. This resulted in an average of 42.84 MW_{ac}/km^2. For the full list of the stations, their attributes, and further calculations, see Appendix 7.1.2.1. In conclusion, the validation results were aligned with IRENA (2022) and Pfennig et al. (2023), and therefore, a similar scale PD for PV was deemed appropriate for this work.

Concerning wind turbine PDs, there was quite a big variation among the studies. Pfennig et al. (2023) used a value of 15 MW_{ac}/km^2, which is three times higher than the value used by IRENA (2022) and almost double the value used by Fasihi and Breyer (2020). When reviewing the sources used by IRENA (2022), the value of 5 MW_{ac}/km^2 was not identified. Enevoldsen and Jacobson (2021) analyzed data from 16 onshore wind farms in five countries/continents and found that the mean installed PD varied from 16.5 MW/km² in Chile to 48 MW/km² in China. G. C. Wu et al. (2015, p. 39) used what they refer to as a land use factor of 9 MW/km² for onshore wind to estimate LCOE in Africa.

The validation approach used for PV was not feasible in the case of onshore wind as the parallel Wikipedia list did not provide information regarding the area size of wind farms. Nonetheless, a FfE study (Kigle et al., 2022) optimized wind farms configuration in Germany and found that PDs varied greatly, ranging from 9 MW_{ac}/km^2 to 60 MW_{ac}/km^2, with an average of 29.3 MW_{ac}/km^2. These variations can be attributed to topographic and climatic conditions and the wind rotor diameter affecting the distance needed between wind turbines (Kigle et al., 2022, p. 7).

According to Bolinger and Bolinger (2022, p. 590), outdated PD values are too low and thus can cause significant overestimation of land requirements. Nonetheless, this study opted for a conservative approach as a base scenario to not overestimate hydrogen potentials and enable a more insightful comparison of the results with other studies. Therefore, the PDs were selected from the range of values used by IRENA (2022) and Pfennig et al. (2023). Taking the observation made by Bolinger and Bolinger (2022, p. 590) into consideration, the upper limits of the range were selected, that is, a PD of 45 MW_{ac}/km^2 for PV (Pfennig et al., 2023) and a PD of 15 MW_{ac}/km^2 for onshore wind (IRENA, 2022). Furthermore, to assess the sensitivity of hydrogen potentials to PDs, a second scenario was examined with higher PD values, which were based on

up-to-date recommendations of 69 MW_{ac}/km^2 for PV (Bolinger & Bolinger, 2022, p. 590) and 29.3 MW_{ac}/km^2 for onshore wind (Kigle et al., 2022, p. 7).

With the determined PDs, the system land requirements per cell were derived, and hydrogen potentials were calculated by allocating the eligible land for hydrogen production according to the system's needs. As previously mentioned, the LCOH was optimized for the three possible scenarios of system configuration in each cell. While a hybrid scenario saw the best LCOH outcome in some cells, it was produced by a single technology scenario in other cells. Accordingly, the land allocation process considered the cost-effectiveness of each configuration scenario. In the following, the process of land allocation is described.

To demonstrate the land allocation process, an example is illustrated below for one cell. First, the input data for land allocation is presented in Table 3. Using the baseline PD values, the installed capacities provided by Martínez Pérez (2022) were converted to the system land requirements. The final input for the land allocation process is the eligible land per cell. For the sake of simplicity, the example below is based on an LE scenario where the cell area was entirely eligible for both PV and onshore wind.

Table 3: Cell optimization output data (Martínez Pérez, 2022) and conversion to land requirements

System configuration scenario	LCOH (€/kg)	Installed capacity (MW)		Land required (km²)	
		PV	Onshore wind	PV	Onshore wind
Hybrid	7.22	0.17	0.22	0.004	0.015
Onshore wind only	7.64	-	0.36	-	0.024
PV only	11.11	0.63	-	0.014	-

The land allocation process was performed in three steps, one for each system configuration scenario. Starting with the system configuration scenario with the lowest LCOH and ending with the highest LCOH. The land allocation model assumed that in a hybrid scenario, eligible areas could be maximally utilized for both RE installations synchronously without depreciating their PDs. While literature indicates that the co-existence of PV and onshore wind in a shared area does lead to some reduction in their PDs, this reduction is negligible and is estimated to affect less than 1% of land (Mamia & Appelbaum, 2016, p. 713). On the other hand, the shadowing effect of wind turbines on PV installations could lower the latter's power productivity by 1-8% (McKenna et al., 2022, p. 9). The shadowing effect is not accounted for in this work and could, therefore, result in a slight overestimation of hydrogen potentials. Additionally, the allocation

model enabled the parallel land allocation for more than one system type. For instance, land might have been allocated for both a PV-only system and a wind-only system. To better understand this methodology, the demonstration continues below where the land allocation process of the exemplified cell from Table 3 is illustrated in Figure 6.

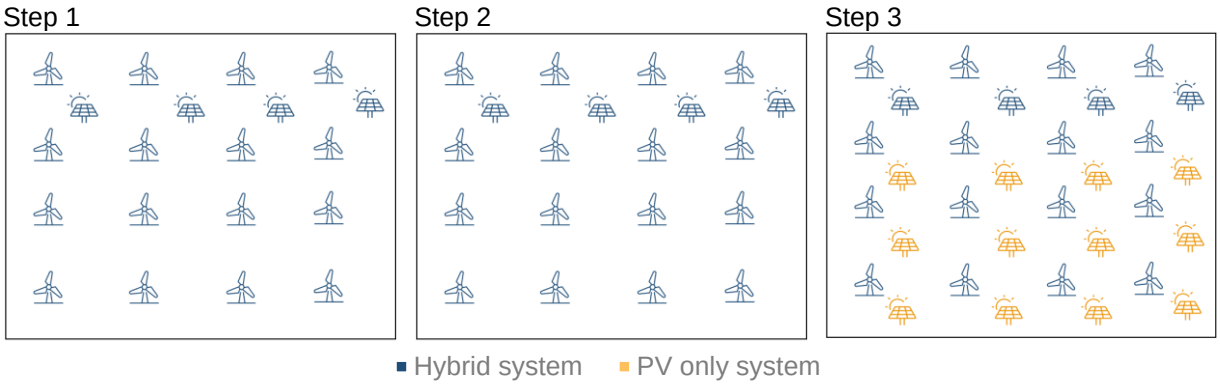

Figure 6: Cell land allocation process

When allocating land for a hybrid system, the ratio between the land requirements of each system component must be kept to maintain the ratio of their installed capacities. In the hybrid scenario exemplified in Table 3, the ratio between onshore wind and PV is approximately 4:1. Before upscaling the configured system, the limiting system upscaling component was determined. That is, the system component with lower upscaling possibility, given its land requirements and land availability. In cases where land availability was equal for both PV and onshore wind, the limiting component was always the one with the larger land requirements. When land availability was not equal for both RES, the limiting system upscaling determinator was subjected to change.

The first step in Figure 6 illustrates the ratio of the hybrid system, where onshore wind installations cover all eligible land and PV installations cover only 25% of it to maintain the ratio. The next scenario in the allocation process was of onshore wind only. However, as the eligible land for this technology was fully utilized in the first step, no additional land was allocated. In the third step, the remaining land for PV installation was fully allocated for the PV-only system. The land allocation results are presented in Table 4.

Table 4: Cell land allocation and system upscaling results

Step	System configuration scenario	LCOH (€/kg)	Land (km²)						No. of systems/ kg H_2 per hour
			Available		Allocated		Remaining		
			PV	Wind	PV	Wind	PV	Wind	
1	Hybrid	7.22	3,653	3,653	932	3,653	2,720	0	245,845
2	Onshore wind only	7.64	2,720	0	0	0	2,720	0	0
3	PV only	11.11	2,720	0	2,720	0	0	0	192,913
								Total	438,758

In each step of the allocation process, the allocated land is calculated, and subsequently, the remaining eligible land feeds into the following step, as highlighted in Table 4. The number of systems that fit into the eligible land is the equivalent of the hourly hydrogen production potential, considering the system was designed to fulfill a demand of 1 kg of hydrogen per hour. In the example above, the total hydrogen potential in the cell was estimated at 439 tons per hour. Yearly potentials were calculated by multiplying the hourly potentials by the number of hours in 2020. Furthermore, as over-costly hydrogen potentials are less or completely irrelevant, the output structure maintained the disaggregation of the three LCOH levels per cell, allowing for costly potentials to be filtered in a later stage.

The land allocation and hydrogen potentials process was scripted in SQL, and the results were saved into the FfE database. In accordance with the different LE and PD scenarios, hydrogen potentials were calculated for each combination of the two. The scripts and database table structure are presented in Appendix 7.1.2.2.

Finally, the aggregation of hydrogen potentials with respect to their costs provided the green hydrogen cost-potential curve. This work aimed not only to paint the global picture of the green hydrogen landscape but also to provide insights into the geographic distribution of hydrogen potentials and enable analysis at a country or region level. To achieve these goals, an interactive dashboard that provides analysis flexibility was created. The author hopes that this form of communicating the results will benefit various users and decision-makers. The interactive dashboard was created using Tableau, a business intelligence tool that provides an online platform for publicly sharing data visualizations (Tableau, 2023).

4 Results and Discussion

In the following chapter, the results are presented and discussed with respect to the three research questions posed by this thesis. The discussion corresponds to the order of the working steps taken in this work, starting with the systematic literature review to define the LE for global hydrogen analysis. Then, the results of the applied LE are examined, and finally, the global hydrogen costs and potentials are discussed.

4.1 Systematic Literature Review of Green Hydrogen Land Eligibility

This part discusses the results of the systematic review literature related to green hydrogen LE and site selection, which defined the LE applied in this work. The results are analyzed to identify general green hydrogen LE trends and to pinpoint the most important criteria to be considered in this global analysis. Selected criteria are then analyzed in depth for the purpose of their application in this work.

4.1.1 Criteria Identification

The systematic literature review included 27 publications, of which 22 were peer-reviewed articles, and another five were classified as reports or gray literature. See Appendix 7.2.1.1 for the full list of publications. The review considered only studies focusing on hydrogen powered by solar PV or onshore wind (or a combination of both). However, some publications included additional RES. A total of 15 publications included both solar and wind energies, while seven included solar and five included wind exclusively. In terms of geographic focus, five publications had a global scope, four publications dealt with a large-scale region such as MENA or Europe, and the remaining 18 publications studied a country or a region within a country. Interestingly, 33% of publications were affiliated with a German institute. A detailed geographic distribution of the publications can be seen in Figure 7.

As Müller et al. (2023, p. 2) pointed out, the application of GIS is needed to deal with the complex considerations of hydrogen infrastructure planning. This was evident in this review, as 17 of the 27 publications used GIS in their site selection methodologies. Moreover, when GIS was not used, studies often emphasize this limitation and importance of GIS (Almutairi, 2022, p. 5892; Bhandari, 2022, p. 810; Y. Wu, Deng, et al., 2021, p. 15).

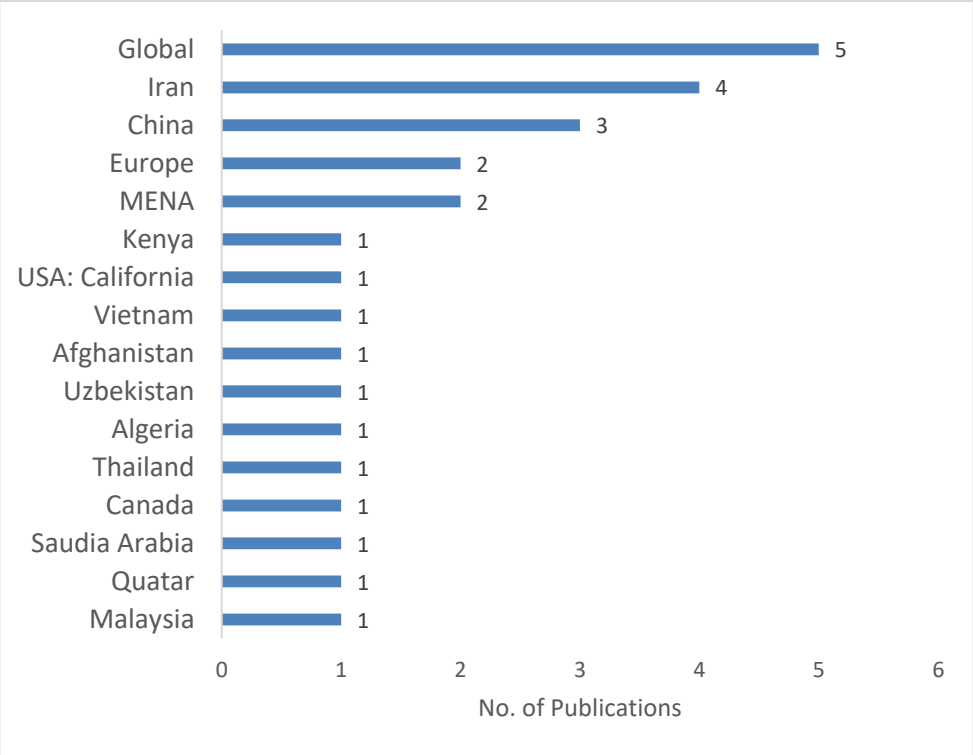

Figure 7: Geographic scope of publications

When reviewing the publications, all criteria that indicated (un)suitability of locations for hydrogen production were collected and summarized in a tabular form. As explained in 2.3, criteria are usually divided into exclusion criteria (EC) and assessment criteria (AC). Some publications included one type of criteria, and some included both. While some reviews in the field of RES separated the two types when collecting data and discussing the results (Spyridonidou & Vagiona, 2020, 2023), others grouped them together (Rediske et al., 2019; Ryberg et al., 2017). Due to the rather small sample of publications, this work followed the latter approach. Furthermore, as the phrasing of criteria differed across studies, they were generalized as much as possible to provide an insightful aggregation (Ryberg et al., 2017, p. 5). Criteria that had only one record were grouped under Other.

The summary of criteria is presented in Table 5, where the criteria are ordered by their importance, no.1 being the most important. The importance is based on the distinct number of publications (NP) that mentioned these criteria. A distinct count is used as some criteria appeared more than once within a study (e.g., as an EC and AC or in different variations of the same criteria, like different types of land use or land cover). Nonetheless, the frequency of occurrence (FO) is also presented, accounting for all types and variations in which the criteria were applied. The EC with limits column indicates whether the criteria were used with a lower limit (LL), i.e.,

values lower than the LL were excluded, or with an upper limit (UL), i.e., values greater than the UL were excluded. For land cover and land use, the class to be excluded was usually specified, e.g., forest or cropland. Additional information is provided for certain criteria regarding the indicator used to evaluate them. For instance, water availability can be measured by regional water stress or by the distance to a water source. For clarification, in criteria where a distance indicator was used with an LL, the exclusion also refers to the area where the distance is measured from, e.g., a protected area. The AC preference column indicates the more suitable values of the criteria. For example, lower slope values are preferable. It is possible that a criterion had both LL and UL or both low and high preferences. For example, the proximity to road networks was considered desirable. However, it was recommended to keep a certain buffer.

In total, 41 general criteria were identified (including the "Other" criterion). Similar results can be seen in RES LE literature. In a systematic review of wind turbine siting, Spyridonidou and Vagiona (2020) identified 28 EC for onshore wind. Ryberg et al. (2017) reviewed 50 LE studies of various RES technologies, and Rediske et al. (2019) reviewed determinant factors for PV site selection projects; both studies listed 28 criteria as well. On the other hand, Spyridonidou and Vagiona (2023) reviewed PV siting studies and identified 83 EC. The variation in the number of criteria can be the result of the level of criteria generalization. The higher the level of generalization, the smaller the list of criteria. It is worth mentioning that the generalization and aggregation of criteria might cause a discrepancy between the number of criteria used in a publication as recorded in this review and the number of criteria specified at the source.

When comparing the results of this review to other reviews in the RES LE field, naturally, there were many similarities as green hydrogen is generated using RES. Few studies made a clear distinction between criteria related to RE plant or hydrogen plant requirements. For instance, Pfennig et al. (2023) divided the EC into general EC and PtX-related EC. However, most studies categorized criteria into technical, physical, environmental, and socioeconomic groups, often making it challenging or impossible to distinguish whether a criterion was hydrogen-related without further details.

Table 5: Criteria for green hydrogen land eligibility and site selection

No.	Criteria	NP	FO	EC with limits	AC preference	NP	FO
1	Land Cover & Land Use	16	67	Class + Distance LL	Class	14	49
				Class + Utilization Factor UL	Class	3	15
				Suitability Score	Class	1	3
2	Road Network	15	21	Distance LL	Far	8	9
				Distance UL	Near	12	12
3	Water Availability	13	19	Distance UL	Near	9	10
				Water Stress UL	Low	3	5
				Precipitation LL	High	3	3
				Water Potential[10] LL	High	1	1
4	Slope of Terrain	13	16	UL	Low	13	16
5	Protected Areas	12	21	Distance LL	Far	12	21
6	Elevation	11	13	Height above sea level LL	High	2	2
				Height above sea level UL	Low	9	11
7	Wind Energy Potential[11]	11	17	LL	High	11	17
8	Population Density	10	10	LL	High	7	7
				UL	Low	3	3
9	Settlement Areas	10	19	Distance LL	Far	10	14
				Distance UL	Near	4	5
10	Solar Energy Potential[12]	8	8	LL	High	8	8
11	Electricity Grid	7	10	Distance LL	Far	4	4
				Distance UL	Near	6	6
12	Public Support	7	7	LL	High	7	7
13	Other	6	8	Various	-	5	8
14	Hydrogen Production Potential	5	5	LL	High	5	5
15	Gas Pipelines	4	5	Distance LL	Far	2	2
				Distance UL	Near	2	2
				Other	-	1	1
16	Railway Network	4	6	Distance LL	Far	4	4
				Distance UL	Near	2	2
17	Air Emissions Reduction Potential	4	5	LL	High	4	5
18	Employment Potential	4	4	LL	High	4	4
19	Skilled Labor & Knowledge Base	4	5	LL	High	4	5
20	Refineries	4	5	No. of Refineries LL	High	4	5
				Distance UL	Near		
21	Ecological Impact	4	5	UL	Low	4	5

[10] "Water potential was calculated using the formula Wp = L/A, where L is the total length of water resources and A is the area of the province" Mostafaeipour, Dehshiri, et al. (2020).
[11] Relevant for wind energy only
[12] Relevant for solar energy only

No.	Criteria	NP	FO	EC with limits	AC preference	NP	FO
22	Local Electricity/Hydrogen Demand	5	5	LL	High	5	5
23	Logistics & Infrastructure	4	9	LL Distance UL	High Near	3 1	8 1
24	Size of Consumption Area	4	4	UL	Low	4	4
25	Average Air Temperature	3	3	UL	Low	3	3
26	Archeological, Historical, Religion and Cultural Heritage Sites	3	5	Distance LL	Far	3	5
27	Relative/Average Humidity[12]	3	3	UL	Low	3	3
28	Other Political & Institutional Conditions	3	6	Various	-	3	6
29	Climate Hazard Zones	3	3	Distance LL Probability UL	High Low	3	3
30	Hours of Sunlight[12]	3	3	LL	High	3	3
31	Government Support	3	3	LL	High	3	3
32	Other Socioeconomic Conditions	3	4	Various	-	3	4
33	Other Financial and Market Conditions	2	6	Various	-	2	6
34	Rate of Industrial Development	2	2	LL	High	2	2
35	Ports	2	2	Distance UL No. of Ports LL	Near High	1 1	1 1
36	Precipitation[12]	2	2	UL	Low	2	2
37	Daily Dust[12]	2	2	UL	Low	2	2
38	Net Renewable Energy Potential	2	3	LL	High	2	3
39	Minimum Required Contiguous Area	2	2	LL	High	2	2
40	LCOE/LCOH	2	4	UL	Low	2	4
41	Noise Impact	2	2	UL	Low	2	2

In general, it was noted that criteria related to the physical attributes of the land, such as topography and land cover, were mostly related to PV or wind turbines, which is reasonable considering these have larger spatial requirements. The only physical attribute associated with the electrolysis process was the additional distance from marine protected areas, which is needed due to the repercussions of water desalination in coastal areas. Nonetheless, some criteria were unique to hydrogen LE. A prominent example was water availability, as water is an integral component in hydrogen production (IRENA, 2022, p. 8). Other unique hydrogen criteria are access to gas pipelines, number of refineries, access to ports, and local hydrogen demand. The

vast majority of studies included not only technical and economic criteria but also socio-political criteria. However, the latter group was mostly used as AC rather than EC. Compared to RES literature, socio-political criteria had slightly more presence in the reviewed hydrogen studies. Nonetheless, these criteria are discussed in greater detail in 4.1.3.

The most important criteria identified in this study were very similar to those in RES LR. Rediske et al. (2019) found that the detrimental factors for PV site selection were, in order of importance, solar radiation, distance to transmission lines, slope, distance to roads, distance from urban areas, and land use. Spyridonidou and Vagiona (2023) found that the most recorded EC in PV siting were the distance from urban areas, distance from water surfaces, distance from protected areas, slope, and distance to roads. With regard to onshore wind siting, Spyridonidou and Vagiona (2020) had a similar result to the aforementioned study, with the exception of aviation areas, which had more records than water surfaces. Many local hydrogen studies in this review ranked the most important criteria using methodologies such as stepwise weight assessment ratio analysis (SWARA). For instance, S. J. H. Dehshiri and Zanjirchi (2022, p. 13374) found that the most important AC were wind speed, the number of refineries in a region, and the rate of industrial development. Y. Wu, Deng, et al. (2021, p. 15) mentioned that the wights given to criteria are subject to the geographic scope of a study, which aligns with the findings of this review, as local studies tended to have a different set of priorities in comparison to this global analysis.

The three inconsistencies in LE literature detected by Ryberg et al. (2017), i.e., ”the inconsistent use of datasets, inconsistent methodologies and inconsistent criteria definitions”, were very much present in this review as well. In the application of LE as part of this study, it was evident that the choice of dataset, its data integrity and its spatial resolution had an impact on the results. Criteria definitions tended to vary most significantly across studies. Nonetheless, Spyridonidou and Vagiona (2023, p. 2954) pointed out that EC definitions are subjected to many factors, such as climatic conditions, laws and policies, data availability and the objective of the site selection process. Considering this, it should be mentioned that when conducting a global LE analysis, criteria definitions are unlikely to fit national or local requirements everywhere. Therefore, the results in this study and other global studies should be interoperated with caution and not considered precise estimations. Ryberg et al. (2017, p. 4) also pointed out that oftentimes, LE methodologies are not explained in detail or not at all, and this review echoes that. For example, in some cases, there were no sources or reasoning for determining a certain threshold for an EC. Ryberg et al. (2017, p. 4) also expressed that all LE researchers must rely on their own judgment

at some point in the process, and the same was true in this work. This emphasizes the need for further green hydrogen LE research and the development of international policies and guidelines for large-scale hydrogen projects.

The average number of criteria used by studies in this review was eight, as well as the mode value, while the minimal number was two and the maximal was 14. The average number of criteria noted by Spyridonidou and Vagiona (2023, p. 2954) was eight as well. Nonetheless, Spyridonidou and Vagiona (2023, p. 2972) conclude that a higher number of EC is advisable for future planning, as well as stricter exclusion limits. They further explain that while this approach will downsize suitable areas, it has the potential to increase environmental sustainability and social acceptance of projects. Considering this, it was decided to apply the eight most important criteria in this work, as these criteria are rather generalized and extensive. While solar and wind energy potential ranked high in their importance, they were excluded from the list to be applied in this work, as areas with insufficient energy potentials had unattractive LCOH that was eliminated in the later stages of this work. Therefore, EC no.7 was not included, and EC no.9 took its place. Furthermore, in line with the recommendation of Spyridonidou and Vagiona (2023), a more restrictive approach was used when defining the criteria for the LE in this work in the hope of fostering sustainable hydrogen production. In the following section, the eight selected criteria are discussed in the context of the scope of this work. The criteria definitions across studies are compared with the goal of finding the appropriate criteria definitions for this global hydrogen LE.

4.1.2 Criteria Analysis and Definition

EC no. 1: Land Cover and Land Use

The terminology and level of detail in criteria definition varied across studies. While there is a difference between land use and land change, some studies made the distinction between the two, and others used the terms interchangeably. It was therefore decided to aggrege the two into one general criterion. Furthermore, some studies listed the different classes of land cover and land use (e.g., water bodies), while others noted a general criterion named land cover and/or land use. To examine which classes of land cover and land use are typically excluded, a disaggregated list of land cover and land use classification is presented in Table 6. The terminology used here is also somewhat aggregated. When no classification was mentioned, a general land use class was used. In some cases, the different land use and land cover classes were excluded with a certain

buffer area or a utilization factor. Therefore, each class was further examined from that perspective.

Table 6: Land cover and land classes considered in green hydrogen land eligibility

Land cover and land use classes	NP
Water Bodies	10
Forest, Woodlands and Tree Regions	6
Agricultural Land and Cropland	6
Aviation Areas	5
Land Use	5
Built-up Areas and Industrial Zones	4
Barren	3
Wetlands	3
Snow-Covered and Permafrost Areas	3
Grassland	2
Scrubland	2
Military Zone	2
Other	6

The exclusion of **water bodies** was the most frequent, with 10 records, from which six publications included buffer zones ranging from 100 to 1000 meters. The different buffer values are presented in Table 7 according to the underlying RES for hydrogen, as well as values recommended by RES literature reviews (N/A was marked when the entry was not relevant for one of the RES). In global studies, a buffer zone from water bodies was not applied or applied to a small extent. Local studies, on the other hand, took a stricter approach. It was generally observed that a buffer zone of 400-500 was often used in local studies, both for PV and onshore wind. These values were aligned with the recommendations of RES literature reviews like Spyridonidou and Vagiona (2020) and Ryberg et al. (2017). A buffer zone of 400 meters was therefore selected for both PV and onshore wind.

After water bodies, **forests** and agricultural land had the most records. Only one study (Okunlola et al., 2022) used a distance of 1km from forests both for PV and onshore wind. The mode value in both onshore wind and PV reviews (Spyridonidou & Vagiona, 2020, 2023) was zero distance. Only one study did not exclude forests for onshore wind completely but applied a utilization factor of 15% (Lux et al., 2021, p. 4). Based on these findings, forests were excluded completely for both PV and onshore wind without an additional buffer zone.

Table 7: Distances from water bodies in the reviewed studies

Type	Publication	Criteria in source	Distance (meters)	
			PV	Onshore Wind
Global & Regional	Agora Energiewende and AFRY Management Consulting (2021)	Water bodies	-	-
	Franzmann et al. (2023)	Coasts	100	100
		Creeks	100	0
		Lakes	100	100
		Rivers	0	100
		Water surface	100	100
	Lux et al. (2021)	Water bodies	0	0
	Pfennig et al. (2023)	Land use: water bodies	0	0
Local	Ali et al. (2022)	Distance to Water Bodies & Ways (km) Lower Limit	500	0
	Messaoudi et al. (2019)	Water Bodies and Waterways	N/A	1000
	Mostafaeipour et al. (2020)	Rivers	N/A	400
	Okunlola et al. (2022)	Water bodies (rivers, streams, lakes, and encroaching coastal waters)	500	500
	Wang et al. (2019)	Water head	-	-
	Wu, He, et al. (2021)	Water area	N/A	500
PV/Wind Literature Review	Spyridonidou and Vagiona (2020)	Water surfaces	N/A	400
	Spyridonidou and Vagiona (2023)	Distance from Water Surfaces	0	N/A
	Ryberg et al. (2017)	Water Bodies	300	300
		Water Bodies: Lakes	400	400
		Water Bodies: Rivers	200	200
		Water Bodies: Coast	1000	1000

Concerning **agricultural land**, a distinction was made between PV and wind in some of the studies. According to IRENA (2022, p. 17), onshore wind turbines can be installed on agricultural land with little impact on crops, while PV installations can cause harm. Accordingly, the study excluded cropland for PV installations only. Nonetheless, IRENA (2022, p. 17) differentiated between land covered with 100% cropland and land covered between 40% to 60% cropland, also referred to as a "cropland natural" class. A utilization factor of 40% was used for the latter. On the other hand, Lux et al. (2021, p. 4) excluded "cropland natural" completely, both for onshore wind and PV, and applied a 30% utilization factor for onshore wind in regular cropland. Furthermore, Ali et al. (2022, p. 6) defined agricultural land as moderately suitable for the installation of PV. While PV installation is theoretically possible in combination with certain crops and the appropriate technology (Fraunhofer ISE, 2020 as cited in IRENA, 2022, p.17), applying this approach in a global LE analysis is complex (IRENA, 2022, p. 17).

Spyridonidou and Vagiona (2023, p. 2958) recorded 42 studies (51% of their reviewed studies) that excluded agricultural land and cropland for PV. While they noted that several studies applied utilization factors for certain agricultural land and crop classes, they did not specify how many studies and what utilization factors were applied to which cropland. They further mentioned that in international literature, most reviewed studies excluded all types of crops (Spyridonidou & Vagiona, 2023, p. 2954). For onshore wind, Spyridonidou and Vagiona (2020, p. 7) recorded nine studies (32% of their reviewed studies) that excluded cropland. No additional recommendations supporting installing onshore wind or PV on agricultural land were identified in the reviewed literature. It was therefore decided to exclude any type of cropland for both RES technologies. Moreover, in both reviews (Spyridonidou & Vagiona, 2020, 2023), it was predominant that studies did not use any buffer distance from croplands, and no buffers were recorded in this review as well. Following this, no buffer zones were used in this analysis. Nonetheless, it is recommended that the co-existence of green hydrogen production with agriculture be further examined.

Aviation areas were excluded by five studies. One was a global study (Franzmann et al., 2023) that excluded aviation areas for onshore wind with a distance of 4 km for large airports and 1.5 km for small airports. No additional distance was applied for PV sites. Three local studies excluded aviation areas for onshore wind as well, using different buffers of 1 km (Okunlola et al., 2022, p. 5), 3 km (S. S. H. Dehshiri & Dehshiri, 2022, p. 24576), and 3.5 km (Mostafaeipour, Dehshiri, et al., 2020, p. 33176). Only one local study used a buffer distance from PV sites of 100 m (Okunlola et al., 2022, p. 5). One local study (Almutairi, 2022, p. 5886) used the number of airports in a region as an indicator that has a negative impact on suitability for wind farms. Similar to the findings of this literature review, Spyridonidou and Vagiona (2020, p. 7) identified 22 onshore wind studies that used this criterion with a mode value of 2.5 km and 3 km. Spyridonidou and Vagiona (2023, p. 2958) showed a more restrictive trend in PV siting, where they identified nine studies with a mode value of a 3 km buffer zone. As the sample size of Spyridonidou and Vagiona (2020; 2023) was significantly higher than the sample of this work, it was decided to follow their recommendations for both RES, applying a buffer zone of 3km from aviation areas.

Military zones were excluded with a buffer zone of 400 meters from wind sites and no buffer from PV sites, following the criterion definition of Franzmann et al. (2023) that applied this EC globally.

The class of **built-up areas and industrial zones** was recorded only four times. However, as seen in Table 5, criteria no. 9 refers to **settlement areas** that can also fall under the "built-up" category, depending on the definition. For clarification, when a record used the term "built-up areas" or a description of an economic activity area, it was recorded under built-up areas and industrial zones land use class. When settlement types were used to describe a criterion, they were recorded under settlement areas. From the perspective of this work, built-up areas are equivalent to settlement areas. For this criterion's definition, the latter's records were examined. Regarding buffer zones, some studies separated urban and rural settlements, where turban areas were typically excluded with lower buffer distances. For simplicity, this analysis will not discuss rural settlements. For urban/residential settlements, two global studies (Franzmann et al., 2023; Pfennig et al., 2023) applied a buffer zone of 1km for onshore wind, while only one global study (Pfennig et al., 2023) applied the same buffer zone for PV. IRENA (2022) applied no buffer zone for both PV and onshore wind. Spyridonidou and Vagiona (2023) found that the mode value of 71 studies of PV siting was zero. Accordingly, it was decided to apply a 1 km buffer zone for wind turbines and no buffer zone for PV sites.

Wetlands were excluded completely in four studies (Franzmann et al., 2023; IRENA, 2022; Lux et al., 2021; Okunlola et al., 2022), and **snow-covered and permafrost areas** were excluded entirely in three studies (Franzmann et al., 2023; Okunlola et al., 2022; Pfennig et al., 2023), while one study (Lux et al., 2021) applied a utilization factor of 12% for wind and 40% for PV. While these land cover classes do not pose a significant siting obstacle, they store carbon that can be released into the atmosphere due to construction and thus threaten the surrounding ecosystem (Okunlola et al., 2022, p. 11). As such, both classes were excluded completely in this work without an additional buffer zone.

When considering barren land, grassland, scrubland, savanna, and low vegetation, they were excluded by only two studies; however, they were excluded with a utilization factor. A similar trend was observed in the literature reviews of Spyridonidou and Vagiona (2020; 2023). The utilization factor applied by the studies can be seen in Table 8.

Table 8: Land cover utilization factors

Class	Onshore Wind		PV	
	Lux et al. (2021)	MENA-Fuels (2022)	Lux et al. (2021)	MENA-Fuels (2022)
Barren	40%	33%	16%	33%
Grassland	30%	33%	20%	33%
Low Vegetation		33%		33%
Savanna	30%		20%	
Scrubland	30%	33%	20%	33%

According to Lux et al. (2021, p. 5), RES potentials are highly sensitive to utilization factors, which vary greatly across studies. They also pointed out that the MENA region has a significant percentage of barren land that can substantially restrict hydrogen potentials. For instance, Egypt, Libya, and Algeria are covered by up to 80% barren land. On the other hand, Ali et al. (2022, p. 6) classify barren land as highly suitable for solar-based green hydrogen, and Mostafaeipour, Dehshiri, et al. (2020, p. 33176) recommended wind-based hydrogen plants to be placed on grasslands, forbs, low shrubs, rangelands, dry farms or land covered with rock, soil, or sand. Based on these findings and considering the increased complexity associated with incorporating utilization factors in this analysis, the choice was made to include 100% of these land cover classes. However, it is recommended that further research be done on the suitability of these classes for hydrogen production.

Regarding data sources, Pfennig et al. (2023, p. 5) identified a land cover data set provided by the Copernicus Climate Change Service, Climate Data Store (2019). This is a raster dataset with a 1 km² spatial resolution that categorizes the world into 22 classes, aligned with definitions of the United Nations Food and Agriculture Organization's (UN FAO) Land Cover Classification System (LCCS). The 22 classes were also categorized according to the Intergovernmental Panel on Climate Change (IPCC) land categories for change detection (Defourny et al., 2021, p. 15), as shown in Table 9. The same aggregation was used in this analysis for categories 1-5, while water bodies and permanent snow and ice remained independent categories. Furthermore, aviation areas and military zones were excluded based on data from OpenStreetMap (2023a) and OpenStreetMap (2023c), respectively.

Table 9: Correspondence between the IPCC land categories used for the change detection and the LCCS legend used in the LC classes. Source: Defourny et al. (2021)

IPCC Classes considered for the change detection		IPCC Classes considered for the change detection LCCS legend used in the CCI-LC maps	
1. Agriculture		10, 11, 12	Rainfed cropland
		20	Irrigated cropland
		30	Mosaic cropland (>50%) / natural vegetation (tree, shrub, herbaceous cover) (<50%)
		40	Mosaic natural vegetation (tree, shrub, herbaceous cover) (>50%) / cropland (< 50%)
2. Forest		50	Tree cover, broadleaved, evergreen, closed to open (>15%)
		60, 61, 62	Tree cover, broadleaved, deciduous, closed to open (> 15%)
		70, 71, 72	Tree cover, needleleaved, evergreen, closed to open (>15%)
		80, 81,82	Tree cover, needleleaved, deciduous, closed to open (>15%)
		90	Tree cover, mixed leaf type (broadleaved and needleleaved)
		100	Mosaic tree and shrub (>50%) / herbaceous cover (< 50%)
		160	Tree cover, flooded, fresh or brackish water
		170	Tree cover, flooded, saline water
3. Grassland		110	Mosaic herbaceous cover (>50%) / tree and shrub (<50%)
		130	Grassland
4. Wetland		180	Shrub or herbaceous cover, flooded, fresh-saline or brackish water
5. Settlement		190	Urban
6. Other	Shrubland	120,121,122	Shrubland
	Sparse	140	Lichens and mosses
	vegetation	150, 151, 152,153	Sparse vegetation (tree, shrub, herbaceous cover)
	Bare area	200,201,202	Bare areas
	Water	210	Water
	Ice	220	Permanent snow and ice

In addition to the croplands identified in the data set above, Pfennig et al. (2023, p. 7) used the Global Food Security-Support Analysis Data (GFSAD) dataset (Teluguntla et al., 2016) to ensure the exclusion of croplands. This dataset is a global 1 km² raster data that classifies five different types of croplands and a non-cropland category. The same approach was also applied in this work, where all types of croplands were excluded.

EC no. 2: Road Network

The distance to a road network was the second most important criterion and had both LL and UL records. The LL distance from roads was recommended due to safety reasons (Ryberg et al. 2017,

p.5; Wu et al., 2021, p.5) and equipment protection reasons (S. S. H. Dehshiri & Dehshiri, 2022, p. 24575). The distances taken from roads by different studies are presented in Figure 8.

a)

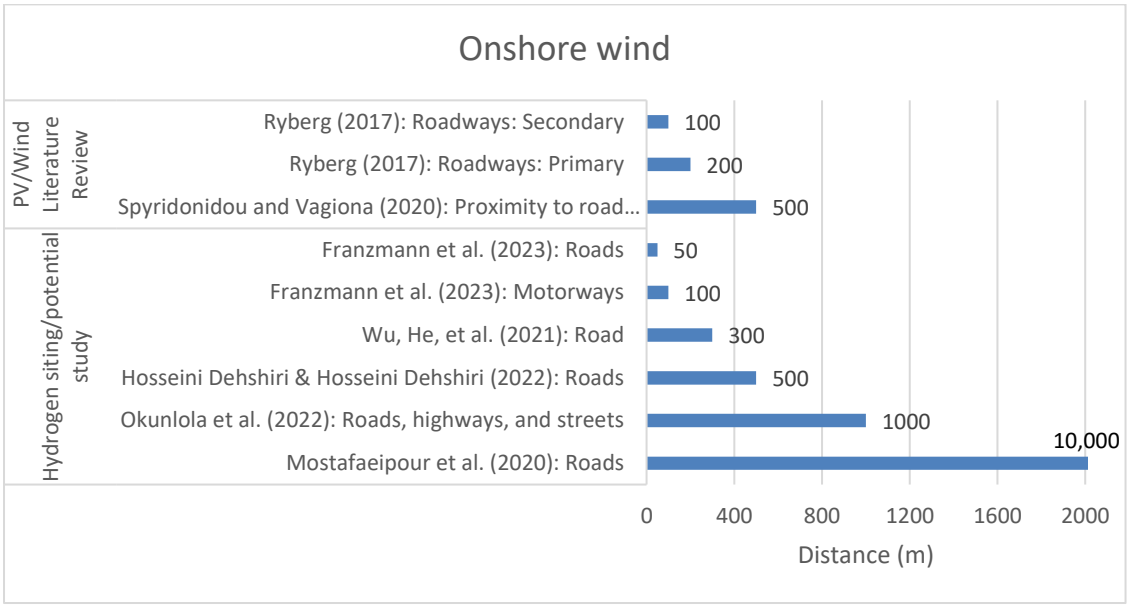

b)

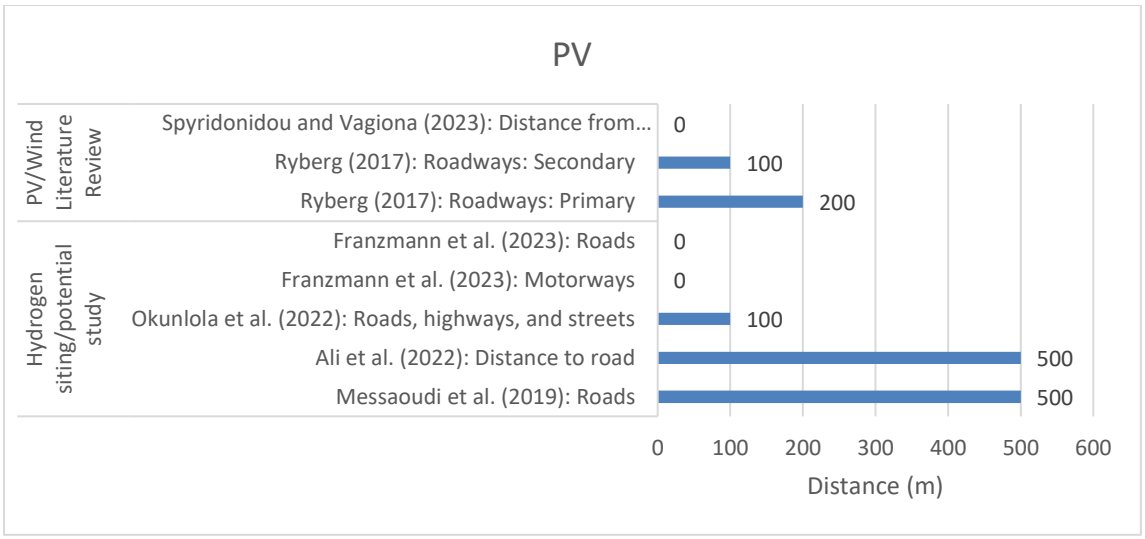

Figure 8: Distance from Road Network LL, (a) Onshore wind, (b) PV

Only one global study (Franzmann et al., 2023) applied this criterion for onshore wind while distinguishing between roads and motorways. This distinction is based on the work of Ryberg et al. (2017), which used the OpenStreetMap (2023e) database. This database provides data on roadways and their classification (OpenStreetMap, 2023b). This study followed the categorization made by Ryberg et al. (2017, p.30) that classified motorway, trunk, and primary ways as primary roads and secondary and tertiary ways as secondary roads. Distances from onshore wind sites were generally higher than those from PV sites. It was decided to use a 500

meters distance from onshore wind sites to primary roads and 250 meters to secondary roads. Franzmann et al. (2023) applied no distance between roads and PV sites, and the literature review by Spyridonidou and Vagiona (2023) also showed a mode value of zero distance. Nonetheless, it was decided to apply a minimal safety distance of 100 meters for primary roads and 50 meters for secondary roads. It is worth mentioning that the data is provided in a line geometry type without any information on the width of roads. Therefore, a minimal buffer must be considered for the road itself.

The accessibility to a road network, i.e., the UL distance from roads, was even more important, as expressed in 12 local studies. This criterion was important from an economic perspective, as longer transportation distances or lack of transportation infrastructure could increase costs (Ali et al., 2022, p. 5; IRENA, 2022, p. 40). No global study applied this criterion; however, IRENA (2022, p. 40) addressed this limitation. They pointed out that while remote areas have attractive hydrogen prices, investing in infrastructure construction (when feasible) would significantly increase the overall costs. Breitschopf et al. (2022, p. 21) stated that already established infrastructure is key for developing hydrogen markets. While the study does not use the UL distance to roads as an EC, it extensively assessed a country's infrastructure system based on many other indicators. In a Canadian study, Okunlola et al. (2022, p. 18) noted that a lack of infrastructure-related EC can lead to overestimations of hydrogen potentials and, consequently, misleading guidance for decision-makers. Considering these, it was decided that this EC is critical to apply in this work. It is worth noting that incomplete data can lead to excess land exclusion. Therefore, it is recommended to evaluate these EC on a smaller geographic scope, using a dataset with a higher level of accuracy.

Most local studies used this criterion as an AC rather than an EC; however, Ali et al. (2022, p. 6) and S. S. H. Dehshiri and Dehshiri (2022, p. 24575) considered sites with no roads in a proximity of 10km not suitable, and Mah et al. (2022, p. 399) used a stricter threshold of 3km. As these studies aimed to identify optimal site locations in a local context, such low thresholds are not suitable for a global analysis. In their RES LE literature review, Ryberg et al. (2017, p.8) found that a typical exclusion threshold was 5km, while a low threshold was 45km. In further research that was not in the framework of this systematic literature review, it was found that Hank et al. (2023, p. 18) evaluated hydrogen's cost and potentials (among other PtX products) in 12 countries around the globe and excluded land without roads in the proximity of 100km. As this threshold was considered appropriate for a global analysis, it was decided to follow the work of Hank et al. (2023).

EC no. 3: Water Availability

As water is needed for the electrolysis process, its availability is crucial. As shown in Table 5, 13 studies mentioned this criterion; however, it was evaluated in various ways. The proximity to a water source was most frequently used as an indicator. Of the nine studies that used this indicator, only three mentioned a distance threshold for exclusion. Pfennig et al. (2023, p. 5) excluded areas without water sources in the proximity of 50km (inland or coastal), as desalinated water is also adequate for electrolysis. IRENA (2022, p. 16) followed the aforementioned study and used the same threshold. On the other hand, Ali et al. (2022, p. 16) used a much lower threshold of 5 km to reduce water transport costs. Nonetheless, according to Müller et al. (2023, p. 6), water costs, including its transportation costs, have a minor impact on the total LCOH. Furthermore, water transport costs are mostly driven by the vertical distance rather than the horizontal distance (Kally & Fishelson, 1993 as cited in Zhou & Tol, 2005). However, evaluating the vertical distance is out of the scope of this work.

Jones et al. (2019, p. 1346) researched the global brine production distribution and found that roughly 80% is produced within 10 km of the coastline and an additional 5% within 50km. Only 15% are produced in greater distances than 50km. Their findings supports the threshold of 50km distance from hydrogen production sites to the coastline used by Pfennig et al. (2023, p. 5). Therefore, this study followed their approach; however, this approach was expanded. Any cell that overlapped with the 50km buffer from water sources was included entirely. This expansion is based on the assumption that the water source does not need to reach all the areas of the cell where RE technologies are installed. However, further consideration should be given to the distance from the RES site to the electrolysis site in the future, and the maximal distance possible between the two sites should be evaluated. It is worth mentioning that in this analysis, no consideration was given to countries' sovereignty over inland water bodies nor their territorial sea, i.e., if the 50km buffer zone from a coast or an inland water body in country A intersected with a cell of country B, the cell was not excluded and was considered eligible from the perspective of this study.

Other studies used other indicators for water availability as well; three local studies (Almutairi, 2022; Ao Xuan et al., 2022; S. J. H. Dehshiri & Zanjirchi, 2022) used the average annual precipitation as an indicator, and three global studies used different indicators to evaluate regional water risk. All three studies used the WRI Aqueduct: Global Water Risk Indicators data set (WRI, 2023a). This data set provides 13 indicators to evaluate water risk. The indicators are

aggregated into three groups using different weights for each indicator. Lastly, the groups are combined into an overall water risk score (Kuzma et al., 2023, p. 2).

The choice of indicator varied among the studies and resulted in different levels of land exclusion. Pfennig et al. (2023, p. 5) applied the most strict approach and excluded areas where the overall water risk exceeds "Low". IRENA (2022, p. 16) used the water stress indicator, excluding areas with a "Low" threshold as well, following the approach of Fraunhofer IEE (2023). As part of the H_2 Potential Atlas (HYPAT) project, Pieton et al. (2023, p. 66) also used the water stress indicator to evaluate regional water risk; however, it was used with a higher threshold of "Medium-High". It is worth mentioning that in prior work of HYPAT, Breitschopf et al. (2022, p. 9) excluded countries with a drought risk greater than "Medium-High" if they had no coasts and less than 1,700m^3 renewable water resources per person and year. The classification of water stress and drought risk categories can be seen in Appendix 7.2.1.2. For further information, see Kuzma et al. (2023, p. 11). The three cases of exclusion were visualized in maps to evaluate the level of exclusion, as seen in Figure 9 (a-c).

It is visible that Pfennig et al. (2023) excluded more land than the other studies, while IRENA (2022) and Pieton et al. (2023) had a similar result; however, the approach taken by IRENA (2022) had a slightly higher level of exclusion, most visibly in North America. As both IRENA (2022) and Pieton et al. (2023) used the water stress indicator, it was decided to use it in this work as well. Since Pieton et al. (2023) applied a combination of criteria, the lower threshold used by IRENA (2022) was selected. The WRI Adequate data set is available from (WRI, 2023a), with further documentation provided by WRI (2023b), and additional information regarding the methodology is given by Kuzma et al. (2023).

Pfennig et al. (2023) and IRENA (2022) made a distinction between inland and coastal areas. When coastal water was available at a maximal distance of 50km, the water scarcity criterion was omitted, as desalinated water can be used. This practice was adopted in this study, applying the same expended approach as in the water proximity criteria (including entire cells when they intersected with the 50km buffer from a water source). For this criteria, the Maritime Boundaries and Exclusive Economic Zones dataset was used (Flanders Marine Institute, 2019). Nonetheless, this approach should be assessed from a sustainable development perspective as water usage might be prioritized for other sectors in water-scarce regions (Tonelli et al., 2023, p. 3) and might impact the allocation of desalinated water as well. Moreover, as the brine byproduct of desalinated water production can have severe environmental reciprocations, and brine management is costly and challenging (Jones et al., 2019, p. 1354).

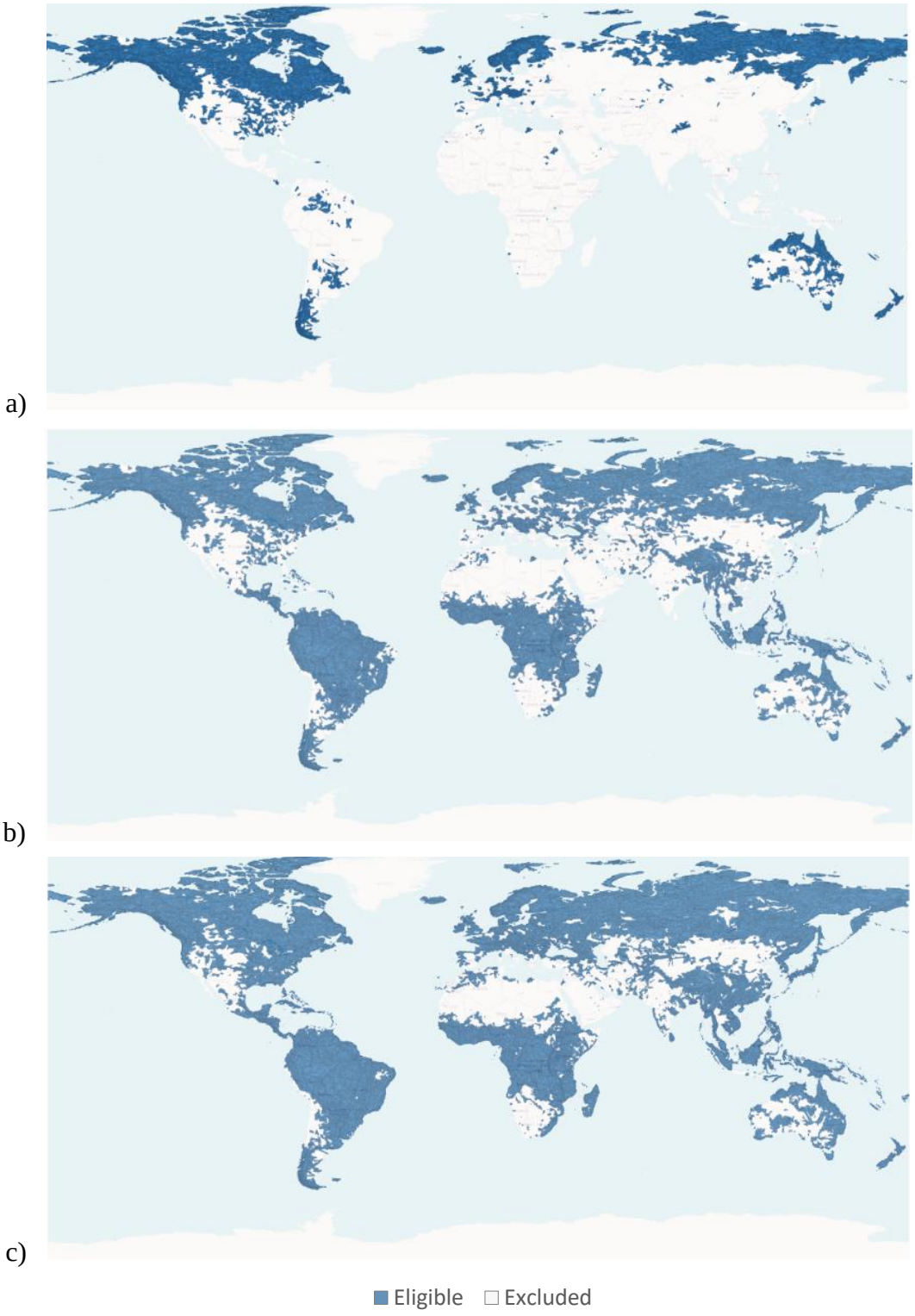

Figure 9: WRI water risk indicators as applied in reviewed studies

(a) WRI Overall water risk >"Low", as applied in Pfennig et al. (2023), (b) WRI water stress greater than “Low”, as applied in IRENA (2022), (c) WRI water stress greater than “Medium-High”, as applied by Pieton et al. (2023). Source: own work, based on data from WRI (2023a)

EC no. 4: Slope of Terrain

The slope of the terrain is a crucial factor in estimating the land suitability for both PV and wind-based hydrogen sites, as steep slopes can challenge vehicles' accessibility to the sites and increase construction costs (Ali et al., 2022, p. 8; S. S. H. Dehshiri & Dehshiri, 2022, p. 24576; Messaoudi et al., 2019, p. 31817). When it comes to the threshold of this EC, there are two variables that must be taken into account. The first is the UL of the slope gradient, and the second is the spatial resolution (SR) of the slope dataset. While a slope dataset with higher spatial resolution leads to better accuracy (Grohmann, 2015), in the context of a global analysis, accuracy might be compromised to allow faster processing of the data. Figure 10 (a-b) shows the thresholds used in global and large regional studies, including the spatial resolution (when it was available).

a)

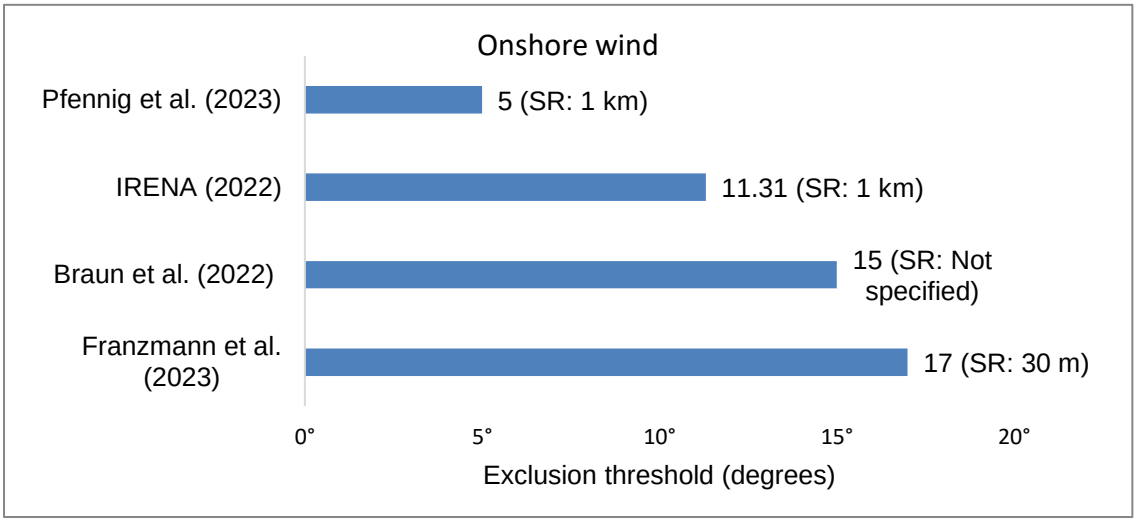

b)

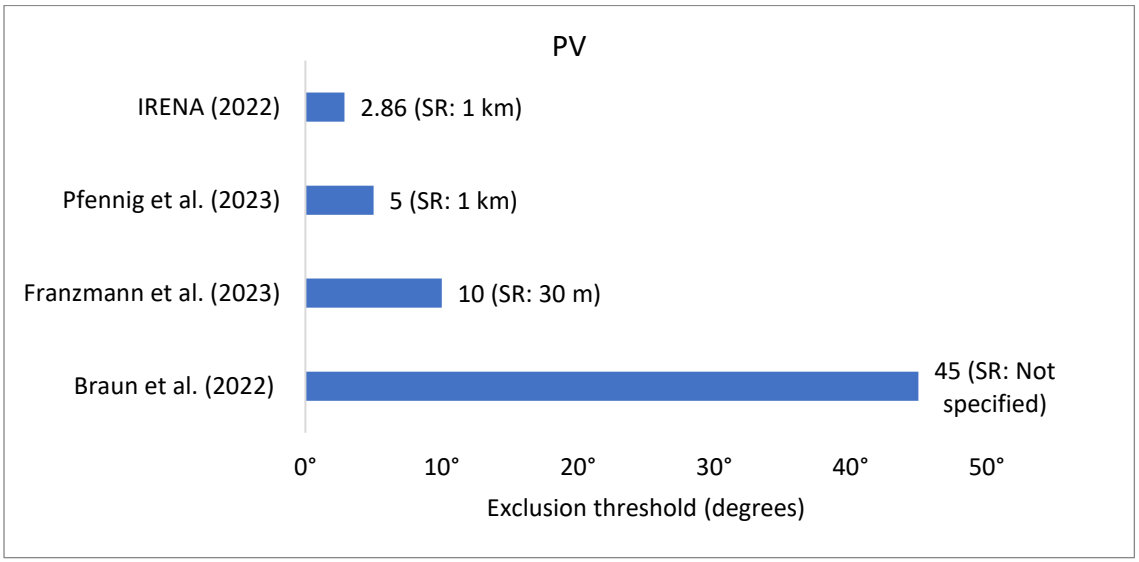

Figure 10: Slope of terrain UL. (a) Onshore wind, (b) PV

IRENA (2022) and Pfennig et al. (2023) were the only two studies that applied this EC on a complete global scale[13], and both studies used a dataset with a spatial resolution of 1km. Accordingly, the same spatial resolution was selected for this analysis to enable efficient running time. The selected dataset was based on the data used by IRENA (2022), which was developed by Amatulli et al. (2018) and is available from EarthEnv (2023). With regard to the UL of the slope gradient, the threshold for onshore wind was generally greater than for PV. Franzmann et al. (2023) applied higher thresholds in comparison to IRENA (2022) and Pfennig et al. (2023); however, they used a dataset with a higher spatial resolution. Braun et al. (2022) used an exceptionally high threshold for PV; however, no spatial resolution was indicated in their study. In their systematic review of wind site selection literature, Spyridonidou and Vagiona (2020) found that the mode value used for onshore wind was 5.71 degrees, similar to the value used by Pfennig et al. (2023). Spyridonidou and Vagiona (2023) also found that a threshold of 2.86 degrees is most frequently used for PV, as applied by IRENA (2022). Accordingly, these thresholds were applied in this study.

EC no. 5: Protected Areas

All the global and large regional studies except Braun et al. (2022) excluded protected areas to some extent. All the studies that specified their data source used the World Database on Protected Areas (WDPA) (UNEP-WCMC, 2023). Therefore, the same dataset was used in this work. This dataset includes protected areas defined by the International Union for Conservation of Nature (IUCN) and the Convention on Biological Diversity (CBD). The protected areas are classified according to the IUCN Protected Area Management Categories (UNEP-WCMC, 2019, pp. 8–10). Table 10 presents the IUCN categories that were excluded by the reviewed studies.

Breitschopf et al. (2022, p. 15) excluded only categories Ia, Ib and, II and pointed out that excluding all IUCN categories will significantly reduce hydrogen potential. They further recommend that hydrogen plant construction in protected areas be examined in the context of the specific location and ensure sufficient protection (Lattemann, 2010, as cited in Breitschopf et al., 2022). Most studies excluded all IUCN categories; thus, the same was applied in this study. While some protected areas have no IUCN category assigned to them, this does not mean they are of lesser importance, nor do they need less protection (UNEP-WCMC, 2019, p. 11). Accordingly, every protected area entry in the dataset was excluded in this work, regardless of its IUCN classification or its absence.

[13] Pfennig et al. (2023) did not include the European Economic Area

Table 10: IUCN Protected Area Management Categories excluded by reviewed studies

IUCN Protected area category	Breitschopf et al. (2022)	Franzmann et al. (2023)[14]	Heuser et al. (2020)[14]	Pfennig et al. (2023)	IRENA (2022)	Lux et al. (2021)[15]
Ia. Strict Nature Reserve	V	V	V	V	V	V
Ib. Wilderness Area	V	V	V	V	V	V
II. National Park	V	V	V	V	V	V
III. Natural Monument		V	V	V	V	V
IV. Habitat/ Species Management		V	V	V	V	V
V. Protected Landscape/ Seascape		V	V	V	V	V
VI. Managed Resource Protected Area				V	V	V

In addition to the WDPA dataset, Pfennig et al. (2023, p. 5) used another source to ensure the quality of this criteria: the Global Critical Habitat Screening Layer (UNEP-WCMC, 2017). This dataset is classified according to the International Finance Corporation's Performance Standard 6 (IFC PS6) criteria and has two levels of critical habitat, "potential" and "likely" (Brauneder et al., 2018, 4). In this work, both levels were excluded.

Five studies (Ali et al., 2022; S. S. H. Dehshiri & Dehshiri, 2022; Franzmann et al., 2023; Okunlola et al., 2022; Pfennig et al., 2023) applied a buffer zone around protected areas ranging 100 meters to 1 km. Franzmann et al. (2023) used different distances according to the RES and the protected area type. For example, bird-protected areas were given a 100 meter buffer zone for PV and a 1 km buffer zone for wind turbines. Pfennig et al. (2023, p. 5) applied a 1 km distance from all protected areas both for PV and wind turbines. A larger distance of 4 km was taken from marine protected areas to avoid pollution from the desalination process. Pieton et al.

[14] Based on the work of Ryberg et al. (2017). This work had another category which has no parallel IUCN category: "Protected biosphere proximity and Protected bird proximity are given as WPDA features with "bio" or "bird," respectively, within the area's English designation."
[15] Specific categories were not listed in this work and therefore it was assumed all IUCN categories were exclude.

(2023, p. 66) also used a 4 km distance from marine protected areas. Spyridonidou and Vagiona found that a buffer zone was predominantly not used both from onshore wind sites (2020, p. 7) and PV sites (2023, p. 2957). They did find, however, that most commonly, a 1 km distance is used between protected landscapes and wind turbines (2020, p. 7). In an LE review of various RE technologies, Ryberg et al. (2017, p. 8) found that typically a 500 meter distance was taken from protected flora, fauna, and habitats, while a distance of 1 km was taken from protected landscapes, designated parks, nature reserves, and natural monuments.

Based on the findings above, it was decided to use a distance of 1 km from all protected area categories and critical habitats for both RE technologies, with the exception of marine protected areas, where a 4 km buffer zone was applied. The WDPA (UNEP-WCMC, 2023) dataset has two types of marine protected areas: "coastal: marine and terrestrial" and "predominantly or entirely marine" (UNEP-WCMC, 2019, p. 16), a 4km buffer was applied for both. Since the Global Critical Habitat Screening Layer (UNEP-WCMC, 2017) dataset does not distinguish between terrestrial and marine habitats, critical habitats were classified as marine habitats when they intersected with maritime boundaries (Flanders Marine Institute, 2019).

The selected buffer zones in this work were used to ensure the highest level of environmental protection on a global scale. However, this approach might be too strict in an analysis with a smaller geographic scope and can be reexamined based on the local environmental conditions and regulations.

EC no. 6: Elevation

The viability of RES diminishes significantly at high elevations due to challenges related to accessibility, installation expenses, and reduced resources, such as lower air density and increased cloud cover (Ryberg et al., 2017, p. 6). At the same time, there were studies that considered high altitude as a positive factor both for PV (Ali et al., 2022; Mostafaeipour, Rezayat, & Rezaei, 2020) and onshore wind (Rezaei et al., 2020). Nonetheless, it can be assumed that these studies did not refer to extreme elevation levels. Three large regional studies (Agora Energiewende and AFRY Management Consulting, 2021; Braun et al., 2022; Lux et al., 2021) applied this EC, but only Braun et al. (2022) specified the threshold for exclusion, which was 3000 meters above sea levels for both onshore wind and PV sites. Local studies typically had a lower threshold of 1000-2000 meters. It was decided to use a less strict approach in this case, as it was assumed that when it comes to the accessibly related challenges, the slope of terrain criteria

will exclude the most problematic areas. Therefore, a threshold of 3000 meters was set for both RES.

EC no. 7: Population Density

Most studies that evaluated this criterion were local studies that used it as an AC with a high preference, i.e., a preference for populated regions with high consumption potential. In the context of this thesis, this aspect was less relevant, as one of the objectives of this work was to estimate hydrogen potentials on a global level and identify potential hydrogen exporters. Nonetheless, the LL of this criterion was recorded in three global/regional studies that applied it in order to exclude areas that were too populated for the development of hydrogen infrastructure (Agora Energiewende and AFRY Management Consulting, 2021; IRENA, 2022; Pfennig et al., 2023). A threshold of 50 inhabitants/ km² was used by Pfennig et al. (2023), while a less strict approach was used by IRENA (2022), which applied a threshold of 130 inhabitants/ km². This work followed the stricter approach used by Pfennig et al. (2023). The population density dataset (Center for International Earth Science Information Network - CIESIN - Columbia University, 2018) identified by Pfennig et al. (2023) was also found suitable for this work, as it projected the population density for the year 2020, the same year of the economic parameters in the optimization model (Martínez Pérez, 2022).

EC no. 8: Settlement Areas

The LL of distance to settlement areas was discussed in the land use and land cover criterion. The UL for this criterion was mostly used to indicate the proximity to the potentially high-consuming locations and minimize transportation costs to these locations (Ali et al., 2022; S. S. H. Dehshiri & Dehshiri, 2022; Okunlola et al., 2022). Pfennig et al. (2023, p. 4) made the assumption that the proximity to large cities can be used as an indicator of the availability of skilled workers, which are necessary for large-scale PtX projects. They further explained that such projects have the potential to create jobs for nearby residents. Similar notions were also expressed in other studies but were recorded as standalone criteria such as “Skilled Labor & Knowledge Base” (Almutairi, 2022; Ao Xuan et al., 2022; Breitschopf et al., 2022; S. J. H. Dehshiri & Zanjirchi, 2022) and “Employment Potential” (S. J. H. Dehshiri & Zanjirchi, 2022; Gao et al., 2021; Mostafaeipour, Dehshiri, et al., 2020; Rezaei et al., 2020). These criteria were evaluated with different indicators, such as the unemployment rate (Rezaei et al., 2020) and labor market assessment (Breitschopf et al., 2022), and were mostly used as AC.

In the context of a global LE analysis, it is challenging to quantify such criteria. However, the UL of the distance to settlements was feasible to apply globally. Pfennig et al. (2023, p. 4) applied this criterion with a threshold of 200 km using the World Cities Database (simplemaps, 2023). The free version of this dataset contained about 43 thousand entries of "prominent cities". When examining the global coverage of this dataset, it appeared to be insufficient or too restrictive. To enhance the global settlement coverage in this work, roughly 1.5 million entries were also considered based on data from OpenStreetMap. Only locations classified as cities, towns, or villages (OpenStreetMap, 2023d) were taken into account. While villages and towns might not be considered "large cities", some entries from the World Cities Database (simplemaps, 2023) had similar population sizes. Future work could explore what minimal population size threshold should be used. On a smaller geographic scope, other indicators like those mentioned above are also recommended for evaluation.

4.1.3 Criteria for Sustainable Development

The literature review identified various criteria considering socio-political and sustainable development perspectives. These criteria are not only crucial for ensuring the sustainable supply of hydrogen to import countries but also for strengthening the economies of export countries (Müller et al., 2023, p. 2) and fostering energy justice (Scott & Powells, 2020). On a local level, these criteria evaluated the domestic prosperity potential of hydrogen with indicators such as public support. These criteria were mostly not measurable using spatial data, but interestingly, one case was recorded where social impact was evaluated based on GIS. Reed et al. (2022, p. 28231) used a tool that maps poor air quality in California to identify the vulnerable communities that might be affected. However, this tool was relevant only for the LE of hydrogen based on thermochemical and steam methane reforming (SMR) technologies.

Other studies evaluated such criteria from an import-export perspective. For example, Franzmann et al. (2023, p. 11) analyzed hydrogen potentials according to government regime types to evaluate future hydrogen supply security. Certain studies used complex methodologies concerning these aspects. One example of such a methodology can be seen in the HYPAT (Breitschopf et al., 2022, p. 8). The study defined a set of minimal requirements a country must fulfill to be considered a hydrogen exporter within a sustainable development compliance framework. These requirements evaluated countries from three perspectives: renewable energy potential, water resources, and political stability. The authors further recommended that these

requirements be considered for any evaluation of future hydrogen import-export, also outside of the HYPAT project. Accordingly, this work followed this recommendation; however, as conducting such an evaluation was beyond the scope of this thesis, the results of Breitschopf et al. (2022) were used as input instead. As water resources were considered sufficiently examined under EC no. 3, this minimal requirement was not included. The other two requirements are briefly described below.

a) **Net renewable potential in 2050**: A country's renewable energy potential and its energy demand were estimated for 2050, taking into account hydropower, geothermal, wind, and solar energy. The demand was calculated based on current consumption and future trends, then subtracted from the generation potential to determine the net renewable energy potential. A threshold of 100 terawatt hours (TWh) net renewable potential with costs up to 70 euro per megawatt hour (MWh) was selected by Breitschopf et al. (2022) according to Germany's hydrogen demand in 2030, which is estimated at 90 to 110 TWh in 2030. They further explain that the relatively high price limit is due to more expensive RE technologies such as solar thermal and wind technologies. Finally, 118 countries did not fulfill this requirement; the list can be found in Breitschopf et al. (2022, p. 62). Nonetheless, this condition affected only 91 countries in this work, as some countries are very small and were not assigned to any MERRA-2 cell. Of these 91 countries, 89 were in the fourth quartile in terms of land size. Thus, their RE potential is relatively low due to their spatial limitations. Nonetheless, sizable countries such as Indonesia and India were also included in this list.
b) **Political stability**: According to Breitschopf et al. (2022, p. 9), political and institutional stability are vital components for a successful hydrogen operation. The study used four political (in)stability indices to determine if a country is sufficiently stable. For each index, the 20 lowest-ranking countries were selected. Countries that were recorded in all four lists were classified as politically unstable. The evaluation resulted in 10 countries that did not meet this requirement: Afghanistan, Burundi, Democratic Republic of the Congo, Iraq, Yemen, Nigeria, Somalia, South Sudan, Sudan and Central African Republic. For the list of indices and further information, see Breitschopf et al. (2022, p. 9).

It is important to mention that the set of criteria above only examines minimal requirements and not optimal requirements. Breitschopf et al. (2022, p. 48) further proceed to identify the most suitable hydrogen export countries (focusing on Germany as the importer country). In the later stages of their work, they asses the reliability of countries that are subjected to a foreign or domestic conflict. At the time of their analysis, they found Russia, Ukraine, Turkey, Iran,

Colombia, Mexico, Egypt, Brazil, and Saudi Arabia to be less suitable. In this study, only the minimal requirements are taken into consideration. Another remark must be made here about the current war between Russia and Ukraine. While both countries meet the minimal export requirements, as defined by Breitschopf et al. (2022, p. 9), their political climate must be considered in future hydrogen markets. Pfennig et al. (2023, p. 10) also conducted a thorough socioeconomic analysis and stated that due to its ongoing war, it was impossible to carry out the evaluation for Russia.

Since the requirements above are mostly relevant from an importer perspective, and the results of this thesis are meant to provide insights for domestic hydrogen use cases as well, they were not considered EC in the LE analysis. Nonetheless, the impact of these criteria on the hydrogen cost-potential curve was assessed and is discussed later in this work. Furthermore, political and economic instabilities were also reflected in the LCOH in this work, as the optimization model (Martínez Pérez, 2022) incorporated the CRP in the cost computation (see 2.2).

The final set of EC applied in this LE analysis, as well as their definitions and data sources, are presented in Table 11. Subsequently, for ease of reference, the names of criteria were abbreviated as indicated in Table 12 and are used in this work from this point onwards. When criteria were applied with ULs of distance, such as UL distance to roads, they were replaced with the term "access to", e.g., access to roads. Additionally, when discussing access to roads and settlements (EC 2.2 and EC 8) simultaneously, they were referred to as access-related EC or access-related criteria.

Table 11: EC applied in global land eligibility analysis for green hydrogen

No.	EC	Indicator	Unit	Exclusion threshold		Data Source
				Onshore wind	PV	
1.1	Distance from Water Bodies LL	Distance	Meters	400	400	Copernicus Climate Change Service, Climate Data Store (2019) & NASA EOSDIS Land Processes DAAC (2017)
1.2	Distance from Agricultural Land & Cropland LL	Distance	Meters	0	0	
1.3	Distance from Settlement Areas LL	Distance	Meters	1000	0	
1.4	Distance from Forests LL	Distance	Meters	0	0	
1.5	Distance from Wetlands LL	Distance	Meters	0	0	
1.6	Distance from Snow-Covered & Permafrost Areas LL	Distance	Meters	0	0	
1.7	Distance from Aviation Areas LL	Distance	Meters	3000	3000	OpenStreetMap (2023a)[16]
1.8	Distance from Military Zone LL	Distance	Meters	400	0	OpenStreetMap (2023c)[17]
2.1	Distance from Road Network LL	Distance	Meters	Primary: 500 Secondary: 250	Primary: 100 Secondary: 50	OpenStreetMap (2023b)[18]
2.2	Distance from Road Network UL	Distance	Kilometers	100	100	
3.1	Distance from Water Bodies UL[19]	Distance	Kilometers	50	50	Copernicus Climate Change Service, Climate Data Store (2019)
3.2	Water Stress Risk UL[20]	Risk Category	Category	Low	Low	WRI (2023a)
4	Slope of Terrain UL	Gradient	Degrees	5.71	2.86	Amatulli et al. (2018)
5	Distance from Protected Areas & Critical Habitat LL	Distance	Kilometers	Terrestrial: 1 Marine: 4	Terrestrial: 1 Marine: 4	UNEP-WCMC (2023) &UNEP-WCMC (2017)
6	Elevation UL	Height from Sea-level	Meters	3000	3000	Amatulli et al. (2018)
7	Population Density UL	Population Density	Inhabitants/ km²	50	50	Center for International Earth Science Information Network - CIESIN - Columbia University (2018)
8	Distance from Settlement Areas UL	Distance	Kilometers	200	200	Simplemaps (2023) & OpenStreetMap (2023d)[21]

[16] OSM tag: aeroway=*
[17] OSM tag: military=*
[18] OSM tag: highway, primary in ('motorway', 'trunk', 'primary'), secondary in ('secondary', 'tertiary')
[19] Cells that overlapped with the 50km buffer from inland or coastal water sources were included entirely.
[20] Water-scarce cells that overlapped with the 50km buffer from coastal waters were included entirely.
[21] OSM tag: 'place' in ('city', 'town', 'village')

Table 12: Abbreviated names of EC

No.	EC
1.1	Water Bodies
1.2	Agricultural Land
1.3	Settlement Areas
1.4	Forests
1.5	Wetlands
1.6	Snow-Covered Areas
1.7	Aviation Areas
1.8	Military Zone
2.1	Road Network
2.2	Access to Road Network
3.1	Access to Water Bodies
3.2	Water Stress
4	Slope of Terrain
5	Protected Areas
6	Elevation
7	Population Density
8	Access to Settlement Areas

4.2 Land Eligibility Analysis

In this section, the results of the LE analysis are presented and discussed. Focus is given to identifying key restrictions to land eligibility for hydrogen production and, thus, hydrogen potentials. This part of the results does not aim to quantify the global hydrogen potentials, as this aspect is discussed in the following section.

The results were analyzed from two aspects: land availability for hydrogen production and hydrogen potentials. Both indicators were calculated pre and post application of the LE. The impact of LE was measured by examining the exclusion share or eligible share of both indicators. Table 13 provides an overview of the analyzed scenarios in this analysis. To clarify, S_0 denotes a theoretical scenario where hydrogen potentials were estimated with no land restrictions.

Table 13: LE and hydrogen potential scenarios

Scenario	Description
S_0	No LE applied
S_1	LE applied with all EC
S_2	LE applied with all EC excluding EC 2.2 and EC 8 (access to roads and settlements)

4.2.1 Assessing Land Exclusion Impact on Land Availability

Firstly, the results are presented in the context of eligible land. To visualize the result of the applied LE in this work, Figure 11 exemplifies the land exclusion in Argentina for each EC group. Additionally, the disaggregation of EC 1, i.e., land use and land cover, is presented in Figure 12. It can be seen from both figures that Argentina is highly restricted due to land cover and land use, which is mostly driven by agriculture and forest. Water availability also excludes a substantial area. On the other hand, Argentina is hardly affected by access to roads and settlements.

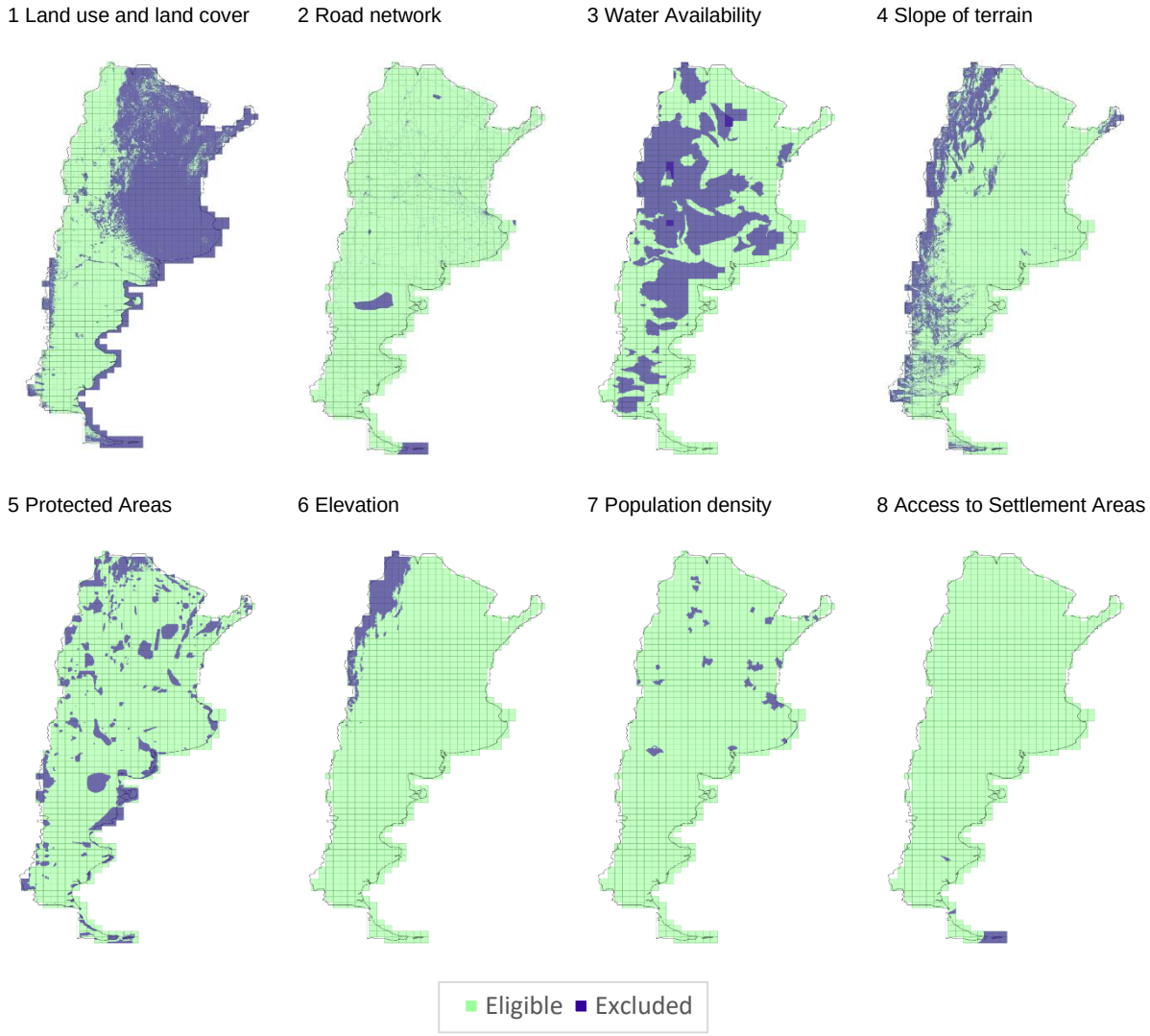

Figure 11: Land eligibility of Argentina by EC

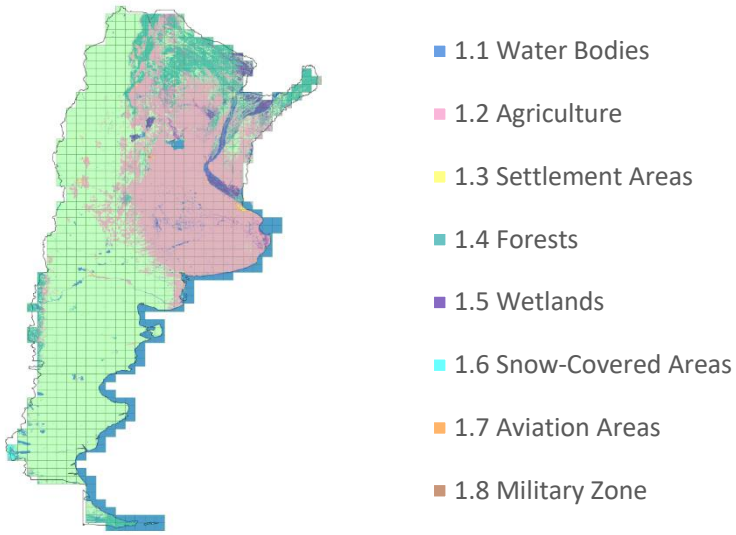

Figure 12: Land use and land cover in Argentina

Finally, the remaining available land for hydrogen production can be seen in Figure 13. While Figure 13.a is a simple unification of all EC, Figure 13.b visualizes areas in which EC are overlapping. Darker shades represent a higher number of EC that overlap. Having said that, this work did not research the overlapping of criteria but rather analyzed each criterion individually. Nonetheless, this topic could be further examined in future work.

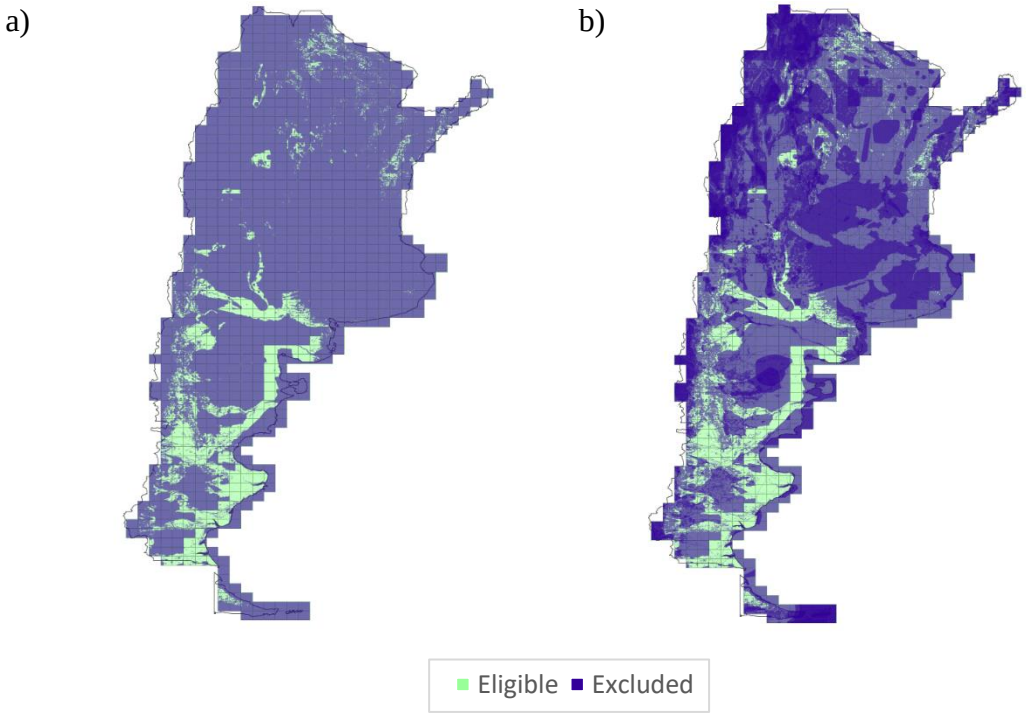

Figure 13: Land eligibility in Argentina under S_1. (a) union of all EC (b) overlapping EC

Under S_1, the global eligible land for hydrogen production was over 5 million km². This figure was roughly double the value reported by Pfennig et al. (2023, p. 9). The aforementioned study did not take the European Economic Area (EEA) into account. However, considering the small share of the eligible land Europe represents, the difference is still rather significant. This difference can be the result of the LE methodology applied by Pfennig et al. (2023), which was stricter in comparison to that applied in this study. The geographic distribution of land, as reported by Pfennig et al. (2023), is presented in Figure 14 for comparison. North America had the largest share of eligible land, accounting for 34%, while in this work, it only accounted for 10% under S_1. The variation might be related to access to roads EC, which was not applied by Pfennig et al. (2023). It can also be assumed that the available land in Africa was greater in this work as a less strict threshold was used for the water stress EC compared to the one used by Pfennig et al. (2023). On the other hand, the eligible land shares of Oceania and Asia in the study above were more similar when compared to those estimated in this work.

The allocation of available land by RES is presented for each scenario in Figure 15. Hybrid sites were disaggregated by the land share of each RES in those sites and are represented by Hybrid PV and Hybrid Onshore wind. It is worth mentioning that due to possible dual allocation to both RES technologies, the RES land share was calculated from the cumulative sum of land allocation rather than the actual size of the land.

The distribution of land is showing similar trends in both scenarios. Hybrid sites spread over roughly two-thirds of land, in which onshore wind is the dominant land occupier. However, Pfennig et al. (2023, p. 9) showed a different site composition, with a land distribution of 38% wind sites, 26% PV sites, and 36% hybrid sites, which tended to have more wind turbines presence. Nonetheless, the overall land use of onshore wind turbines was greater than that of PV both in this work and in the work of Pfennig et al. (2023, p. 9). There are two plausible distinctions that could explain the difference between the two studies. First, Pfennig et al. (2023) estimated hydrogen potentials and costs for 2050, which can impact the LCOE of RES, therefore leading to different technology prioritizations. Second, the methodology of land allocation in this study enabled more than one type of site on the same land.

Table 14: Global land availability for hydrogen production

Scenario	Continent	Share from global eligible land		
		PV	Wind	Hybrid
S_1	Africa	30.6%	29.2%	30.8%
	Asia	24.9%	25.0%	24.9%
	Europe	1.1%	1.6%	1.1%
	North America	9.9%	10.6%	9.8%
	Oceania	13.4%	12.5%	13.4%
	South America	20.0%	21.2%	20.0%
	Total area (km^2)	5.11 M	5.88 M	5.01 M
S_2	Africa	23.5%	21.9%	23.5%
	Asia	27.3%	28.7%	27.3%
	Europe	0.8%	1.1%	0.8%
	North America	22.0%	22.4%	22.2%
	Oceania	11.1%	10.1%	11.1%
	South America	15.2%	15.7%	15.1%
	Total area (km^2)	6.87 M	8.07 M	6.77 M

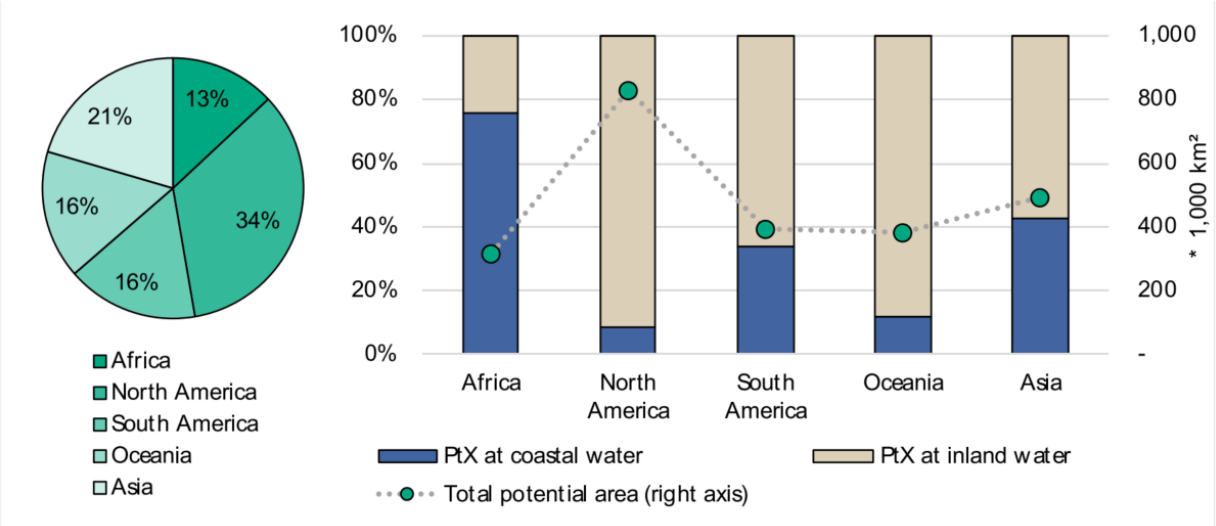

Figure 14: "Percentage distribution and total area of the preferred PtX regions divided by water supply source". Source: Pfennig et al. (2023, p.10).

As can be deducted from the difference in PD of each RES, PV requires less space in comparison to wind turbines. Thus, it is logical that the latter holds a higher share of land. However, another interesting comparison can be made here by examining the distribution of RES from a perspective of power rather than land. This comparison will be examined later in the discussion.

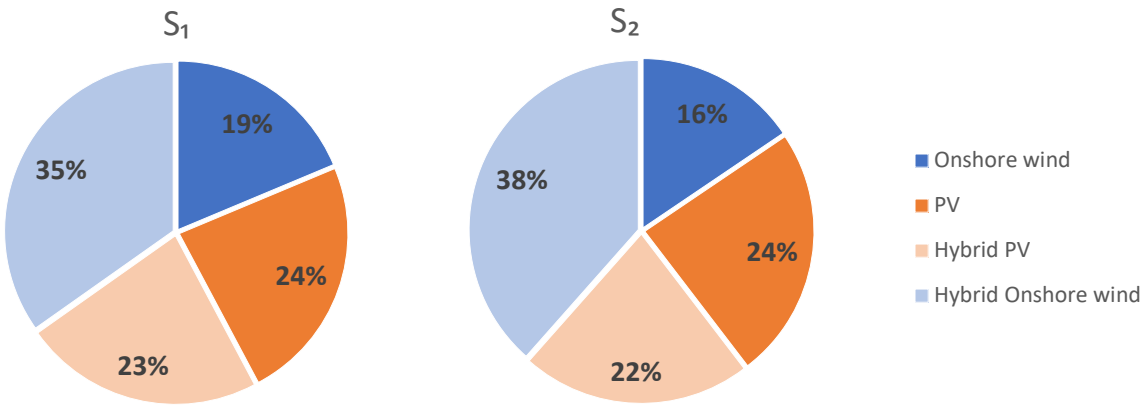

Figure 15: RES land share for hydrogen production by scenario

The exclusion share of land was calculated for each EC individually to identify the most land-restrictive criteria. The results are presented in Figure 16, where the metric is presented for both PV and onshore wind. Water stress was the most restricting criterion, excluding 34% of land. Protected areas and forests were the next most restrictive, with an exclusion share of about 30% of land. The exclusion of land for PV by the slope of terrain was roughly 10% greater than that of wind. The lack of access to a road network also led to a significant land exclusion of 16%.

The interactive dashboard (Barak, 2023) created as part of this thesis provides further insights on a country and continental level. The figure above is available as an interactive visualization as part of the dashboard and enables the user to drill down to an area of interest. The interactive visualization also includes the overall land exclusion when all EC were applied. For example, in the case of Saudia Arabia, water stress is the most restrictive EC, with an 85% exclusion share. IRENA (2022, p. 8) on the other hand, reported a highest exclusion share of 92% in this country. While the same threshold was used for water stress levels both in this work and the study above, the definition of this EC varied with regard to coastal areas (see 4.1.2), which can explain the difference in land exclusion shares. This emphasizes the need to evaluate the reasonable maximal distance between hydrogen sites and their water sources, especially in water-scarce regions.

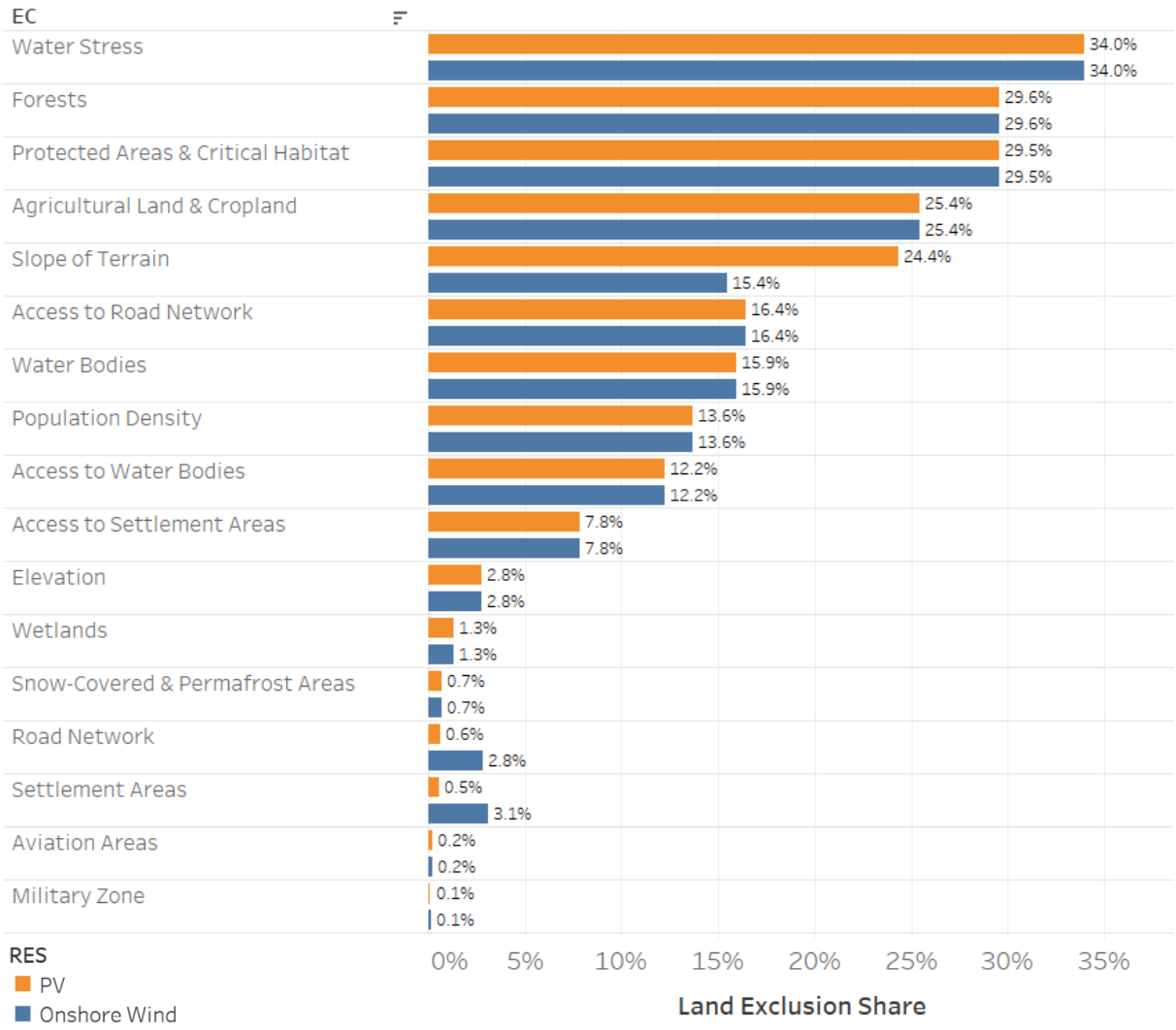

Figure 16: Global land exclusion by EC and RES

In comparison to IRENA (2022), the general level of land exclusion in this study was higher, which is in line with the stricter LE methodology that was applied in this work. In the case of Germany, for instance, the LE applied by IRENA (2022, p. 19) resulted in the land exclusion of roughly 95% and 35% for PV and onshore wind, respectively. While in this work, no eligible land was identified for both RES in Germany. One driver for the difference in exclusion levels could be the different definitions and datasets used for the agricultural land EC. While in this work, all types of cropland were excluded for both PV and onshore wind turbines, IRENA (2022) did not exclude croplands for onshore wind turbines and only partially excluded them for PV, depending on the cropland class. Further examination of the datasets used for this EC revealed that the dataset provided by NASA EOSDIS Land Processes DAAC (2017) led to the exclusion of 71% of land in Germany, while the dataset provided by Copernicus Climate Change Service,

Climate Data Store (2019) excluded only 42% of land. On a global level, the difference was less significant, with the first excluding 20% and the latter excluding 18% of land. Nonetheless, it is advisable to reassess the definition of this EC in future work in the context of crop types and local requirements. Another possible explanation for the difference in land exclusion in Germany between this study and IRENA (2022) was the lower population density threshold used in this work compared to the study above (see 4.1.2).

Finally, the current LE methodology applied in this study under S_1 resulted in 82 countries having less than 0.1% of eligible land for hydrogen production; see the full list of countries in Appendix 7.2.2.2. Another interesting indicator of land eligibility was the average eligible land per cell. It was observed that certain studies used this measure for estimating hydrogen potentials instead of defining the actual eligible areas for hydrogen production. For instance, Fasihi and Breyer (2020, p. 5) assumed a 10% eligible land per cell for both PV and wind. However, the average eligible share calculated in this study was significantly lower. In S_1, only 3.3% and 3.8% of the land were eligible for hydrogen production from PV and onshore wind energy, respectively. Even when access to roads and settlements was not considered in the LE under S_2, only 5.3% was eligible for PV, and 6.4% was eligible for onshore wind.

4.2.2 Assessing Land Exclusion Impact on Hydrogen Potentials

In this part of the discussion, the analysis examines the LE results in terms of hydrogen potentials. More specifically, the exclusion share of hydrogen potentials from the theoretical potentials under S_0, induced by the application of LE. However, the analysis did not consider all hydrogen potentials, but rather narrowed the consideration to those deemed economically feasible. Consequently, a decision was made to confine the assessment to hydrogen potentials with a maximal LCOH of 12 €/kg. This specific threshold was chosen, as it encapsulates 75% of the global hydrogen potential, and it deviates by about a 1.5 factor from the HYDRIX[22] index that estimates the price for green hydrogen in Germany in 2023 (European Energy Exchange AG, 2023). The rationale behind this selection is to support the analysis that comprehensively captures a substantial portion of global hydrogen potential while remaining in a plausible cost range for its production. Furthermore, the restrictions to hydrogen potentials are compared against those

[22] The HYDRIX index is the unweighted arithmetic mean of pricing data provided by companies (European Energy Exchange AG, 2023).

of the land. This analysis aims to elucidate the distinctions between these approaches and underscore the divergent outcomes that arise from each of them.

Firstly, a general overview of each scenario is pretested in Table 15. This overview includes the global share of eligible land and hydrogen potentials by scenario, as well as the variation between both measures. The delta column is the subtraction of the eligible land share from the eligible hydrogen potential share, while the percentage change is the rate of change. It can be seen that the levels of both measures are similar. However, the delta shows that land eligibility share is slightly lower than hydrogen potentials share, especially when compared to PV land eligibility. When looking at the percentage change column, the difference is more visible for PV, with about 17% change. This could indicate that either the land exclusion was less impactful in economically attractive areas or that the eligible land itself was more productive in terms of hydrogen potentials, i.e., more hydrogen could be produced per one surface unit.

Table 15: Eligible land and H_2 share by scenario

Scenario	H2	Land		Delta		Percentage change	
		PV	Onshore wind	PV	Onshore wind	PV	Onshore wind
1	4.02%	3.45%	3.97%	0.57%	0.05%	16.55%	1.28%
2	5.46%	4.64%	5.45%	0.82%	0.01%	17.76%	0.26%

Figure 17 provides the distribution of hydrogen potentials by the underlying power for hydrogen production. The shares of each RES in hybrid sites were determined by the ratio of their installed capacities and are denoted as hybrid PV and hybrid onshore wind. It can be seen that in both LE scenarios, hybrid sites generated approximately 80% of hydrogen potentials. PV was the dominant RES, both in hybrid sites and in the overall production, generating almost 75% of hydrogen potentials. Nonetheless, hydrogen production from wind turbines slightly increased under S_2, indicating that wind energy was limited due to access criteria in S_1. The perspective of the hydrogen potentials by RES depicts a different picture than the land distribution perspective (see Figure 15), in which onshore wind was the dominant RES. The results are aligned with IRENA (2022) and Franzmann et al. (2023), which also concluded that PV was the main RES for green hydrogen production.

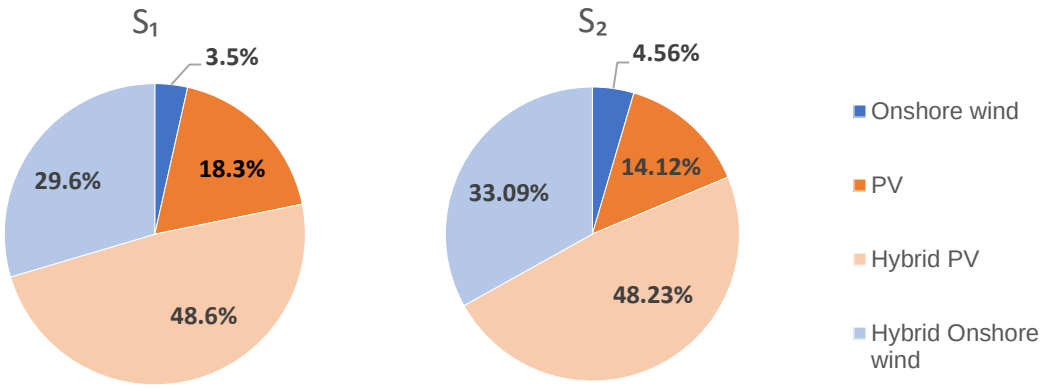

Figure 17: Hydrogen potentials distribution by RES and scenario

To examine the impact of the different EC on hydrogen potentials, first, the influence of each criterion was examined with respect to the cost-potential curve. For this analysis, a curve was created for multiple scenarios where only one EC was applied, and the lower PD values were used. The results are presented in Figure 18. For better visibility, the curve is curtailed at LCOH of 30 €/kg, which represented 98% of global hydrogen potentials. It is worth noting that the figure does not provide final hydrogen estimates but rather alludes to which criteria had the most impact on the curve and to what extent.

The primary factors limiting hydrogen potentials exhibit similarities to those restricting the land for its production. The impact of water stress here is evident, restricting far more than any other individual criteria. Nonetheless, there are subtle differences between the two indicators. When examining the land exclusion shares, forests had a higher level of restriction in comparison to agricultural land (see **Error! Reference source not found.**, Figure 16). However, in the case of hydrogen potentials, the latter was more restrictive. To further assess the differences between land and hydrogen potentials, a comparison of exclusion shares of both measures is presented in Table 16. Only hydrogen potentials with a threshold of LCOH 12 €/kg were considered to maintain the economic relevancy of potentials. For EC in which the exclusion definition varied between PV and onshore wind, the land exclusion values are presented separately, as well as for the hydrogen potentials exclusion share, i.e., the exclusion share is disaggregated by the underlying RES that provides the electric power. The delta column in this case is the subtraction of the excluded hydrogen potentials share from the excluded land share.

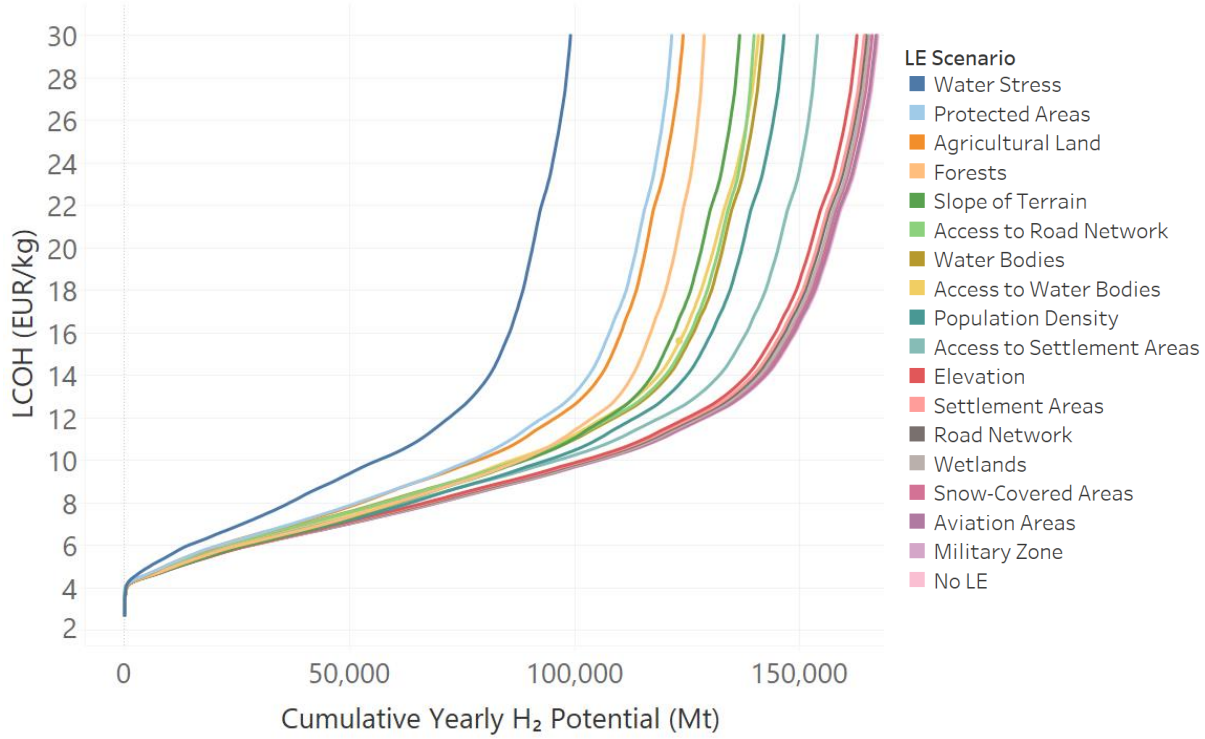

Figure 18: Global green hydrogen cost-potential curve by EC

Comparable to the findings in Table 15, the general exclusion trend is rather similar between land and hydrogen exclusion. However, in some EC, the difference was more substantial. Higher delta levels are represented in green shading, marking a positive implication, as the levels of excluded hydrogen potentials were lower than the share of excluded land. For example, forests excluded 10% more land compared to hydrogen potentials. However, in the case of water stress, the exclusion share hydrogen potentials was 10% greater. When looking at the slope of the terrain, the exclusion share of hydrogen potentials was lower than that of land. A connection could be made here between the climatic or topographic conditions and hydrogen potentials. For example, water-scarce regions are exposed to plenty of sun and, therefore, have more PV potential (Tonelli et al., 2023, p. 3).

Agriculture was also a main exclusion driver, with an exclusion share of 25% both for land and hydrogen, indicating that agricultural land has hydrogen production potential at attractive costs. It is therefore recommended that further research be conducted on the possibility of combining agriculture with green hydrogen production in order to provide future LE recommendations in this field. Additionally, the substantial losses of hydrogen potentials due to water stress provoke questions like whether RES and electrolysis must be located at the same site or what reasonable

distances of water transportation are to the location of electrolysis. As noted in 4.1.2, the latter question was not widely discussed in the literature.

Table 16: Global exclusion share of land and hydrogen potentials by EC

No.	EC	H_2		Land		Delta	
		PV	Wind	PV	Wind	PV	Wind
1.1	Water Bodies	15.7%		15.9%		0.3%	
1.2	Agricultural Land	25.8%		25.4%		-0.3%	
1.3	Settlement Areas	1.8%	3.5%	0.6%	3.1%	-1.3%	-0.4%
1.4	Forests	19.3%		29.6%		10.3%	
1.5	Wetlands	1.0%		1.3%		0.3%	
1.6	Snow-Covered Areas	0.7%		0.7%		0.0%	
1.7	Aviation Areas	0.3%		0.2%		0.0%	
1.8	Military Zone	0.12%	0.15%	0.09%	0.10%	-0.03%	-0.05%
2.1	Road Network	1.4%	2.6%	0.6%	2.8%	-0.8%	0.2%
2.2	Access to Road Network	16.3%		16.4%		0.2%	
3.1	Access to Water Bodies	17.5%		12.2%		-5.3%	
3.2	Water Stress	44.2%		34.0%		-10.2%	
4	Slope of Terrain	20.4%	8.5%	24.4%	15.4%	3.9%	7.0%
5	Protected Areas	28.0%		29.5%		1.5%	
6	Elevation	3.1%		2.8%		-0.3%	
7	Population Density	12.0%		13.7%		1.6%	
8	Access to Settlement Areas	7.8%		7.8%		0.0%	

To examine which geographic regions were most affected by which criteria, the land and hydrogen potentials exclusion shares were broken down into a continent level and are presented in Table 17. For each continent, the five EC that were most restrictive to hydrogen potentials were selected. Additionally, the hydrogen potentials share generated by each continent is noted for each scenario.

The most restricting EC appear to be similar among the different continents, with some variations. Water availability, agricultural land, and protected areas had a major hydrogen exclusion in almost all continents. Water stress was the most restrictive EC in all continents except Europe and South America. Across continents, Africa stands out as the region most significantly affected by this criterion, experiencing a comparatively higher exclusion share of hydrogen potentials in comparison to the rest of the world. Furthermore, the exclusion of

hydrogen potentials due to this EC in Africa was 22% greater than land exclusion, indicating that land is restricted in highly productive and cost-efficient areas. This finding could be one of the reasons Africa represents 30% of land but only 23% of hydrogen potentials. On the other hand, agricultural land in Africa seems to be less attractive for hydrogen production, with hydrogen potentials being reduced by 9% less than land.

Table 17: Exclusion share of land and hydrogen potentials by EC and continent

Continent & share from global H_2	EC	H_2		Land		Delta	
		PV	Wind	PV	Wind	PV	Wind
Africa	Water Stress	68.1%		45.6%		-22.5%	
S_0: 19%	Access to Water Bodies	46.5%		30.9%		-15.6%	
S_1: 23%	Protected Areas	26.7%		26.7%		-0.1%	
S_2: 17%	Access to Road Network	20.8%		14.0%		-6.8%	
	Agricultural Land	14.4%		23.2%		8.8%	
Asia	Water Stress	46.9%		38.4%		-8.5%	
S_0: 33%	Agricultural Land	31.5%		28.4%		-3.1%	
S_1: 26%	Slope of Terrain	29.1%	11.9%	32.5%	22.6%	3.4%	10.7%
S_2: 28%	Population Density	22.5%		21.5%		-1.0%	
	Protected Areas	20.5%		22.3%		1.7%	
Europe	Agricultural Land	51.1%		48.0%		-3.1%	
S_0: 6%	Protected Areas	46.0%		44.5%		-1.5%	
S_1: 1%	Water Bodies	30.4%		28.1%		-2.3%	
S_2: 1%	Population Density	23.0%		22.4%		-0.6%	
	Forests	22.7%		28.1%		5.4%	
North America	Water Stress	36.9%		28.6%		-8.3%	
S_0: 19%	Water Bodies	27.1%		28.0%		0.9%	
S_1: 11%	Protected Areas	26.7%		28.7%		2.1%	
S_2: 24%	Forests	26.3%		33.5%		7.3%	
	Agricultural Land	25.3%		19.9%		-5.5%	
Oceania	Water Stress	47.5%		38.1%		-9.3%	
S_0: 11%	Access to Water Bodies	37.4%		30.9%		-6.5%	
S_1: 20%	Protected Areas	32.2%		36.0%		3.8%	
S_2: 17%	Access to Road Network	18.0%		20.2%		2.2%	
	Water Bodies	14.9%		22.6%		7.8%	
South America	Protected Areas	41.1%		45.9%		4.8%	
S_0: 11%	Forests	36.5%		44.5%		7.9%	
S_1: 18%	Agricultural Land	30.5%		27.2%		-3.3%	
S_2: 13%	Slope of Terrain	26.0%	10.4%	25.9%	15.9%	-0.1%	5.5%
	Water Stress	14.6%		12.2%		-2.4%	

Europe generated only 1% of hydrogen potentials when LE was applied, in comparison to 6% in the theoretical scenario, in which land use was not restricted. Agricultural land was the main excluding factor, reducing hydrogen potentials by half. Thus, it is advisable to examine the possible synergy of RE-powered hydrogen in this area. Ryberg et al. (2020) found that when it comes to onshore wind turbines, the most restricting criteria were wind speed, slope of terrain, UL distance from power lines, and LL distance from settlements. Forests and agricultural land were not used as EC in this study; however, it was noted that almost 49% of the eligible land already had agricultural use, and 38% was covered with some type of woodland, therefore aligning with the results of this work.

To evaluate which areas were most affected by access EC, Table 18 displays the hydrogen potentials exclusion shares by LE scenario on a continental level. North America is where access EC were most restrictive, reducing hydrogen potentials by 4.4%. Developing access infrastructure in remote areas on this continent could potentially improve the suitability of areas with economic viability. However, the costs of such operations must be accounted for. While Africa appears to be highly affected by the lack of access to roads in Table 17, the comparison of the two LE scenarios reveals that in the overall impact, this criterion did not significantly exclude additional land to that already excluded by other EC. This indicates that even if access infrastructure is to be created, land in Africa will still be restricted due to other factors, most likely due to water scarcity. Furthermore, this finding emphasizes the limitation of this work with regard to the lack of analysis of criteria intersection. It is worth noting the level of accuracy of the underlying dataset (OpenStreetMap, 2023b) is unknown. Therefore, the results must be interpreted with caution, as incomplete data can lead to excess exclusion.

Table 18: Exclusion share of hydrogen potentials by EC and scenario and continent

Continent	H_2		Delta
	S_1	S_2	
Africa	95.3%	95.2%	0.1%
Asia	96.8%	95.4%	1.4%
Europe	99.0%	99.0%	0.0%
North America	97.7%	93.3%	4.4%
Oceania	92.8%	91.8%	0.9%
South America	93%	93%	0%

For a country-level analysis, an interactive map of hydrogen exclusion shares highlights which countries were most or least restricted by a criterion of interest that the user may select. Furthermore, the user has the ability to set the range of LCOH to be taken into account. Figure 19 exemplifies one use case for this visualization, in which shares of hydrogen potentials excluded by water stress with the LCOH threshold of 12 €/kg are depicted.

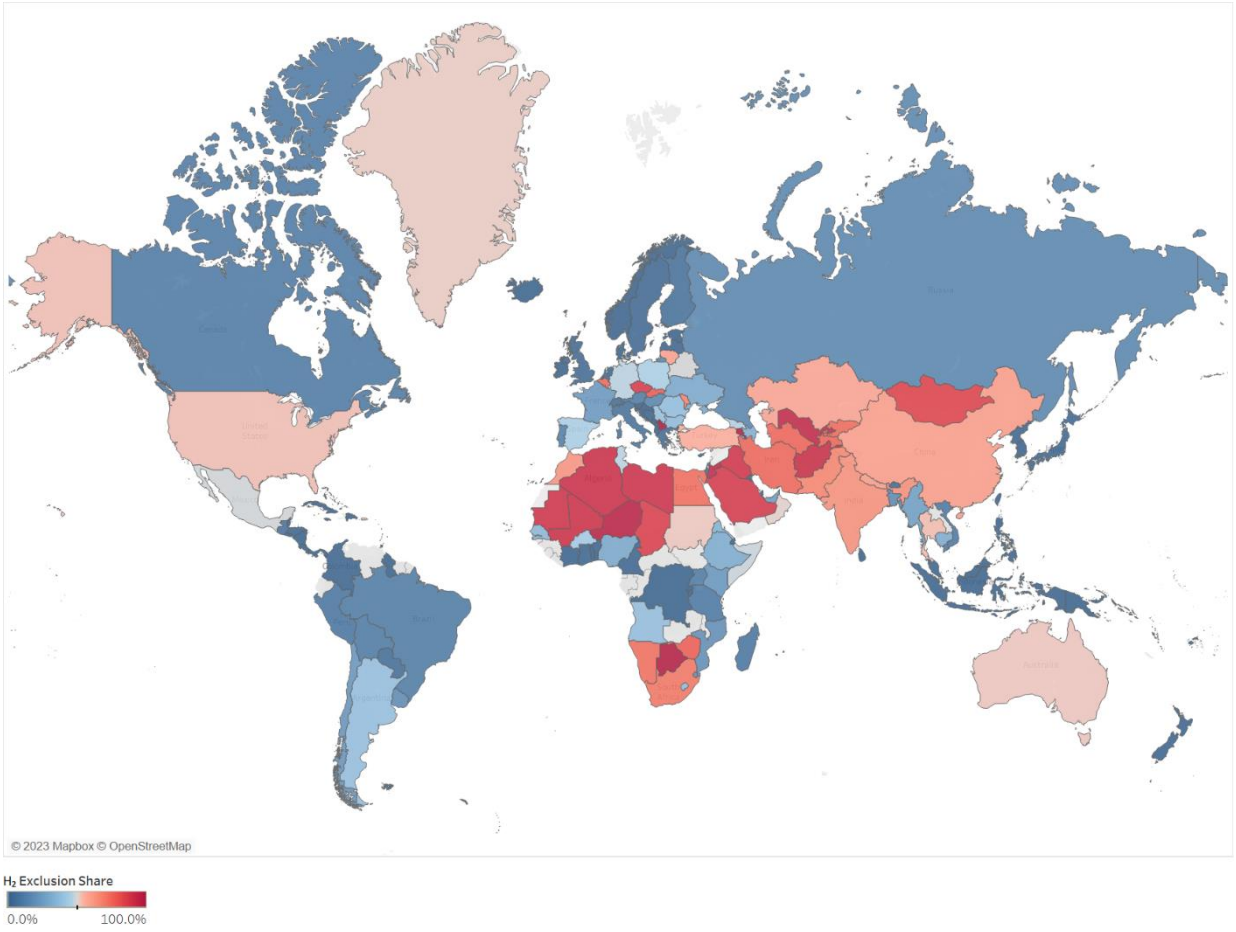

Figure 19: Map of hydrogen potentials exclusion share by water stress, LCOH UL: 12 €/kg

From Figure 19, it is visible that countries most significantly restricted due to water stress are highly concentrated in the MENA region, as well as some countries in Asia, like Afghanistan, Uzbekistan, and Mongolia. Southern Africa is also under a relatively high level of water stress, particularly in Botswana. Tonelli et al. (2023, p. 10) examined the water scarcity exacerbation caused by green hydrogen demand in 2050 globally and showed that water-scarce regions, similar to those in Figure 19, were subjected to an increase in water scarcity up to 5%. On the other hand, hydrogen demand did not increase water scarcity in regions that did not experience it to begin with. This underscores that the development of future hydrogen projects in water-

scarce regions, as economically appealing as they might appear to be, is unlikely to uphold the principles of a sustainable development approach.

Thus far, the analysis above has provided LE-related insights mainly on the cumulative hydrogen potentials level. Therefore, an interactive visualization was created to illustrate the influence of LE at different LCOH levels. Figure 20 demonstrates this visualization, in which the global hydrogen potentials and the level of their restrictions are illustrated under the constraint of water stress. The LCOH bin represents the lower limit of the bin, e.g., bin 5 represents LCOH between 5 to 6. The user may filter the data to a specific country or continent, as well as the LCOH range.

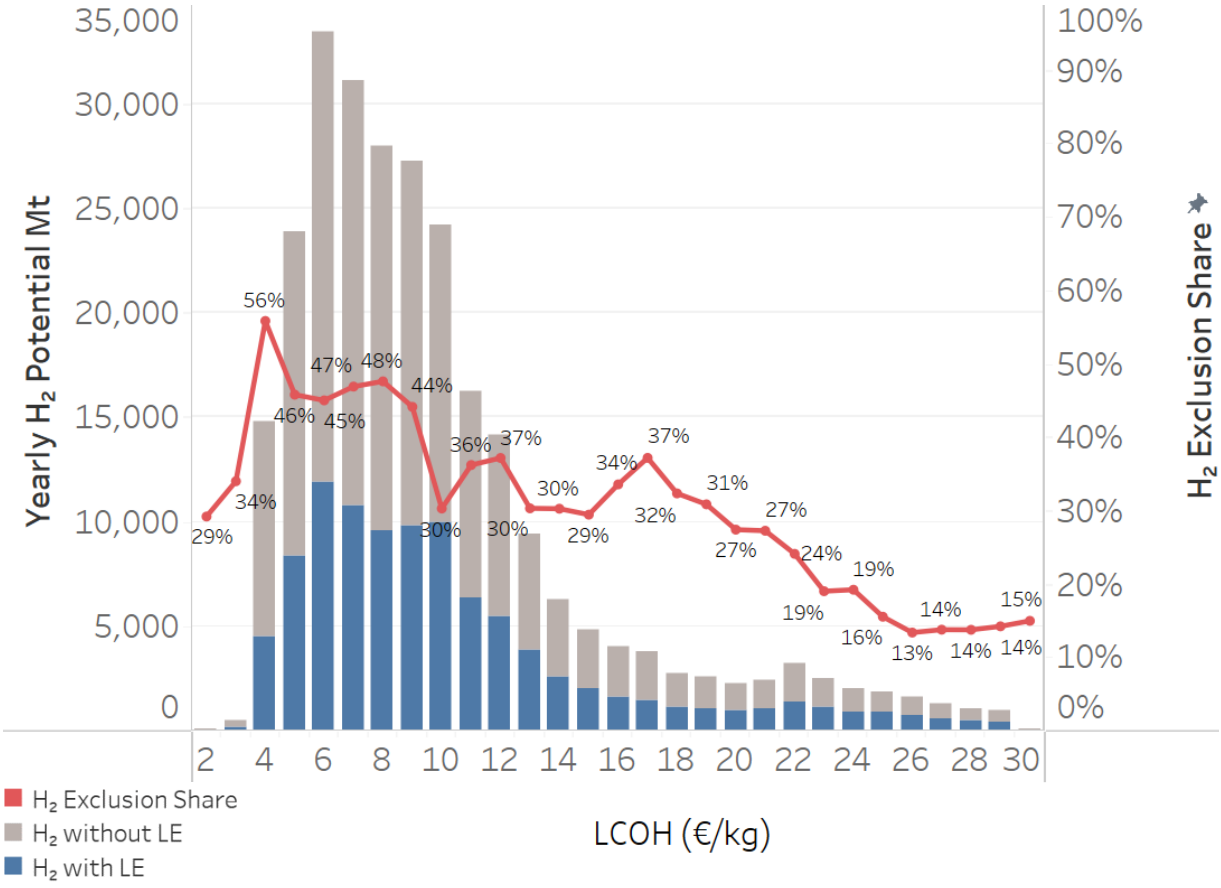

Figure 20: Water stress hydrogen potentials exclusion share by LCOH

The figure illustrates that hydrogen potentials are highly restricted at attractive LCOH levels, peaking at 4 €/kg, with a 56% share of exclusion. However, in absolute terms, hydrogen potentials are experiencing the most significant losses at a cost range of 6-7 €/kg. Unfortunately, it can be observed that there is a negative correlation between LCOH and exclusion share caused by water stress, i.e., higher levels of LCOH are experiencing less reduction in potentials. On the

other hand, this trend is reversed when looking at potentials exclusion caused by forests, as illustrated in Figure 21. These trends accentuate the relationship between climatic and topographic land attributes and their hydrogen potentials and costs.

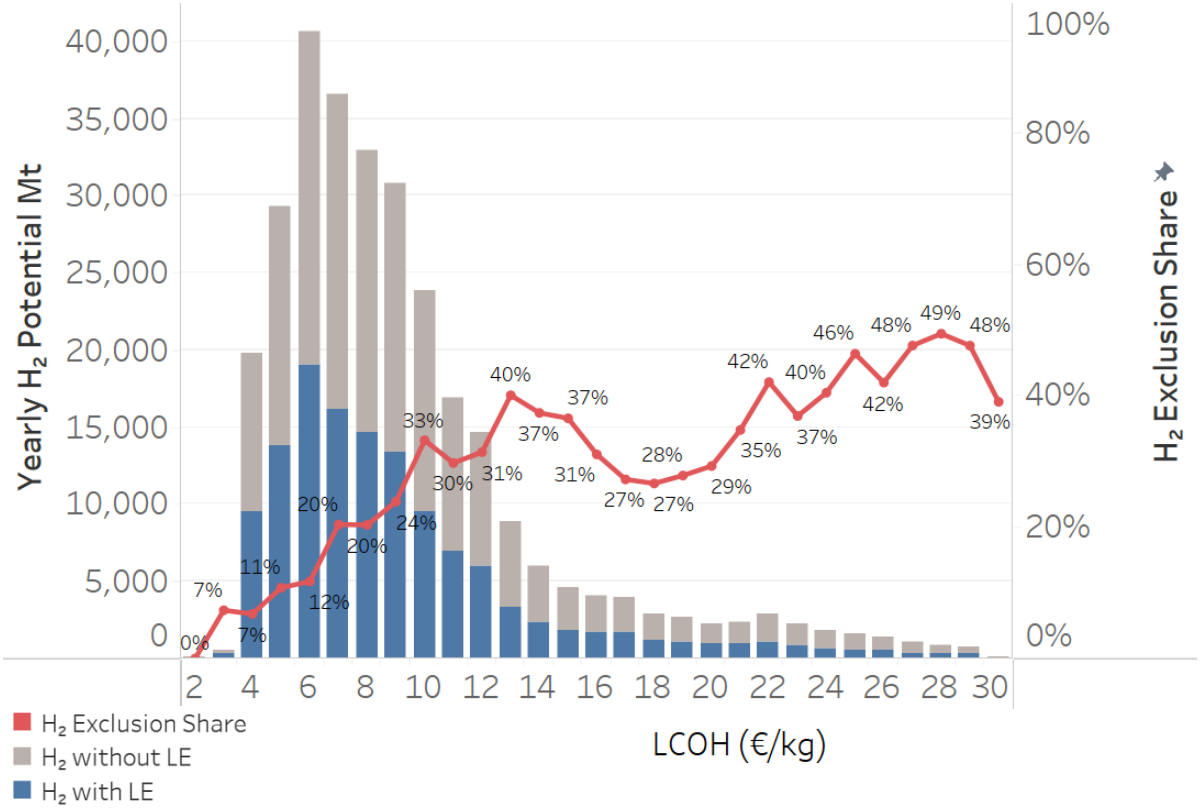

Figure 21: Forests hydrogen potentials exclusion share by LCOH

4.3 Global Costs and Potentials of Green Hydrogen

This section focuses on estimating global hydrogen potentials and costs for 2020, the year on which the economic assumptions in the optimization model (Martínez Pérez, 2022) were based. First, the global cost-potential curve is illustrated, then the global distribution of hydrogen potentials is discussed, and finally, the results are compared against existing studies.

4.3.1 Green Hydrogen Cost-Potential Curve

The global cost-potential curves under S_1 and S_2 are depicted in Figure 22. The curves were calculated using the bassline scenario of PD values, i.e., lower PD values (see 3.3). For the rest of this section, unless specified otherwise, the results are always calculated using the baseline PD scenario.

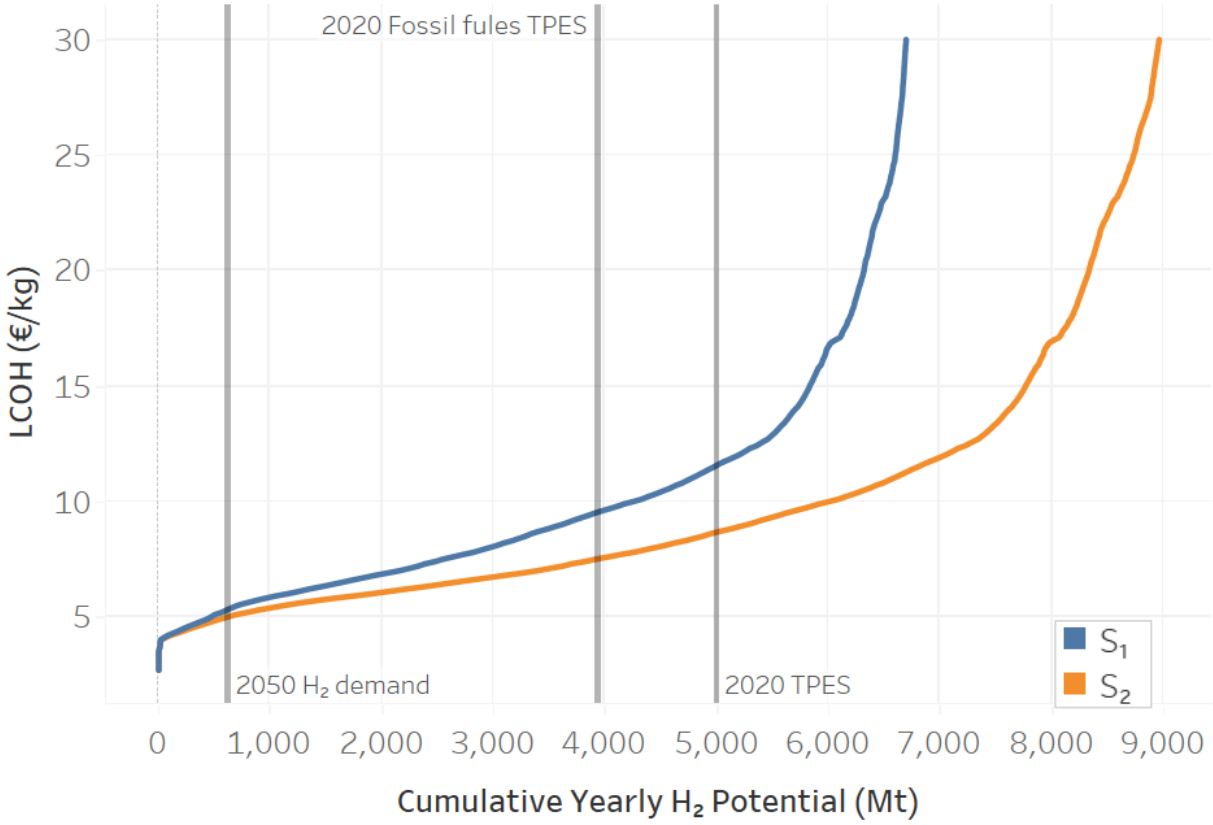

Figure 22: Global hydrogen cost-potential curve by LE scenario with low PD

In total, 6,856 Mt of hydrogen potentials were estimated based on S_1. When considering the LCOH threshold of 12 €/kg, potentials were reduced to 5,193 Mt. For reference of scale, Figure 22 also marks the total primary energy supply (TPES)[23,24] by all energy carries, as well as by fossil fuels exclusively, in 2020 as reported by IRENA (2023). The figure also includes the projected hydrogen demand in 2050, as reported by IRENA (2022)[24]. The S_1 curve intersects with the fossil fuels TPES at a potential of 3,950 Mt and LCOH of 9.6 €/kg and with the overall TPES at a potential 5,000 Mt and LCOH of 11.6 €/kg. These points of intersection offer a degree of validation, suggesting that the order of magnitude of the results is reasonable. When it comes to the demand side, the curves intersect with the projected 616 Mt demand at LCOH of 5 €/kg and 5.3€/kg for S_1 and S_2, respectively. The relatively negligible cost variation indicates that global hydrogen production might be able to meet future demand without additional access

[23] TPES "refers to the total amount of energy that is produced and consumed in various forms around the world. It includes all the energy sources that are used to produce electricity, power transportation, heat buildings and homes, and power industrial processes. Renewables include hydro, solar, wind, bioenergy, geothermal and ocean energy" IRENA (2023).)

[24] Values were reported in exajoule (EJ) and converted to Mt based on the low heating value (LHV)

infrastructure development. Nonetheless, this assumption is only valid for a scenario in which all eligible land is allocated for hydrogen production. Therefore, further evaluation is needed to understand the influence of insufficient access to roads and settlements on hydrogen potentials.

As discussed in 3.3, an additional scenario examined the outcome of estimating potentials while applying higher PDs. The influence of the S_1 cost-potential curve by the PD scenario is presented in Figure 23. The impact of PDs is evident, as the total hydrogen potentials nearly doubled using high PDs. This amplification is aligned with ratios of PDs between the two scenarios, which had a factor of 2 and 1.5 for wind turbines and PV, respectively. As already pointed out by Bolinger and Bolinger (2022), outdated and thus insufficient PD values can lead to grossly overestimating land requirements, and in this case, it could lead to underestimating hydrogen potentials. The high sensitivity to PD values in this work underscores the much-needed research in this field for enhanced precision in future energy potentials and land requirement estimations. Furthermore, as PDs tend to vary among geographic regions (Enevoldsen & Jacobson, 2021), it is worth exploring an approach in which PDs are variable with respect to regions.

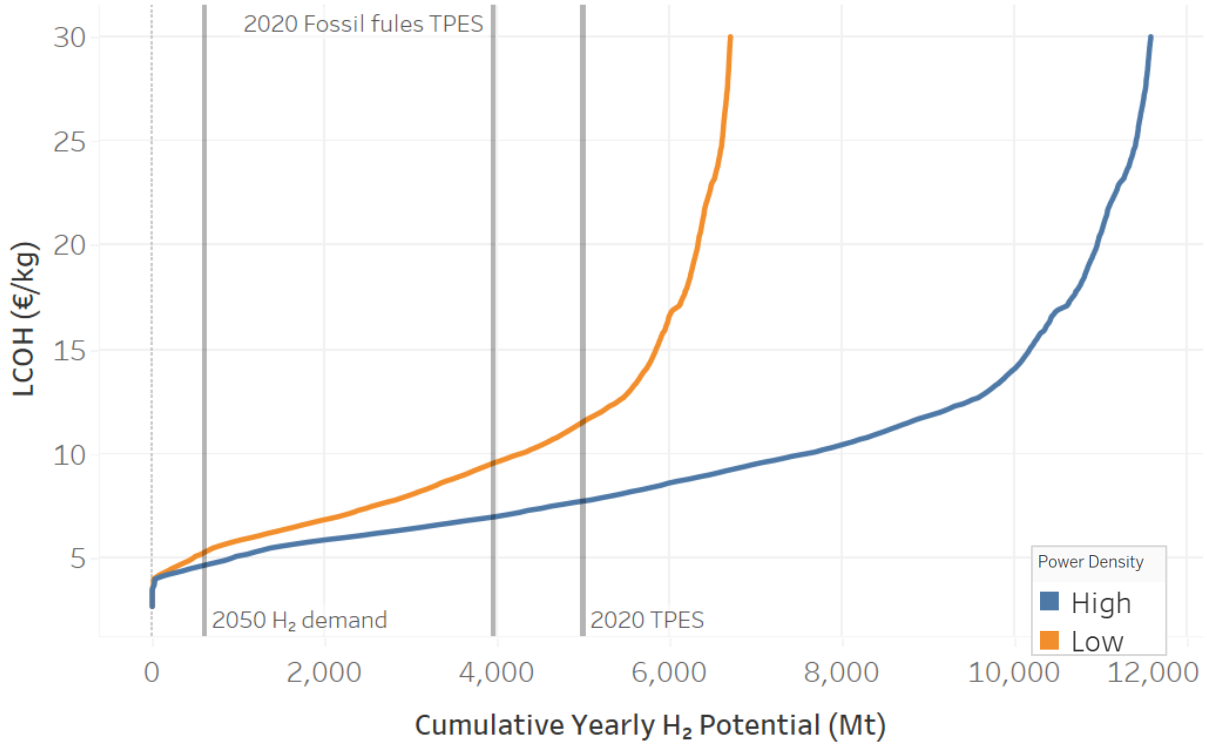

Figure 23: Global hydrogen cost-potential curve by power density under S_1

For an examination from an import-export perspective, Figure 24 illustrates the impact of minimal requirements for hydrogen export countries (Breitschopf et al., 2022) on hydrogen costs and potentials (see 4.1.2 for further information). The cost-potential curves are presented for S_1 and S_1 without countries that did not fulfill the minimal requirements. Fortunately, the curves diverge at costlier levels of hydrogen, indicating that countries with high potentials at attractive costs were able to fulfill the set of requirements. Nonetheless, as these are only minimal standards, further analysis is needed to evaluate future hydrogen international cooperations.

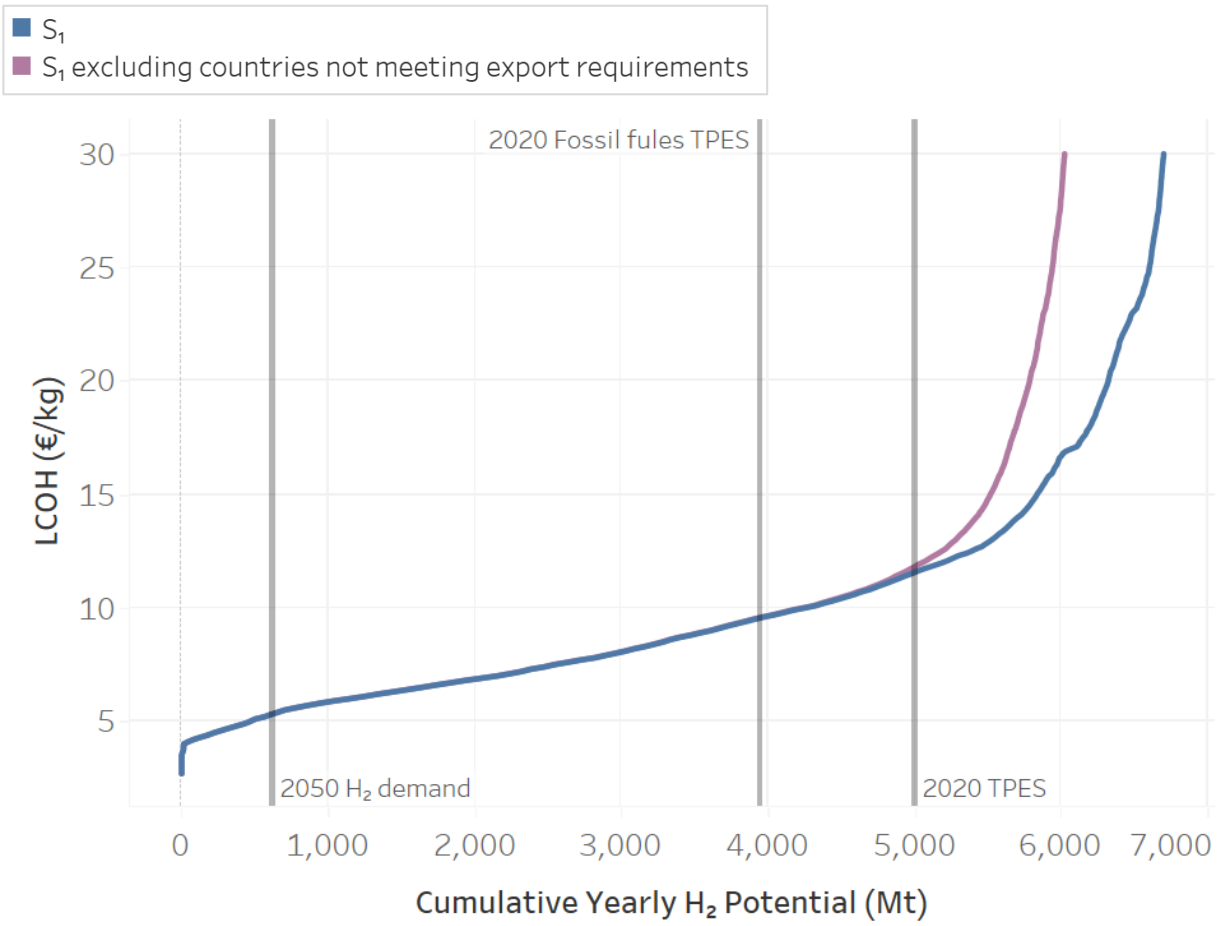

Figure 24: Minimal export requirements impact on the global hydrogen cost-potential curve under S_1

4.3.2 Global Distribution of Green Hydrogen Potentials

In this part of the discussion, the geographic distribution of hydrogen potentials is evaluated to identify productive regions and countries. The yearly hydrogen potentials per MERRA-2 cell are illustrated for different scenarios in Figure 25 (a-c). Figure 25.a and Figure 25.b depict the potentials under S_1, where the first considers all potentials, and the latter considers only potentials with a maximal LCOH of 12 €/kg. The comparison of the two figures alludes to areas that might

be rich in potentials but economically unattractive. In Figure 25.c, potentials are also curtailed at 12 €/kg, but under S_2, demonstrating the economically viable potentials lost in S_1 due to access criteria.

Coastal areas in the MENA region exhibited high levels of potentials, which is likely enabled by omitting the water stress EC in these areas. Conversely, equatorial regions were often characterized by lower potentials. Substantial potentials were also identified in South America, especially in Brazil and Argentina. When comparing the three figures for these two countries, their potentials were not affected in a significantly visible manner, indicating that these potentials are economically attractive and that these regions are well accessible by roads and settlements. On the other hand, when comparing all potentials under S_1 in Figure 25.a to the economically constrained potentials in Figure 17.b, hydrogen potentials were completely eliminated in some areas in Central Africa, and notable reductions were also observed in Russia. When looking at Figure 25.c, vast potentials were found in areas approaching the Arctic Circle. However, these potentials were greatly diminished when considering access to roads and settlements EC, as seen under S_1 in Figure 25.b. In light of this, it is worthwhile exploring the additional costs incurred by developing the necessary access infrastructure within these regions.

Further analysis revealed that global hydrogen potentials were highly concentrated in very few countries. Table 19 shows that only 15 countries generated 74% of global hydrogen potentials under S_1, noting that only potentials with LCOH of 12 €/kg and less were considered for this analysis. Australia alone represented 20% of global hydrogen potentials and was followed by Kazakhstan, Brazil, Argentina, and the United States, generating about 6-7% each.

The resulting localized concentration of hydrogen potentials in this work was aligned with the findings of Pfennig et al. (2023, p. 9), who reported that only 10 countries generated 80% of the identified potentials in their study. Nonetheless, the countries with the highest hydrogen potentials in the aforementioned study diverged to some extent from those identified in this work and were as follows (in order of importance): the United States, Australia, Argentina, and Russia. The lesser contribution of the United States in this study could be the result of the access to roads EC, which was not applied by Pfennig et al. (2023) in their LE analysis. Pfennig et al. (2023) further indicated that in comparison to Argentina, the United States and Australia had a higher socioeconomic suitability for importing PtX products to Europe, while an evaluation for Russia from this perspective was not feasible due to the war on Ukraine.

a)

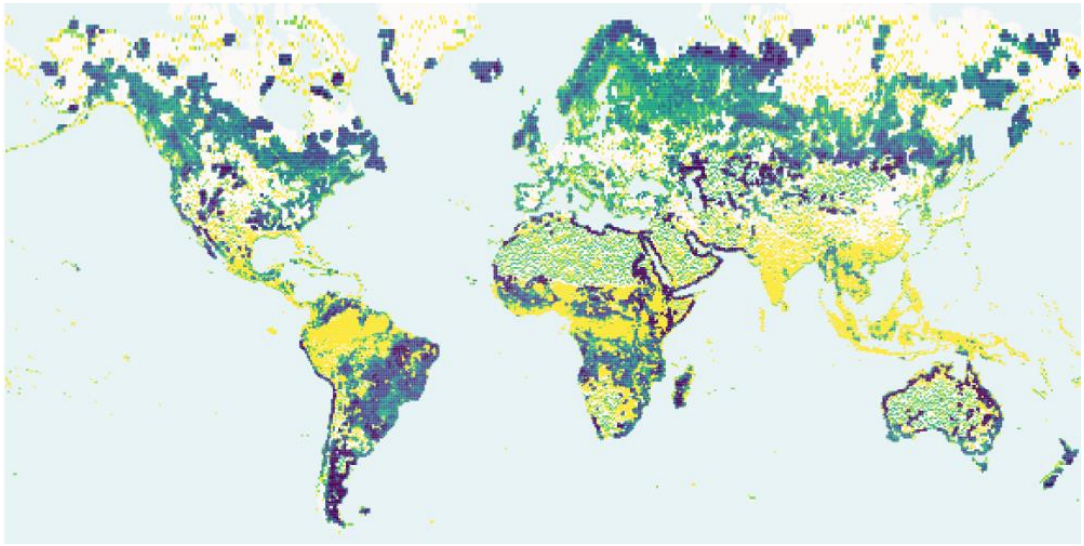

b)

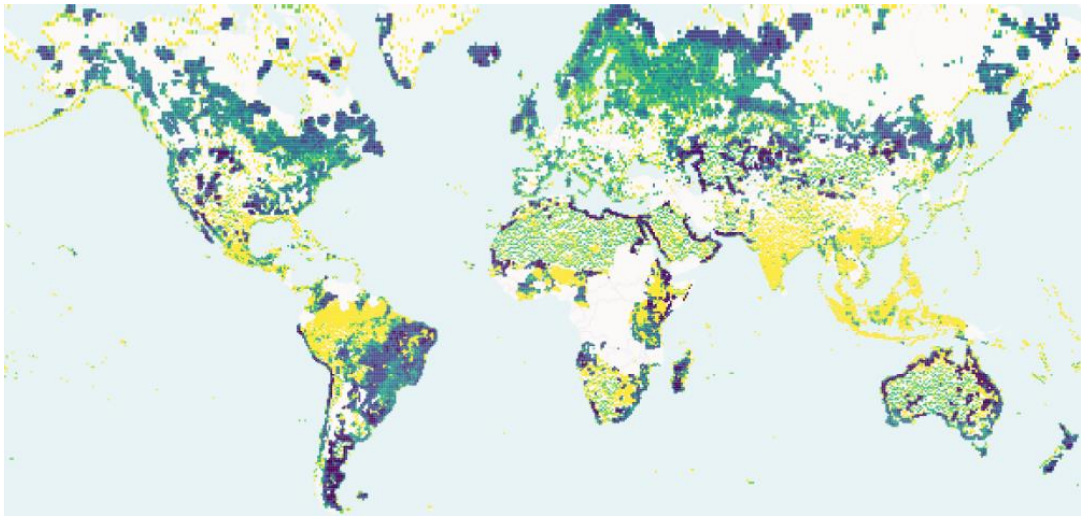

c)

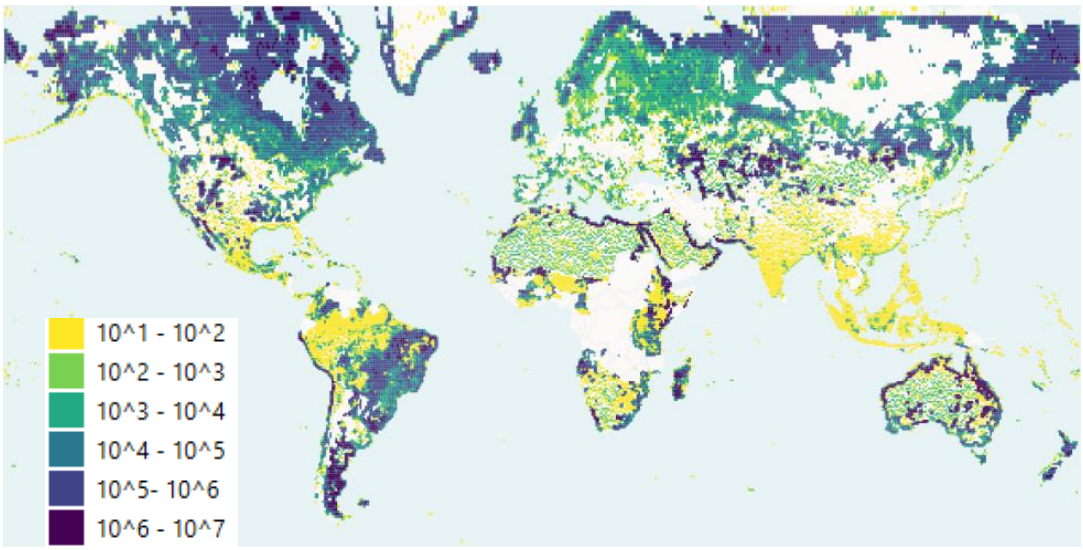

Figure 25: Map of yearly hydrogen potentials by MERRA-2 cell

(a) S_1 (b), S_1 with a 12 €/kg LCOH limit (c) and S_2 with a 12 €/kg LCOH limit

Table 19: Leading countries in yearly hydrogen potentials S_1 with a 12 €/kg LCOH limit

Country	H_2 (Mt)	Share from global H_2	Cumulative global H_2 share
Australia	1,006	19.4%	19.4%
Kazakhstan	391	7.5%	26.9%
Brazil	374	7.2%	34.1%
Argentina	346	6.7%	40.8%
United States of America	308	5.9%	46.7%
Russian Federation	301	5.8%	52.5%
Canada	177	3.4%	55.9%
China, People's Republic	161	3.1%	59.0%
Egypt	160	3.1%	62.1%
Ethiopia	116	2.2%	64.3%
Saudi Arabia	115	2.2%	66.5%
Libya	109	2.1%	68.6%
Mauritania	92	1.8%	70.4%
Madagascar	87	1.7%	72.1%
Kenya	86	1.7%	73.8%
Rest of the world (159 countries)	1,363	26.2%	100.0%
Total	5,193	100%	

For further analysis concerning the rest of the world or any region of interest, two dashboards provide additional information. First, an interactive map highlights primary hydrogen producers, in which the user is able to control the LCOH range. For instance, Figure 26 highlights dominant countries when considering a 12 €/kg LCOH limit under S_1. And second, a cost-potential curve dashboard that can be filtered to a specific country or continent. Furthermore, the dashboard indicates the geographic distribution of hydrogen potentials at each LCOH point on the curve by county and continent, as well as the distribution of hydrogen potentials by RES. Figure 27 provides an overview of the interactive cost-potential curve dashboard.

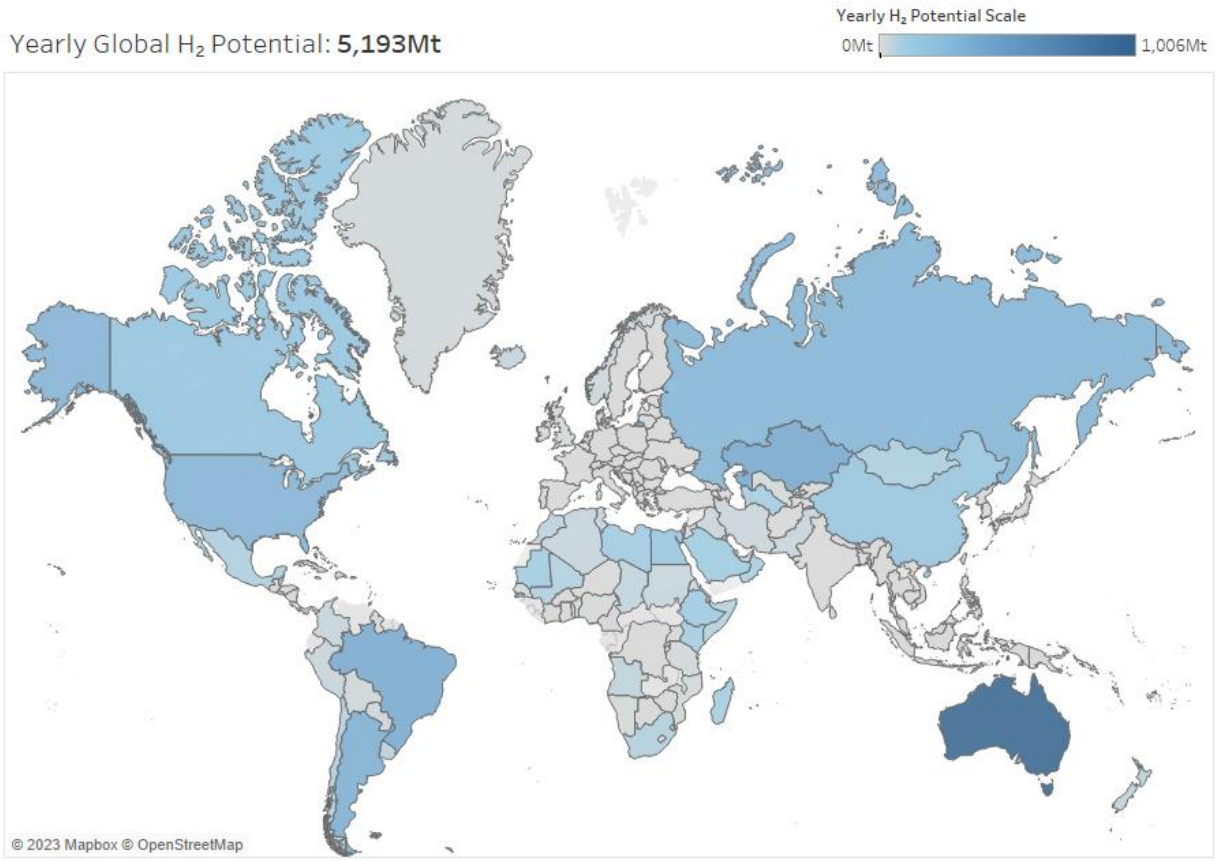

Figure 26: Map of yearly hydrogen potentials by country with a 12 €/kg LCOH limit under S_1

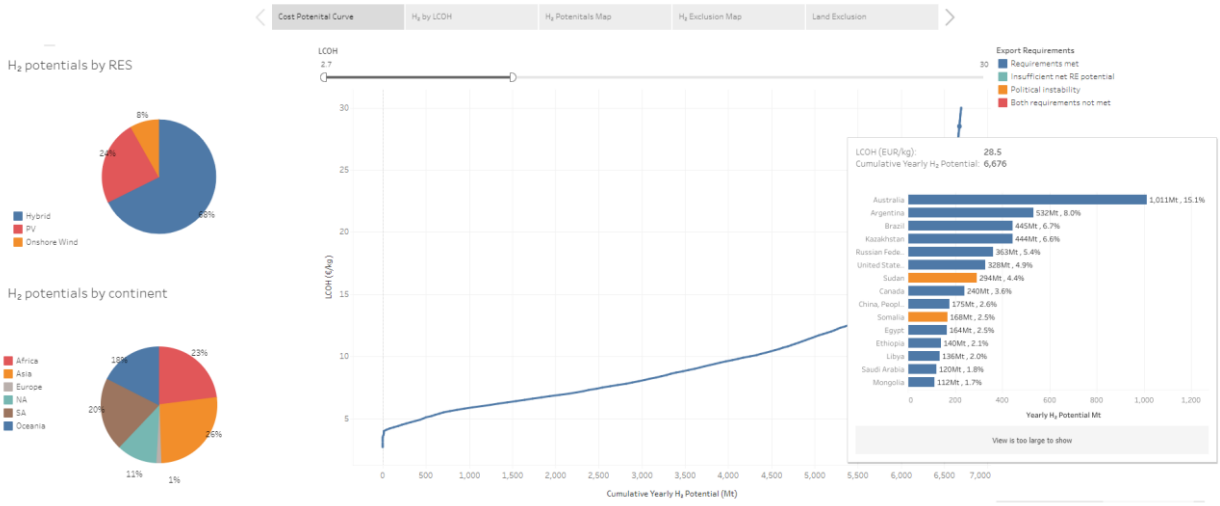

Figure 27: Cost-potential curve interactive dashboard

4.3.3 Comparative Analysis with Existing Studies

This section compares the calculated global hydrogen potentials against estimates of equivalent studies. This comparison aims to validate the results of this study from an order of magnitude perspective. Six studies were considered, five with a global or a large regional scope and one with a country-level analysis. The studies were selected based on the similar attributes they shared with this work, but nonetheless, there were still significant differences in LE and cost-potential calculation methodologies.

As noted by IRENA (2022, p. 6), the potential of green hydrogen "is not a single value; it is a continuous relationship between cost and renewable capacity." Hence, comparing potentials against other studies is not a straightforward evaluation. Most of the compared studies projected future scenarios of cost-potentials, while this thesis deals with cost-potentials for the year 2020. Accordingly, the cost element was of lesser relevance for this specific analysis. Accordingly, the maximal potentials reported in the studies were recorded without considering their associated LCOH. The list of studies and their attributes can be seen in Table 20. Moreover, Table 21 presents the EC that were considered in the applied LE analysis in the studies.

Table 20: Hydrogen potentials comparative analysis studies

Publication	Potential year	RES				Electrolyzer	Weather data		Geographic scope	PD (MW/km²)	
		Onshore wind	PV	Hybrid	Other		Source	Year		PV	Wind
Fasihi and Breyer (2020)	2020-2050	x	x	x		Alkaline	NASA	2005	Global	74	8.4
Franzmann et al. (2023)	2020-2050	x	x	x		PEM	MERRA-2 GWA[25]	2019	Global (28 countries)		
IRENA (2022)	2030, 2050	x	x	x	Offshore wind	Alkaline	ERA5	2018	Global	45	5
Lux et al. (2021)	2030, 2050	x	x		Offshore wind CSP Rooftop PV	PEM SOEC	ERA5	2010	MENA (10 countries)		50-57
Okunlola et al. (2022)	2019	x	x			PEM	GWA[25] GSA[26]	n.d.	Canada		
Pfennig et al. (2023)	2050	x	x	x		PEM	ERA5	2008-2012	Global w/o EEA (98 countries)	40	15
FfE	2020	x	x	x		PEM	MERRA-2	2012	Global	45/69	15/29.3

[25] Global Wind Atlas (GWA)
[26] Global Solar Atlas (GSA)

Table 21: EC applied in existing hydrogen potentials studies

	Water Bodies	Agricultural Land	Settlement Areas	Forests	Wetlands	Snow-Covered Areas	Aviation Areas	Military Zone	Road Network	Access to Road Network	Access to Water Bodies	Water Stress	Slope of Terrain	Protected Areas	Elevation	Population Density	Access to Settlement Areas
Publication	1.1	1.2	1.3	1.4	1.5	1.6	1.7	1.8	2.1	2.2	3.1	3.2	4	5	6	7	8
Fasihi and Breyer (2020)																	
Franzmann et al. (2023)	x	x	x	x	x	x	x	x	x				x	x			
IRENA (2022)		x	x	x	x						x	x	x	x		x	
Lux et al. (2021)	x	x	x	x	x	x							x	x	x		
Okunlola et al. (2022)	x		x	x			x		x					x			
Pfennig et al. (2023)	x	x	x	x		x					x	x	x	x		x	x
S_1	x	x	x	x	x	x	x	x	x	x	x	x	x	x	x	x	x

It is important to note that while the compared studies used some parallel EC, their definitions and underlying datasets were not identical to those in this work. Furthermore, certain studies included EC that were not included in the applied LE analysis in this thesis. Below are additional LE details that may lead to variations in hydrogen potentials:

- Fasihi and Breyer (2020) did not apply an LE analysis, but instead, they assumed a land eligibility rate of 10% per cell.
- Franzmann et al. (2023) excluded the following from their study as well: historical areas, leisure and camping, mining, pastures, power lines, railways, recreational areas, salt flats, and sandy lands.
- IRENA (2022) excluded croplands for PV only, where the "cropland" class was excluded completely, and the "cropland-natural" class had a 40% utilization factor.
- Lux et al. (2021) allowed the usage of barren land, forests, grassland, savanna, scrubland, snow areas, and croplands with utilization factors ranging from 15% to 40%.
- Okunlola et al. (2022) examined additional scenarios. Each scenario included all EC listed in Table 21, adding one of the following criteria: wetlands (defined as snow-covered areas and peatlands), distance to power transmission lines, distance to gas pipelines, and distance to major population clusters. To the author's best understanding,

each criterion's impact on hydrogen potentials was examined exclusively by adding it separately to the study's baseline LE scenario.

- Pfennig et al. (2023) applied an LCOE threshold of 30 €/MWh for PV and 40 €/MWh for wind turbines, as well as a UL for distance to ports and pipelines.

Since the studies deal with different geographical scopes, the compared hydrogen potentials were calculated for each study accordingly with the effort of having as similar scope as possible[27]. While hydrogen potentials were reported in different units among studies, they were converted to match the units reported in this study[28]. Furthermore, as potentials were often communicated in graphs, exact total potentials could not always be identified but rather approximated based on the visible data in these figures. The comparison of hydrogen potentials is presented in Table 22. Additionally, as certain studies had multiple scenarios in their results, the specific scenarios used for this comparison are mentioned in Table 22 as well.

The hydrogen potentials were compared with the results calculated under S_1 and for both PD scenarios in this work (see 3.3). The ratio column is the proportion between the estimate of the compared publication to that of this thesis. Furthermore, another comparison is made against each study's most compatible scenario (MCS), an LE scenario more similar to the one applied in the compared study. In some cases, a tailor-made MCS was created, and in others, a more general scenario was used. The MCS for each study are as follows:

- The MCS for Fasihi and Breyer (2020) mimicked the LE methodology applied by the study, using an eligible land rate of 10% per cell.
- Franzmann et al. (2023) and Lux et al. (2021) did not exclude water-scarce areas, nor did they exclude remote areas, i.e., areas without access to roads and settlements. Therefore, these three EC were not applied in the MCS for these studies. While there are other differences in LE methodologies, these three absent EC were more restrictive.
- Two scenarios were evaluated from the work of Okunlola et al. (2022): a baseline scenario and another one in which areas without access to major population clusters in a proximity of 160km were excluded. Two MSCs were created in this case based on the same EC listed in Table 21 for each scenario.

[27] Franzmann et al. (2023) analyzed 28 countries, and Lux et al. (2021) considered eight countries from the MENA regions. The same set of countries was used for the comparison of each study. Pfennig et al. (2023) had a global analysis excluding EEA, the comparison was made accordingly, excluding the countries listed in eurostat (2020).
[28] Conversions of energy units were made based on the low heating value (LHV) unless results were reported in high heating values (HHV) by studies.

- The MCS for IRENA (2022) applied the same list of EC as applied in their study, as seen in Table 21. In the case of agricultural land, the EC definition could not be replicated precisely to allow a 40% utilization factor for PV installation on "cropland-natural" class. Therefore, all types of agricultural land were excluded completely for PV but included for onshore wind turbines. Furthermore, this thesis used two data sets for agricultural land exclusion: Copernicus Climate Change Service, Climate Data Store (2019) and NASA EOSDIS Land Processes DAAC (2017). The latter was more restrictive and therefore was also removed from the MCS in this case.
- Pfennig et al. (2023) was the only study that applied more EC and had stricter definitions for some criteria. As these EC could not be added, no MCS was created.

While adapting the hydrogen potentials as much as possible, it is important to note that EC definitions still vary between this work and the comparable studies, as well as other system attributes and commutation methodologies.

Table 22: Hydrogen potentials comparative analysis

Scope	Publication	Potential yea	Scenario	Publication H_2 (Mt)	H_2 comparison (Mt)				Ratio			
					Low PD		High PD		Low PD		High PD	
					S1	MCS	S1	MCS	S1	MCS	S1	MCS
Global	Fasihi and Breyer (2020)	2020	Onsite	25,374	6,856	17,063	11,852	29,196	3.7	1.5	2.1	0.9
	Franzmann et al. (2023)	2050[29]		45,005	3,480	13,349	6,084	23,333	12.9	3.4	7.4	1.9
	IRENA (2022)[30]	2050	Optimistic	83,333	6,856	33,544	11,852	59,056	12.2	2.5	7.0	1.4
	Pfennig et al. (2023)	2050		3,510	6,781	-	11,716	-	0.5	-	0.3	-
MENA	Lux et al. (2021)	2030	WACC 7%	3,660	558	2,400	962	4,148	6.6	1.5	3.8	0.9
Australia	IRENA (2022)[30]	2030	Optimistic	4,983	1,011	2,335	1,754	4,115	4.9	2.1	2.8	1.2
Canada	Okunlola et al. (2022)	2019	Baseline	2,346	240	2,517	431	4,501	9.8	0.9	5.4	0.5
		2019	Access to major population clusters[31]	1,146	240	1,360	431	2,417	4.8	0.8	2.7	0.5
USA	IRENA (2022)[30]	2030	Optimistic	3,208	328	2,494	571	4,478	9.8	1.3	5.6	0.7

[29] While this study discussed a 2020 scenario as well, a comparable value of hydrogen potentials was not identified for this year.

[30] "The definition of the different scenarios depends on the assumptions regarding the CAPEX of the components of the standalone systems, the efficiency of the electrolyser and the WACC" (IRENA, 2022)

[31] This scenario applies the same EC as in the baseline scenario in this study, and additionally, it excludes areas with no major population clusters (defined with a population density of 3236 people/km²) in the proximity of 160 km.

Ratio values highlighted in red mean hydrogen potentials were higher compared to this study, while blue highlights indicate the opposite. When looking at S_1 with low PD, all studies, except Pfennig et al. (2023), had higher potential estimates. Most notably, Franzmann et al. (2023) had the highest ratio compared to the potentials calculated under S_1 in this study. However, the MCS ratio is significantly lower. This difference emphasizes the significance of EC related to remoteness and water scarcity. Franzmann et al. (2023, p. 11) also discussed the latter in their work, pointing out the future limitations it sets for hydrogen potentials.

In comparison to IRNEA (2022), the results of this study were also significantly lower. The comparison to MCS reduces the difference substantially, which can be attributed to the lack of remoteness EC, a limitation noted by IRENA (2022) as well. The different definitions of the agricultural land EC are also likely to play a key variation driver here, as this EC has a rather significant restriction level (see 4.2.2). Another possible contributor to the potentials difference is the inclusion of offshore wind by IRNA (2022). The study provided the hydrogen production RES share breakdown for a few selected countries, such as Australia and the United States. For both countries, offshore wind was not mentioned in the RES mix. Therefore, a country-level comparison was made, and in both cases, the potential ratios were significantly lower than the global ratios. This evaluation emphasizes the additional value offshore wind could provide to the global hydrogen arena. It is worth mentioning that incorporating this RES in the optimization model (Martínez Pérez, 2022) is already underway within the framework of the FfE.

Fasihi and Breyer (2020) used a different approach for LE, taking 10% of land per cell. When comparing to the MCS, the difference between hydrogen potentials decreased drastically, bringing the potentials under high PD closer to equivalence. As noted in Table 20, the compared study used a significantly higher PD for PV, which may be another driver for the differences in potentials. While the wind PD used by Fasihi and Breyer (2020) was lower by almost half, wind power accounted for only a third of the hydrogen underlying RES in this work. Therefore, hydrogen potentials were more sensitive to the PD of PV. Interestingly, the eligible land share of 10% used by Fasihi and Breyer (2020) was about three times the average eligible land share per cell calculated in this work, and a similar ratio was found between the hydrogen potentials under S_1 with low PD. However, this argument does not apply when considering higher PD values. Another interesting perspective here is with relation to the LCOH, as the potential year is identical to that of this study, i.e., 2020. The study reported hydrogen potentials of 507 Mt under 2.6 €/kg, while under S_1 results, the same amount of hydrogen could be produced with a threshold

of 5.1 €/kg and 4.6 €/kg for a low PD and high PD, respectively. Nonetheless, analyzing what drives these cost variations was not in the scope of this study.

Okunlola et al. (2022) calculated hydrogen potentials in Canada for various scenarios, two of which were used in this comparison. Potentials were 10 times greater in their baseline scenario than in this study. When Okunlola et al. (2022) included the EC of access to major population clusters, their estimate shrank by 50%. However, the estimated potentials were still five times the potentials in this work. When looking at the MSC under low PD, potentials were almost equivalent in both scenarios. This comparison indicates not only the high restriction level of the access EC in this region but also other EC that were not considered in the respective MCS. For example, slope of terrain, agricultural areas, and water stress each excluded roughly 10% of hydrogen potentials in Canada under S_1. Nonetheless, the intersection of criteria was not analyzed in this work. Therefore, it is not to say that the potentials excluded by these EC can be summed together (e.g., to 30%), but it may be that the excluded land by these EC was overlapping.

The only study with more EC and some EC with stricter definitions, compared to this work, was the study by Pfennig et al. (2023). For instance, as shown in Figure 9 in section 4.1.2, this study used the most strict approach regarding water scarcity, which was also the most limiting EC on a global level. It is therefore reasonable that the potentials calculated in this work were greater. Nevertheless, the ratio of the potentials in this case was the smallest compared to the rest of the studies. It is worth mentioning that Pfennig et al. (2023) used a different methodology to calculate the global hydrogen potentials. While costs and potentials were calculated on a cell level in this study, Pfennig et al. (2023) selected 600 sites for which they performed optimization and later upscaled the results on a global scale.

As Ryberg et al. (2017) concluded in their study, inconsistent LE methodologies among different studies lead to substantially different results, and the comparison above echoes their findings. Nonetheless, there were other differences between the various studies that were not exclusive to LE methods, and therefore, it is challenging to pinpoint the exact drivers for variations among results. However, it can generally be deduced from the analysis above that hydrogen potentials are highly sensitive to LE definitions. A higher number of EC, as well as stricter EC definitions, lead to less available land, thus resulting in a reduction of hydrogen potentials. While such reductions might be substantial, a restrictive approach is recommended to foster social and environmental sustainability (Spyridonidou & Vagiona, 2023, p. 2972) and simultaneously assure a reliable hydrogen supply.

The reviewed studies unanimously reported that future hydrogen potentials largely exceed their future demand in competitive costs. If a more restrictive LE approach is applied, such as in Pfennig et al. (2023) or this study, it can be assumed that hydrogen potentials will also decrease in regions with attractive costs. As a result, hydrogen potentials with higher costs will be needed to meet future demand. Nonetheless, this assumption should be further examined in future research. Another topic generally absent from discussions was the land use and water demand of other sectors, whether in energy or other fields. Tonelli et al. (2023) addressed this research question and identified countries where future hydrogen production would face competition from other resource consumers and would exacerbate land and water scarcity. They found that hydrogen production is expected to intensify water stress in regions already subjected to it. On the other hand, they found that major hydrogen contributors like Australia and Canada are expected to satisfy domestic hydrogen demand and export it while not adding additional stress on land and water.

5 Conclusions and Outlook

This section encapsulates the findings of this thesis while providing future recommendations and highlighting its limitations. Potential further research and developments based on this work are provided as well.

This thesis developed and applied a land eligibility (LE) framework for a global green hydrogen analysis use case. The LE analysis was designed to uphold the principles of a strict sustainable development approach that supports a just energy transition. Eight extensive exclusion criteria were established (see Table 11) and can be used as a hydrogen LE basis for other large regional analyses. However, considering the global scope for which the LE was designed, it is implausible to suit land use requirements and their policies everywhere, as climatic conditions and regulations are not a geographic constant. Nonetheless, future international policies are needed to provide global guidelines for green hydrogen LE.

The systematic literature review in this thesis echoed the prevalence of LE inconsistencies identified by Ryberg et al. (2017), i.e., the inconsistencies in data usage, methodologies, and criteria definitions, as well as the insufficient documentation of LE methodologies. From the perspective of this work, it is the latter that is most acute. While differences in LE methodologies are frequent as they are shaped by their goal and scope, their detailed documentation can support

a better understanding of results variation among studies. Furthermore, analyzing such variations can provide additional insights.

The LE of green hydrogen is primarily driven by its underlying RES. Nevertheless, there are a few LE features that are unique to hydrogen production. Most critically, the criteria that ensure water availability for electrolysis within the sustainable boundaries of this resource. Assessing LE from this perspective necessitates a comprehensive evaluation of both proximity to water sources and the level of water scarcity. However, definitions of these criteria were not conclusive enough, and their variations led to significant differences of LE. A notable knowledge gap was identified regarding the maximum permissible distance between water sources and hydrogen plants. Additionally, while desalination was considered a viable option in water-scarce regions, it remains uncertain whether this approach might result in additional water stress. Another vital factor for hydrogen LE is the access to a road network that can support the development of a hydrogen infrastructure, along with the proximity to settlements that can provide the required human resources for its operation.

The reviewed literature made it clear that socio-political criteria are fundamental for hydrogen LE to ensure both the benefits of domestic hydrogen projects and the prosperity of hydrogen import-export relations. Concerning the latter, prosperity entails not only securing the hydrogen supply of the importer but also guaranteeing the strengthening of the exporter's economy. As these criteria were addressed only to a minimal extent in this thesis, a thorough analysis of these perspectives is needed in future expansions of this study.

The LE resulted in a global land availability of 5 million km² and 6 million km² for hydrogen production powered by PV and onshore wind, respectively. Additionally, it produced an average eligible land share per cell of 3.3% for PV and 3.8% for onshore wind. These measures can provide input for studies that estimate hydrogen or RES potentials based on a grided approach while excluding the LE analysis step. Among continents, Africa had the largest share of eligible land, representing 30% of the global land availability, while Europe made up only 1% of eligible land. When considered eligible for hydrogen production, remote areas increased land availability by roughly 35% for both RES technologies. A significant portion of this potential land was in North America. Nonetheless, planning large-scale hydrogen projects in such areas must account for the additional costs incurred by access infrastructure developments. Regarding the RES for hydrogen production, while onshore wind occupied more space, PV was the predominant power source, which coincided with its higher power density.

When considering potentials with a levelized cost of hydrogen (LCOH) of up to 12 €/kg, the global primary restrictor to hydrogen potentials was water stress, reducing hydrogen potentials by 45%. The impact of this criterion was most palpable in Africa, where 68% of hydrogen potentials were excluded due to this criterion. Additional significant constraints to hydrogen potentials included protected areas and critical habitat, as well as agricultural areas and croplands, reducing potentials by 28% and 26%, respectively. On a continental level, these dominant restrictors exhibited similar trends with some regional variations. Notably, hydrogen potentials in Europe were reduced by 50% due to agricultural land. This substantial exclusion rate encourages further exploration of the co-existence of agriculture and green hydrogen production, a practice supported by very few studies. Further research on this topic can contribute to shaping land eligibility recommendations.

The restricted land in North America due to inadequate access was also expressed in the loss of hydrogen potentials, exclusively reducing 4.4% of economically viable potentials. That is, the exclusion of potentials, which were not restricted by any other criteria except access criteria. On the other hand, the high level of land restriction due to insufficient connectivity in Africa did not lead to an additional reduction in hydrogen potentials, as other factors already excluded the same land. These findings extenuate the valuable insights that can be derived from the analysis of overlapping criteria, which was one of the limitations of this study.

Delving into the LE impact assessment of hydrogen potentials and their associated costs revealed nuanced insights compared to exclusively evaluating land availability. The exclusion rate variation between land and hydrogen potentials sheds light on the suitability of certain climatic and topographic conditions for hydrogen production. For instance, while forests excluded 30% of the land, they reduced economically efficient hydrogen potentials by only 20%. This finding indicates that a great portion of tree regions do not have favorable conditions for hydrogen production. The slope of the terrain was a significant land restrictor as well, particularly for PV-based hydrogen. However, while it led to the respective land exclusion of 24% and 15% of PV and onshore wind, hydrogen potentials were reduced to a lesser extent of 20% and 8%, respectively. Like forests, areas with steep slopes were less viable for hydrogen production. On the other hand, water-stressed regions exhibit greater appeal for hydrogen production, with hydrogen potentials reducing by an additional 10% compared to land.

The substantial losses in hydrogen potentials due to water stress provoke the need to evaluate the approach of co-location RES and electrolysis facilities or the reassessment of reasonable water transportation distances between both facilities. Another factor that was generally absent in

hydrogen land eligibility analyses and potential estimations, including in this work, was the competition for land and water resources with other sectors and industries. Future research can follow the work of Tonelli et al. (2023) and estimate hydrogen potentials while considering the resource demand of other sectors. With the great economic appeal of RE conditions in water-scarce regions, further research like the study mentioned above is crucial to ensure that hydrogen projects are only implemented if they uphold the principles of sustainable development.

This analysis revealed a global production potential of 6,856 Mt of green hydrogen, from which 5,193 (75%) is achievable within a 12 €/kg threshold based on economic parameters for the year 2020. These estimates notably surpass the anticipated hydrogen demand for the year 2050 by nearly tenfold. When considering a 12 €/kg LCOH limit, Australia is the largest single contributor to hydrogen potentials, accounting for almost a fifth of the global potential. Other major potential countries include Kazakhstan, Brazil, Argentina, the United States, and Russia, each generating between 6% and 7% of the global potential supply. Equatorial regions demonstrate relatively lower hydrogen productivity, and regions approaching the Arctic Circle exhibit considerable potentials, which are significantly curtailed due to the regional lack of access infrastructure.

The restrictive LE approach in this thesis resulted in relatively conservative estimates of global hydrogen potentials compared to similar studies. Even so, there was a unanimous agreement in this study and other literature that future hydrogen production could satisfy its global demand with economic efficiency. Nevertheless, this study revealed that hydrogen potentials are highly sensitive to the underlying LE for their estimation, as well as the defined RES power densities. These sensitivities, coupled with the assumption that practical land allocation may not perfectly align with optimal locations or reach its maximum capacity, introduce uncertainty regarding the precise LCOH level at which future demand could be met. However, there is no indication of whether such deviations from the forecasted LCOH values would be significant. Consequently, it is prudent to consider the outcomes of this study and similar large-scale analyses as approximate estimations and exercise caution in their interpretation. For localized hydrogen planning, it is advisable to rely on analyses with narrower scopes and heightened accuracy levels.

The developed land allocation model for hydrogen production in this thesis enabled the maximal utilization of spatial availability. Nevertheless, the model did not account for wind turbines' shadowing effect on PV installation in hybrid sites. As a hybrid system was the dominant configuration in this study, future developments in this model could precise the result by adding the shadowing effect to its methodology. Additional improvements can enhance the model's accuracy, such as excluding certain class types with a utilization factor, applying variable power

densities according to geographic regions, and adding offshore wind to the RES mix and evaluating its land eligibility analysis.

The results of this thesis have been compiled into an interactive dashboard (Barak, 2023), providing accessibility and enabling flexible analysis across various geographic scopes. Future developments of the dashboard could unlock deeper insights by incorporating supplementary features and enhancing its spatial resolution to a MERRA-2 cell level. The author aspires that the interactive publishing of the results will serve as a valuable resource for diverse users, foster knowledge dissemination, and contribute to the sustainable development of future hydrogen economies.

6 References

Action Renewables. (2019). *How does a wind turbine work? - Action Renewables*. https://actionrenewables.co.uk/news/how-does-a-wind-turbine-work/ (access date: 2023-11-25).

Agora Energiewende and AFRY Management Consulting. (2021). *No-regret hydrogen: Charting early steps for H_2 infrastructure in Europe*. https://static.agora-energiewende.de/fileadmin/Projekte/2021/2021_02_EU_H2Grid/A-EW_203_No-regret-hydrogen_WEB.pdf.

Ali, F., Bennui, A., Chowdhury, S., & Techato, K. (2022). Suitable Site Selection for Solar-Based Green Hydrogen in Southern Thailand Using GIS-MCDM Approach. *Sustainability*, *14*(11), 6597. https://doi.org/10.3390/su14116597

Almutairi, K. (2022). Determining the appropriate location for renewable hydrogen development using multi-criteria decision-making approaches. *International Journal of Energy Research*, *46*(5), 5876–5895. https://doi.org/10.1002/er.7528

Amatulli, G., Domisch, S., Tuanmu, M.-N., Parmentier, B., Ranipeta, A., Malczyk, J., & Jetz, W. (2018). A suite of global, cross-scale topographic variables for environmental and biodiversity modeling. *Scientific Data*, *5*, 180040. https://doi.org/10.1038/sdata.2018.40

Ao Xuan, H., Vu Trinh, V., Techato, K., & Phoungthong, K. (2022). Use of hybrid MCDM methods for site location of solar-powered hydrogen production plants in Uzbekistan. *Sustainable Energy Technologies and Assessments*, *52*, 101979. https://doi.org/10.1016/j.seta.2022.101979

Barak, T. (2023). *Global land eligibility for green hydrogen: costs & potenitlas.* FfE; Technical University of Munich. https://public.tableau.com/views/Globallandeligibilityforgreenhydrogencostspotenitlas/Thesis?language=en-US&:display_count=n&:origin=viz_share_link (access date: 2023-11-14).

Bhandari, R. (2022). Green hydrogen production potential in West Africa – Case of Niger. *Renewable Energy*, *196*, 800–811. https://doi.org/10.1016/j.renene.2022.07.052

Bogdanov, D., & Breyer, C. (2016). North-East Asian Super Grid for 100% renewable energy supply: Optimal mix of energy technologies for electricity, gas and heat supply options. *Energy Conversion and Management*, *112*, 176–190. https://doi.org/10.1016/j.enconman.2016.01.019

Bolinger, M., & Bolinger, G. (2022). Land Requirements for Utility-Scale PV: An Empirical Update on Power and Energy Density. *IEEE Journal of Photovoltaics*, *12*(2), 589–594. https://doi.org/10.1109/JPHOTOV.2021.3136805

Brändle, G., Schönfisch, M., & Schulte, S. (2021). Estimating long-term global supply costs for low-carbon hydrogen. *Applied Energy*, *302*, 117481. https://doi.org/10.1016/j.apenergy.2021.117481

Braun, J., Kern, J., Scholz, Y., Hu, W., Moser, M., Schillings, C., Simon, S., Ersoy, S., & Terrapon-Pfaff, J. (2022). Technische und risikobewertete Kosten-Potenzial-Analyse der MENA-Region. MENA-Fuels: Teilbericht 10 des Deutschen Zentrums für Luftund Raumfahrt (DLR) und des Wuppertal Instituts an das Bundesministerium für Wirtschaft und Klimaschutz (BMWK). Wuppertal, Stuttgart, Saarbrücken.

Brauneder, K. M., Montes, C., Blyth, S., Bennun, L., Butchart, S. H. M., Hoffmann, M., Burgess, N. D., Cuttelod, A., Jones, M. I., Kapos, V., Pilgrim, J., Tolley, M. J., Underwood, E. C., Weatherdon, L. V., & Brooks, S. E. (2018). Global screening for Critical Habitat in the terrestrial realm. *PloS One*, *13*(3). https://doi.org/10.1371/journal.pone.0193102

Breitschopf, B., Thomann, J., Garcia, J. F., Kleinschmitt, C., Hettesheimer, T., Neuner, F., Wittmann, F., Roth, F., Pieton, N., & Lenivova, V. (2022). *Importing hydrogen and hydrogen derivatives: Export countries. HYPAT Working Paper 02/2022.* Karlsruhe:. Fraunhofer ISI (ed.).

Čablová, L., Pates, R., Miovský, M., & Noel, J. (2017). How to Write a Systematic Review Article and Meta-Analysis. In T. F. Babor, K. Stenius, R. Pates, M. Miovský, J. O'Reilly, & P. Candon (Eds.), *Publishing Addiction Science: A Guide for the Perplexed* (pp. 173–189). Ubiquity Press. https://doi.org/10.5334/bbd.i

Capurso, T., Stefanizzi, M., Torresi, M., & Camporeale, S. M. (2022). Perspective of the role of hydrogen in the 21st century energy transition. *Energy Conversion and Management*, *251*, 114898. https://doi.org/10.1016/j.enconman.2021.114898

Center for International Earth Science Information Network - CIESIN - Columbia University. (2018). *Gridded Population of the World, Version 4 (GPWv4): Population Density, Revision 11*. https://doi.org/10.7927/H49C6VHW

Copernicus Climate Change Service, Climate Data Store. (2019). *Land cover classification gridded maps from 1992 to present derived from satellite observations*. Copernicus Climate Change Service (C3S) Climate Data Store (CDS).

https://cds.climate.copernicus.eu/cdsapp#!/dataset/10.24381/cds.006f2c9a?tab=overview. https://doi.org/10.24381/CDS.006F2C9A

Cremonese, L., Mbungu, G. K., & Quitzow, R. (2023). The sustainability of green hydrogen: An uncertain proposition. *International Journal of Hydrogen Energy*, *48*(51), 19422–19436. https://doi.org/10.1016/j.ijhydene.2023.01.350

Damodaran, A. (2023). *Country Default Spreads and Risk Premiums*. https://pages.stern.nyu.edu/~adamodar/New_Home_Page/datafile/ctryprem.html (access date: 2023-11-22).

Defourny, P., Lamarche, C., Marissiaux, Q., Brockmann, C., Boettcher, M., & Kirches, G. (2021). *Product User Guide and Specification: ICDR Land Cover 2016-2020.* UCLOUVAIN; ROCKMANN CONSULT GMBH. https://datastore.copernicus-climate.eu/documents/satellite-land-cover/D5.3.1_PUGS_ICDR_LC_v2.1.x_PRODUCTS_v1.1.pdf.

Dehshiri, S. J. H., & Zanjirchi, S. M. (2022). Comparative analysis of multicriteria decision-making approaches for evaluation hydrogen projects development from wind energy. *International Journal of Energy Research*, *46*(10), 13356–13376. https://doi.org/10.1002/er.8044

Dehshiri, S. S. H., & Dehshiri, S. J. H. (2022). Locating wind farm for power and hydrogen production based on Geographic information system and multi-criteria decision making method: An application. *International Journal of Hydrogen Energy*, *47*(58), 24569–24583. https://doi.org/10.1016/j.ijhydene.2022.03.083

Dillman, K. J., & Heinonen, J. (2022). A 'just' hydrogen economy: A normative energy justice assessment of the hydrogen economy. *Renewable and Sustainable Energy Reviews*, *167*, 112648. https://doi.org/10.1016/j.rser.2022.112648

EarthEnv. (2023). *Global 1,5,10,100-km Topography*. https://www.earthenv.org/topography (access date: 2023-10-03).

Enevoldsen, P., & Jacobson, M. Z. (2021). Data investigation of installed and output power densities of onshore and offshore wind turbines worldwide. *Energy for Sustainable Development*, *60*, 40–51. https://doi.org/10.1016/j.esd.2020.11.004

European Commission. (2020). *Communication from The Commission to The European Parliament, The Council, The European Economic and Social Committee and The Committee of The Regions: A hydrogen strategy for a climate-neutral Europe*. Brussels.

https://eur-lex.europa.eu/legal-content/EN/TXT/PDF/?uri=CELEX:52020DC0301&from=EN.

European Commission. (2022). *Energy systems integration: Hydrogen*. https://energy.ec.europa.eu/topics/energy-systems-integration/hydrogen_en (access date: 2023-08-08).

European Energy Exchange AG. (2023). *EEX HYDRIX*. https://www.eex-transparency.com/hydrogen/germany (access date: 2023-11-13).

eurostat. (2020). *Glossary: European Economic Area (EEA)*. https://ec.europa.eu/eurostat/statistics-explained/index.php?title=Glossary:European_Economic_Area_(EEA) (access date: 2023-11-10).

Fasihi, M., & Breyer, C. (2020). Baseload electricity and hydrogen supply based on hybrid PV-wind power plants. *Journal of Cleaner Production, 243*, 118466. https://doi.org/10.1016/j.jclepro.2019.118466

FfE. (2022, November 28). *ISAaR – Integrated Simulation Model for Unit Dispatch and Expansion with Regionalization - FFE Website*. https://www.ffe.de/en/tools/isaar/ (access date: 2023-03-25).

Flanders Marine Institute. (2019). *Maritime Boundaries Geodatabase: Maritime Boundaries and Exclusive Economic Zones (200NM)*. https://www.marineregions.org/ https://doi.org/10.14284/386. https://doi.org/10.14284/386

Franzmann, D., Heinrichs, H., Lippkau, F., Addanki, T., Winkler, C., Buchenberg, P., Hamacher, T., Blesl, M., Linßen, J., & Stolten, D. (2023). Green hydrogen cost-potentials for global trade. *International Journal of Hydrogen Energy.* Advance online publication. https://doi.org/10.1016/j.ijhydene.2023.05.012

Fraunhofer IEE. (2023, September 7). *Global PtX Atlas*. https://devkopsys.de/ptx-atlas/#flaechenpotenzialanalyse (access date: 2023-09-25).

Gao, J., Men, H., Guo, F., Liang, P., & Fan, Y. (2021). A multi-criteria decision-making framework for the location of photovoltaic power coupling hydrogen storage projects. *Journal of Energy Storage, 44*, 103469. https://doi.org/10.1016/j.est.2021.103469

German Federal Ministry for Economic Affairs and Energy. (June 2020). *The National Hydrogen Strategy*. Berlin. https://www.bmbf.de/bmbf/shareddocs/downloads/files/bmwi_nationale-wasserstoffstrategie_eng_s01.pdf?__blob=publicationFile&v=2.

GitHub. (2023, November 23). *GitHub - FZJ-IEK3-VSA/glaes: Geospatial Land Availability for Energy Systems*. https://github.com/FZJ-IEK3-VSA/glaes (access date: 2023-11-23).

Grohmann, C. H. (2015). Effects of spatial resolution on slope and aspect derivation for regional-scale analysis. *Computers & Geosciences*, *77*, 111–117. https://doi.org/10.1016/j.cageo.2015.02.003

Hank, C., Holst, M [Marius], Thelen, C., Kost, C., Längle, S., Schaadt, A., & Smolinka, T. (05/2023). *POWER-TO-X COUNTRY ANALYSES: Site-specific, comparative analysis for suitable Power-to-X pathways and products in developing and emerging countries*. A cost analysis study on behalf of H2Global. Fraunhofer ISE.

Heuser, P. M., Grube, T., Heinrichs, H., Robinius, M., & Stolten, D. (2020). Worldwide Hydrogen Provision Scheme Based on Renewable Energy, 2020020100. https://www.preprints.org/manuscript/202002.0100/v1.

IEA. (2023). *Global Hydrogen Review 2022*. https://iea.blob.core.windows.net/assets/c5bc75b1-9e4d-460d-9056-6e8e626a11c4/GlobalHydrogenReview2022.pdf.

Ince, A. C., Colpan, C. O., Hagen, A., & Serincan, M. F. (2021). Modeling and simulation of Power-to-X systems: A review. *Fuel*, *304*, 121354. https://doi.org/10.1016/j.fuel.2021.121354

Institute of Energy and Climate Research. (2023). *H2 ATLAS AFRICA*. https://www.h2atlas.de/en/ (access date: 2023-04-08).

IRENA. (2022). *Global hydrogen trade to meet the 1.5°C climate goal: Part III – Green hydrogen cost and potential*, *International Renewable Energy Agency*. Abu Dhabi. https://www.irena.org/publications/2022/May/Global-hydrogen-trade-Cost.

IRENA. (2023). *World Energy Transitions Outlook 2023: 1.5°C Pathway*. International Renewable Energy Agency, Abu Dhabi.

Ishaq, H., Dincer, I., & Crawford, C. (2022). A review on hydrogen production and utilization: Challenges and opportunities. *International Journal of Hydrogen Energy*, *47*(62), 26238–26264. https://doi.org/10.1016/j.ijhydene.2021.11.149

Jahangiri, M., Shamsabadi, A. A., Mostafaeipour, A., Rezaei, M., Yousefi, Y., & Pomares, L. M. (2020). Using fuzzy MCDM technique to find the best location in Qatar for exploiting wind and solar energy to generate hydrogen and electricity. *International Journal of Hydrogen Energy*, *45*(27), 13862–13875. https://doi.org/10.1016/j.ijhydene.2020.03.101

Jones, E., Qadir, M., van Vliet, M. T. H., Smakhtin, V., & Kang, S.-M. (2019). The state of desalination and brine production: A global outlook. *The Science of the Total Environment, 657*, 1343–1356. https://doi.org/10.1016/j.scitotenv.2018.12.076

Kally, E., & Fishelson, G. (1993). Water and peace : Water resources and the Arab-Israeli peace process. https://cir.nii.ac.jp/crid/1130000795462972928.

Kigle, S., Jetter, F., Ebner, M., & Schmid, T. (01/2022). *2 % der Landesfläche für Windenergie: ein geeignetes Maß? FfE-Discussion Paper 2022-01*. Forschungsstelle für Energiewirtschaft e.V. (FfE e.V.). https://www.ffe.de/wp-content/uploads/2022/02/FfE-Discussion-Paper-2-der-Landesflaeche-fuer-Windenergie-ein-geeignetes-Mass.pdf.

Kovač, A., Paranos, M., & Marciuš, D. (2021). Hydrogen in energy transition: A review. *International Journal of Hydrogen Energy, 46*(16), 10016–10035. https://doi.org/10.1016/j.ijhydene.2020.11.256

Kuzma, S., Bierkens, M. F., Lakshman, S., Luo, T., Saccoccia, L., Sutanudjaja, E. H., & van Beek, R. (2023). Aqueduct 4.0: Updated Decision-Relevant Global Water Risk Indicators. *World Resources Institute.* Advance online publication. https://doi.org/10.46830/writn.23.00061

Lux, B., Gegenheimer, J., Franke, K., Sensfuß, F., & Pfluger, B. (2021). Supply curves of electricity-based gaseous fuels in the MENA region. *Computers & Industrial Engineering, 162*, 107647. https://doi.org/10.1016/j.cie.2021.107647

Lux, B., & Pfluger, B. (2020). A supply curve of electricity-based hydrogen in a decarbonized European energy system in 2050. *Applied Energy, 269*, 115011. https://doi.org/10.1016/j.apenergy.2020.115011

Mah, A. X. Y., Ho, W. S., Hassim, M. H., Hashim, H., Muis, Zarina Ab, Ling, G. H. T., & Ho, C. S. (2022). Spatial optimization of photovoltaic-based hydrogen-electricity supply chain through an integrated geographical information system and mathematical modeling approach. *Clean Technologies and Environmental Policy, 24*(1), 393–412. https://doi.org/10.1007/s10098-021-02235-4

Malczewski, J. (2004). GIS-based land-use suitability analysis: a critical overview. *Progress in Planning, 62*(1), 3–65. https://doi.org/10.1016/j.progress.2003.09.002

Mamia, I., & Appelbaum, J. (2016). Shadow analysis of wind turbines for dual use of land for combined wind and solar photovoltaic power generation. *Renewable and Sustainable Energy Reviews, 55*, 713–718. https://doi.org/10.1016/j.rser.2015.11.009

Martínez Pérez, M. Á. (2022). *Modelling of Global Levelized Cost of Hydrogen under Use of an Open- Source Modelling Environment* [Master's Thesis]. Technical University of Munich, Munich. http://hdl.handle.net/10251/190448.

McKenna, R., Mulalic, I., Soutar, I., Weinand, J. M., Price, J., Petrović, S., & Mainzer, K. (2022). Exploring trade-offs between landscape impact, land use and resource quality for onshore variable renewable energy: an application to Great Britain. *Energy*, *250*, 123754. https://doi.org/10.1016/j.energy.2022.123754

Messaoudi, D., Settou, N., Negrou, B., & Settou, B. (2019). GIS based multi-criteria decision making for solar hydrogen production sites selection in Algeria. *International Journal of Hydrogen Energy*, *44*(60), 31808–31831. https://doi.org/10.1016/j.ijhydene.2019.10.099

Mostafaeipour, A., Dehshiri, S. J. H., Dehshiri, S. S. H., & Jahangiri, M. (2020). Prioritization of potential locations for harnessing wind energy to produce hydrogen in Afghanistan. *International Journal of Hydrogen Energy*, *45*(58), 33169–33184. https://doi.org/10.1016/j.ijhydene.2020.09.135

Mostafaeipour, A., Rezayat, H., & Rezaei, M. (2020). A thorough investigation of solar-powered hydrogen potential and accurate location planning for big cities: A case study. *International Journal of Hydrogen Energy*, *45*(56), 31599–31611. https://doi.org/10.1016/j.ijhydene.2020.08.211

Müller, L. A., Leonard, A., Trotter, P. A., & Hirmer, S. (2023). Green hydrogen production and use in low- and middle-income countries: A least-cost geospatial modelling approach applied to Kenya. *Applied Energy*, *343*, 121219. https://doi.org/10.1016/j.apenergy.2023.121219

NASA EOSDIS Land Processes DAAC. (2017). *NASA Making Earth System Data Records for Use in Research Environments (MEaSUREs) Global Food Security-support Analysis Data (GFSAD) 1 km datasets*. https://lpdaac.usgs.gov/documents/172/GFSAD1K_User_Guide_V1.pdf.

NASA Global Modeling and Assimilation Office. (2022). *MERRA-2*. https://gmao.gsfc.nasa.gov/reanalysis/MERRA-2/ (access date: 2023-11-17).

Okunlola, A., Davis, M., & Kumar, A. (2022). The development of an assessment framework to determine the technical hydrogen production potential from wind and solar energy. *Renewable and Sustainable Energy Reviews*, *166*, 112610. https://doi.org/10.1016/j.rser.2022.112610

Ong, S., Campbell, C., Denholm, P., Margolis, R., & Heath, G. (2013). *Land-Use Requirements for Solar Power Plants in the United States.* National Renewable Energy Laboratory (NREL). https://www.nrel.gov/docs/fy13osti/56290.pdf.

OpenStreetMap. (2023a, October 17). *Aeroways - OpenStreetMap Wiki*. https://wiki.openstreetmap.org/wiki/Aeroways#Military_aerodromes (access date: 2023-11-02).

OpenStreetMap. (2023b, October 30). *Key:highway - OpenStreetMap Wiki*. https://wiki.openstreetmap.org/wiki/Key:highway (access date: 2023-11-01).

OpenStreetMap. (2023c, October 30). *Key:military - OpenStreetMap Wiki*. https://wiki.openstreetmap.org/wiki/Key:military (access date: 2023-11-02).

OpenStreetMap. (2023d, October 30). *Key:place - OpenStreetMap Wiki*. https://wiki.openstreetmap.org/wiki/Key:place (access date: 2023-11-02).

OpenStreetMap. (2023e, November 1). *OpenStreetMap*. https://www.openstreetmap.org/#map=16/65.8636/179.9930 (access date: 2023-11-01).

Pfennig, M., Böttger, D., Häckner, B., Geiger, D., Zink, C., Bisevic, A., & Jansen, L. (2023). Global GIS-based potential analysis and cost assessment of Power-to-X fuels in 2050. *Applied Energy*, *347*, 121289. https://doi.org/10.1016/j.apenergy.2023.121289

Pieton, N., Abdel-Khalek, H., Fragoso, J., Franke, K., Graf, M., Holst, M [M.], Kleinschmitt, C., Müller, V. P., Weise, F., Drechsler, B., Lenivova, V., Nolden, C., Voglstätter, C., Wietschel, M., Bergup, E., & Sinha, M. F. A. (02/2023). *Export Potentials of Green Hydrogen – Methodology for a Techno-Economic Assessment, HYPAT Working Paper 02/2023*. Karlsruhe. Fraunhofer ISI (ed.).

PostGIS. (2023). *About PostGIS*. https://postgis.net/ (access date: 2023-11-17).

Rediske, G., Siluk, J. C. M., Gastaldo, N. G., Rigo, P. D., & Rosa, C. B. (2019). Determinant factors in site selection for photovoltaic projects: A systematic review. *International Journal of Energy Research*, *43*(5), 1689–1701. https://doi.org/10.1002/er.4321

Reed, J., Dailey, E., Fong, A., & Samuelsen, G. S. (2022). Time-phased geospatial siting analysis for renewable hydrogen production facilities under a billion-kilogram-scale build-out using California as an example. *International Journal of Hydrogen Energy*, *47*(66), 28224–28243. https://doi.org/10.1016/j.ijhydene.2022.06.179

Rezaei, M., Khalilpour, K. R., & Jahangiri, M. (2020). Multi-criteria location identification for wind/solar based hydrogen generation: The case of capital cities of a developing

country. *International Journal of Hydrogen Energy*, *45*(58), 33151–33168. https://doi.org/10.1016/j.ijhydene.2020.09.138

Ryberg, D. S., Robinius, M., & Stolten, D. (2017, December 21). *Methodological Framework for Determining the Land Eligibility of Renewable Energy Sources*. https://arxiv.org/pdf/1712.07840.

Ryberg, D. S., Robinius, M., & Stolten, D. (2018). Evaluating Land Eligibility Constraints of Renewable Energy Sources in Europe. *Energies*, *11*(5), 1246. https://doi.org/10.3390/en11051246

Ryberg, D. S., Tulemat, Z., Stolten, D., & Robinius, M. (2020). Uniformly constrained land eligibility for onshore European wind power. *Renewable Energy*, *146*, 921–931. https://doi.org/10.1016/j.renene.2019.06.127

Scott, M., & Powells, G. (2020). Towards a new social science research agenda for hydrogen transitions: Social practices, energy justice, and place attachment. *Energy Research & Social Science*, *61*, 101346. https://doi.org/10.1016/j.erss.2019.101346

Shen, W., Chen, X., Qiu, J., Hayward, J. A., Sayeef, S., Osman, P., Meng, K., & Dong, Z. Y. (2020). A comprehensive review of variable renewable energy levelized cost of electricity. *Renewable and Sustainable Energy Reviews*, *133*, 110301. https://doi.org/10.1016/j.rser.2020.110301

simplemaps. (2023, October 5). *World Cities Database*. https://simplemaps.com/data/world-cities (access date: 2023-10-05).

Spyridonidou, S., & Vagiona, D. G. (2020). Systematic Review of Site-Selection Processes in Onshore and Offshore Wind Energy Research. *Energies*, *13*(22). https://doi.org/10.3390/en13225906

Spyridonidou, S., & Vagiona, D. G. (2023). A systematic review of site-selection procedures of PV and CSP technologies. *Energy Reports*, *9*, 2947–2979. https://doi.org/10.1016/j.egyr.2023.01.132

Tableau. (2023). *What is Tableau?* https://www.tableau.com/why-tableau/what-is-tableau (access date: 2023-11-19).

Teluguntla, P., Thenkabail, P., Xiong, J., Gumma, M., Giri, C., Milesi, C., Ozdogan, M., Congalton, R., Tilton, J., Sankey, T., Massey, R., Phalke, A., & Yadav, K. (2016). *NASA Making Earth System Data Records for Use in Research Environments (MEaSUREs) Global Food Security Support Analysis Data (GFSAD) Crop Mask 2010 Global 1 km V001*. https://doi.org/10.5067/MEASURES/GFSAD/GFSAD1KCM.001

Tonelli, D., Rosa, L., Gabrielli, P., Caldeira, K., Parente, A., & Contino, F. (2023). Global land and water limits to electrolytic hydrogen production using wind and solar resources. Advance online publication. https://doi.org/10.21203/rs.3.rs-2724691/v1

UNEP-WCMC. (2017). *Global Critical Habitat Screening Layer*. https://doi.org/10.34892/NC6D-0Z73

UNEP-WCMC. (2019). *User Manual for the World Database on Protected Areas and world database on other effective area-based conservation measures: 1.6*. UNEP-WCMC: Cambridge, UK. http://wcmc.io/WDPA_Manual.

UNEP-WCMC. (2023). *Protected areas map of the world*. https://www.protectedplanet.net (access date: 2023-09-21).

Wang, C.-N., Hsueh, M.-H., & Lin, D.-F. (2019). Hydrogen Power Plant Site Selection Under Fuzzy Multicriteria Decision-Making (FMCDM) Environment Conditions. *Symmetry*, *11*(4), 596. https://doi.org/10.3390/sym11040596

Welder, L., Ryberg, D., Kotzur, L., Grube, T., Robinius, M., & Stolten, D. (2018). Spatio-temporal optimization of a future energy system for power-to-hydrogen applications in Germany. *Energy*, *158*, 1130–1149. https://doi.org/10.1016/j.energy.2018.05.059

Wikipedia (Ed.). (2023). *List of photovoltaic power stations*10/11/2023. https://en.wikipedia.org/w/index.php?title=List_of_photovoltaic_power_stations&oldid=1178305728.

World Energy Council (2021). Working Paper: Hydrogen on the Horizon: National Hydrogen Strategies. https://www.worldenergy.org/assets/downloads/Working_Paper_-_National_Hydrogen_Strategies_-_September_2021.pdf.

WRI. (2023a). *Aqueduct 4.0 Current and Future Global Maps Data*. https://www.wri.org/aqueduct/data (access date: 2023-09-24).

WRI. (2023b). *GitHub - Aqueduct 4.0 Public Documentation*. https://github.com/wri/Aqueduct40/tree/master (access date: 2023-09-25).

Wu, G. C., Deshmukh, R., Ndhlukula, K., Radojicic, T., & Reilly, J. (2015). *Renewable Energy Zones for the Africa Clean Energy Corridor*. https://doi.org/10.13140/RG.2.1.4005.4644

Wu, Y., Deng, Z., Tao, Y., Wang, L., Liu, F., & Zhou, J. (2021). Site selection decision framework for photovoltaic hydrogen production project using BWM-CRITIC-MABAC: A case study in Zhangjiakou. *Journal of Cleaner Production*, *324*, 129233. https://doi.org/10.1016/j.jclepro.2021.129233

Wu, Y., He, F., Zhou, J., Wu, C., Liu, F., Tao, Y., & Xu, C. (2021). Optimal site selection for distributed wind power coupled hydrogen storage project using a geographical information system based multi-criteria decision-making approach: A case in China. *Journal of Cleaner Production, 299,* 126905. https://doi.org/10.1016/j.jclepro.2021.126905

Yates, J., Daiyan, R., Patterson, R., Egan, R., Amal, R., Ho-Baille, A., & Chang, N. L. (2020). Techno-economic Analysis of Hydrogen Electrolysis from Off-Grid Stand-Alone Photovoltaics Incorporating Uncertainty Analysis. *Cell Reports Physical Science, 1*(10), 100209. https://doi.org/10.1016/j.xcrp.2020.100209

Zhou, Y., & Tol, R. S. J. (2005). Evaluating the costs of desalination and water transport. *Water Resources Research, 41*(3). https://doi.org/10.1029/2004WR003749

Declaration of Originality

I declare that this thesis is my own work and that, to the best of my knowledge, it contains no material previously published, or substantially overlapping with material submitted for the award of any other degree at any institution, except where due acknowledgment is made in the text.

Date and Signature of student 30th of November 2023, 

7 Appendix

7.1 Material and Methods supplementary information

7.1.1 Land eligibility analysis

7.1.1.1 LE by exclusion criterion

Exclusion script of aviation area polygons, uniform exclusion for PV and onshore wind

```
SELECT
	id_cell
	, iso_a3
	, country
	, geom
	, cell_area
	, nel_geom
	, el_geom
	, nel_area
	, cell_area - nel_area AS el_area
	, 8 AS ec_id
FROM
	(
	SELECT
		id_cell
		, iso_a3
		, country
		, geom
		, cell_area
		, nel_geom
		, CASE
			WHEN nel_geom IS NULL THEN geom
			ELSE st_difference(geom, nel_geom)
		END AS el_geom
		, CASE
			WHEN st_area(nel_geom::geography) / 1000000> cell_area THEN
cell_area
			WHEN nel_geom IS NULL THEN 0
			ELSE st_area(nel_geom::geography) / 1000000
		END AS nel_area
	FROM
		(
		SELECT
			id_cell
			, iso_a3
			, country
			, geom
			, cell_area
			, ST_Union(nel_gem) nel_geom
		FROM
			(
			SELECT
				m.id_cell
				, m.iso_a3
				, m.country
				, m.geom
				, m.cell_area
				, st_intersection(m.geom
```

```
                        , ec.geom) nel_gem
                    FROM u_tbarak.merra2_cells m
                    LEFT JOIN u_tbarak.airports AS ec
                                ON st_intersects(m.geom, ec.geom)
                ) AS t
            GROUP BY
                    1, 2, 3, 4, 5
        ) AS t
    ) AS t;
```

Exclusion script of slope raster data, exclusion differ for PV and onshore wind

```
WITH merra2_slope_intersection AS (
SELECT
      id_cell
      , iso_a3
      , country
      , nel_pv_geom
      , nel_wind_geom
FROM
      (
      SELECT
            id_cell
            , iso_a3
            , country
            , ST_Polygon(ST_Clip(ST_Reclass(r.rast
            , 1
            , '[2.86-100:1', '4BUI'
            , 0)
            , m.geom))
         AS nel_pv_geom
            , ST_Polygon(ST_Clip(ST_Reclass(r.rast
            , 1
            , '[5.71-100:1'
            , '4BUI'
            , 0)
            , m.geom))
         AS nel_wind_geom
      FROM
            u_tbarak.merra2_cells m
      LEFT JOIN dhm.slope_1km_gmtedmd AS r ON
            ST_Intersects(m.geom, r.rast)
    ) wb
WHERE
      wb.nel_pv_geom IS NOT NULL
      OR nel_wind_geom IS NOT NULL)
SELECT
      *
      , cell_area - nel_pv_area AS el_pv_area
      , cell_area - nel_wind_area AS el_wind_area
      , cell_area - nel_hybrid_area AS el_hybrid_area
      , 0 AS el_pv_only_area
      -- determined by the RES with more strict threshold: pv
      , COALESCE(cell_area - nel_hybrid_area, 0) - COALESCE(cell_area -
nel_pv_area, 0) el_wind_only_area
      --(el_hybrid_area - el_pv_area)
      , 18 AS ec_id
```

```
FROM
	(
	SELECT
		id_cell
		, iso_a3
		, country
		, geom
		, cell_area
		, nel_pv_geom
		, nel_wind_geom
		, nel_pv_geom AS nel_hybrid_geom
		-- determined by the RES with more strict threshold: pv
		, el_pv_geom
		, el_wind_geom
		, el_pv_geom AS el_hybrid_geom
		--  determined by the RES with more strict threshold: pv
		, CASE
			WHEN st_area(nel_pv_geom::geography) / 1000000> cell_area
			THEN cell_area
			WHEN nel_pv_geom IS NULL THEN 0
			ELSE st_area(nel_pv_geom::geography) / 1000000
		END AS nel_pv_area
		, CASE
			WHEN st_area(nel_wind_geom::geography) / 1000000> cell_area
			THEN cell_area
			WHEN nel_wind_geom IS NULL THEN 0
			ELSE st_area(nel_wind_geom::geography) / 1000000
		END AS nel_wind_area
		, CASE
			WHEN st_area(nel_pv_geom::geography) / 1000000> cell_area
			THEN cell_area
			WHEN nel_pv_geom IS NULL THEN 0
			ELSE st_area(nel_pv_geom::geography) / 1000000
		END AS nel_hybrid_area
		-- determined by the RES with more strict threshold: pv
	FROM
		(
		SELECT
			*
			, CASE
				WHEN nel_pv_geom IS NULL THEN geom
				ELSE st_difference(geom, nel_pv_geom)
			END el_pv_geom
			, CASE
				WHEN nel_wind_geom IS NULL THEN geom
				ELSE st_difference(geom, nel_wind_geom)
			END el_wind_geom
		FROM
			(
			SELECT
				m.id_cell
				, m.iso_a3
				, m.country
				, m.geom
				, m.cell_area
				, ST_Union(ST_Intersection(m.geom, ec.nel_pv_geom))
					AS nel_pv_geom
				, ST_Union(ST_Intersection(m.geom, ec.nel_wind_geom))
					AS nel_wind_geom
```

```
                FROM
                        u_tbarak.merra2_cells m
                LEFT JOIN u_tbarak.merra2_slope_intersection AS ec ON
                        ST_Intersects(m.geom, ec.nel_wind_geom )
                                AND m.iso_a3 = ec.iso_a3
                        GROUP BY
                                m.id_cell
                                , m.iso_a3
                                , m.country
                                , m.geom
                                , m.cell_area
            ) AS t
        ) AS t
    ) AS t;
```

LE per cell and EC data structure in database object merra2_ec

Field name	Description
ec_cell_id	Unique identifier for each exclusion criteria (EC) and cell (primary key)
ec_id	EC unique identifier
id_cell	Cell unique identifier
country	Country name
iso_a3	Country ISO alpha-3 codes
geom	Cell geometry
cell_area	Total cell area in km²
nel_pv_geom	Cell excluded geometry for PV
nel_wind_geom	Cell excluded geometry for onshore wind
nel_hybrid_geom	Cell excluded geometry for a hybrid scenario (area is excluded for at least one of RES)
el_pv_geom	Cell eligible geometry for PV
el_wind_geom	Cell eligible geometry for onshore wind
el_hybrid_geom	Cell eligible geometry for a hybrid scenario (area is eligible for both RES)
nel_pv_area	Cell excluded area for PV (km²)
nel_wind_area	Cell excluded area for onshore wind (km²)
nel_hybrid_area	Cell excluded area for a hybrid scenario (km²) (area is excluded for at least one of RES)
el_pv_area	Cell eligible area for PV (km²)
el_wind_area	Cell eligible area for onshore wind (km²)
el_hybrid_area	Cell eligible area for a hybrid scenario (km²) (area is eligible for both RES)

7.1.1.2 Assignment of EC to LE scenarios data structure in database object le_scenarios

Field name	Description
le_scenario_id_ec_id	Unique identifier for each scenario and EC (primary key)
le_scenario_id	LE scenario unique identifier
le_scenario_name	LE scenario description
ec_id	EC unique identifier
include	Binary field indicating if the EC is to be included in the LE scenario

include_onshore_wind	Binary field indicating if the EC is to be included for onshore wind in the LE scenario
include_pv	Binary field indicating if the EC is to be included for PV in the LE scenario

7.1.1.3 LE scenarios

Create LE scenarios script

```
SELECT
	concat(id_cell, '_', le_scenario_id) AS cell_le_scenario
	, le_scenario_id
	, le_scenario_name
	, id_cell
	, iso_a3
	, country
	, geom
	, cell_area
	, nel_pv_geom
	, nel_wind_geom
	, nel_hybrid_geom
	, el_pv_geom
	, el_wind_geom
	, el_hybrid_geom
	, nel_pv_area
	, nel_wind_area
	, nel_hybrid_area
	, cell_area-nel_pv_area AS el_pv_area
	, cell_area-nel_wind_area AS el_wind_area
	, cell_area-nel_hybrid_area AS el_hybrid_area
	, pv_ec_count
	, wind_ec_count
	, hybrid_ec_count
	, (cell_area-nel_pv_area)/ cell_area AS el_pv_share
	, (cell_area-nel_wind_area)/ cell_area AS el_wind_share
	, (cell_area-nel_hybrid_area)/ cell_area AS el_hybrid_share
FROM
	(
	SELECT
		*
		, CASE
			WHEN nel_pv_geom IS NULL THEN geom
			ELSE st_difference(geom, nel_pv_geom)
		END el_pv_geom
		, CASE
			WHEN nel_wind_geom IS NULL THEN geom
			ELSE st_difference(geom, nel_wind_geom)
		END el_wind_geom
		, CASE
			WHEN nel_hybrid_geom IS NULL THEN geom
			ELSE st_difference(geom, nel_hybrid_geom)
		END el_hybrid_geom
		, CASE
			WHEN st_area(nel_pv_geom::geography) / 1000000> cell_area THEN
cell_area
			WHEN nel_pv_geom IS NULL THEN 0
			ELSE st_area(nel_pv_geom::geography) / 1000000
		END AS nel_pv_area
```

```
            , CASE
                  WHEN st_area(nel_wind_geom::geography) / 1000000> cell_area THEN
cell_area
                  WHEN nel_wind_geom IS NULL THEN 0
                  ELSE st_area(nel_wind_geom::geography) / 1000000
            END AS nel_wind_area
            , CASE
                  WHEN st_area(nel_hybrid_geom::geography) / 1000000> cell_area
THEN cell_area
                  WHEN nel_hybrid_geom IS NULL THEN 0
                  ELSE st_area(nel_hybrid_geom::geography) / 1000000
            END AS nel_hybrid_area
      FROM
            (
            SELECT
                  s.le_scenario_id
                  , s.le_scenario_name
                  , id_cell
                  , iso_a3
                  , country
                  , geom
                  , cell_area
                  , st_union(nel_pv_geom) nel_pv_geom
                  , st_union(nel_wind_geom) nel_wind_geom
                  , st_union(nel_hybrid_geom) nel_hybrid_geom
                  , count(nel_pv_geom) AS pv_ec_count
                  , count(nel_wind_geom) AS wind_ec_count
                  , count(nel_hybrid_geom) AS hybrid_ec_count
            FROM
                  u_tbarak.merra2_ec ec
            JOIN u_tbarak.le_scenarios s ON s.ec_id = ec.ec_id
            WHERE
                  include = 1
                  AND s.le_scenario_id NOT IN (
                  SELECT
                        DISTINCT le_scenario_id
                  FROM
                        u_tbarak.merra2_le)
            GROUP BY
                  1, 2, 3, 4, 5, 6, 7
    ) AS t
) AS t;
```

LE scenarios data structure in database object merra2_le

Field name	Description
cell_le_scenario	Unique identifier for each LE scenario and cell (primary key)
le_scenario_id	LE scenario unique identifier
le_scenario_name	LE scenario description
id_cell	Cell unique identifier
iso_a3	Country ISO alpha-3 codes
country	Country name
geom	Cell geometry
cell_area	Total cell area (km²)
nel_pv_geom	Cell excluded geometry for PV
nel_wind_geom	Cell excluded geometry for onshore wind

nel_hybrid_geom	Cell excluded geometry for a hybrid scenario (area is excluded for at least one of RES)
el_pv_geom	Cell eligible geometry for PV
el_wind_geom	Cell eligible geometry for onshore wind
el_hybrid_geom	Cell eligible geometry for a hybrid scenario (area is eligible for both RES)
nel_pv_area	Cell excluded area for PV (km²)
nel_wind_area	Cell excluded area for onshore wind (km²)
nel_hybrid_area	Cell excluded area for a hybrid scenario (km²) (area is excluded for at least one of RES)
el_pv_area	Cell eligible area for PV (km²)
el_wind_area	Cell eligible area for onshore wind (km²)
el_hybrid_area	Cell eligible area for a hybrid scenario (km²) (area is eligible for both RES)
pv_ec_count	Number of EC that resulted of PV land exclusion in cell
wind_ec_count	Number of EC that resulted of onshore land exclusion in cell
hybrid_ec_count	Number of EC that resulted of PV or onshore wind land exclusion in cell
el_pv_share	Share of eligible area for PV from the total cell area (%)
el_wind_share	Share of eligible area for onshore wind from the total cell area (%)
el_hybrid_share	Share of eligible area for both PV and onshore wind from the total cell area (%)

7.1.2 Green hydrogen costs and potentials

7.1.2.1 List of PV stations and power densities calculations

Station	Reference	Commission Date	Area km^2	MW_{dc}	MW_{ac}	$Factor\ ac/dc$	Power density (PD) MW_{dc}/km^2	Power density (PD) MW_{ac}/km^2
Agua Caliente Solar Project	https://en.wikipedia.org/wiki/Agua_Caliente_Solar_Project	2014	9.71	410.0	290	71%	42.2	29.9
Topaz Solar Farm	https://en.wikipedia.org/wiki/Topaz_Solar_Farm	2014	19	711.4	550		37.4	28.9
Antelope Valley Solar Ranch	https://en.wikipedia.org/wiki/Antelope_Valley_Solar_Ranch	2014	8.49	297.5	230		35.0	27.1
Mount Signal Solar	https://en.wikipedia.org/wiki/Mount_Signal_Solar	2014	7.9	266.0	206	77%	33.7	26.1
Desert Sunlight Solar Farm	https://en.wikipedia.org/wiki/Desert_Sunlight_Solar_Farm	2015	16	711.4	550		44.5	34.4
Solar Star	https://en.wikipedia.org/wiki/Solar_Star	2015	13	743.3	579	78%	57.2	44.5
NP Kunta Ultra Mega Solar Park	https://en.wikipedia.org/wiki/NP_Kunta_Ultra_Mega_Solar_Park	2016	32	978.5			30.6	0.0
Tengger Desert Solar Park	https://en.wikipedia.org/wiki/Tengger_Desert_Solar_Park	2016	43	1547.0			36.0	0.0
Mesquite Solar project	https://en.wikipedia.org/wiki/Mesquite_Solar_project	2016	9.3	517.4	400		55.6	43.0
Kamuthi Solar Power Project	https://en.wikipedia.org/wiki/Kamuthi_Solar_Power_Project	2017	10	648.0			64.8	0.0
Mount Signal Solar	https://en.wikipedia.org/wiki/Mount_Signal_Solar	2018	8.1	328.0	254	77%	40.5	31.4
Rewa Ultra Mega Solar	https://en.wikipedia.org/wiki/Rewa_Ultra_Mega_Solar	2018	6.4	750.0			117.2	0.0
Dau Tieng Solar Power Project	https://en.wikipedia.org/wiki/Dau_Tieng_Solar_Power_Project	2018	5	600.0	500	83%	120.0	100.0
Kurnool Ultra Mega Solar Park	https://en.wikipedia.org/wiki/Kurnool_Ultra_Mega_Solar_Park	2019	24	1000.0			41.7	0.0
Mula Photovoltaic Power Plant	https://en.wikipedia.org/wiki/Mula_Photovoltaic_Power_Plant	2019	10	494.0			49.4	0.0

Station	Reference	Commission Date	Area km^2	MW_{dc}	MW_{ac}	$Factor\ ac/dc$	Power density (PD) MW_{dc}/km^2	MW_{ac}/km^2
Techren Solar Project	https://en.wikipedia.org/wiki/Techren_Solar_Project	2019	9.3	517.4	400		55.6	43.0
Mount Signal Solar	https://en.wikipedia.org/wiki/Mount_Signal_Solar	2020	5.1	200.0	154	77%	39.2	30.2
Karapınar Solar Power Plant	https://en.wikipedia.org/wiki/Karap%C4%B1nar_solar_power_plant	2022	20	1300.0			65.0	0.0
Travers Solar Project	https://en.wikipedia.org/wiki/Travers_Solar_Project	2022	13.35	601.5	465		45.1	34.8
Copper Mountain Solar Facility	https://en.wikipedia.org/wiki/Copper_Mountain_Solar_Facility	2008-2021	16	1037.4	802		64.8	50.1

$$Factor_{\ ac/dc} = \frac{MW_{ac}}{MW_{dc}}$$

$$MW_{dc} = \frac{MW_{ac}}{Average\ Factor_{\ ac/dc}}$$

$$PD_{ac} = \frac{MW_{ac}}{km^2}$$

$$PD_{dc} = \frac{MW_{dc}}{km^2}$$

$Average\ Factor_{\ ac/dc}$=0.77

$$PD\,\frac{MW_{ac}}{km^2} = Average\,\frac{MW_{AC}}{km^2} = 40.3$$

$$PD\,\frac{MW_{dc}}{km^2} = Average\,\frac{MW_{dc}}{km^2} \times Avergae\ Factor_{\ ac/dc} = 53.8\,\frac{MW_{dc}}{km^2} \times 0.77 = 41.6\,\frac{MW_{dc}}{km^2}$$

7.1.2.2 Land allocation and hydrogen potentials

Land allocation and hydrogen potentials calculation scripts

```
-- create power_density
CREATE TABLE u_tbarak.power_density
(
    pd_scenario_id   INTEGER PRIMARY KEY,
    pd_scenario_name TEXT,
    pv_pd   REAL,
    wind_pd REAL
);

INSERT INTO u_tbarak.power_density
VALUES (1,'Low',45,15),(2,'High',69,29.3);


-- create cell_scenarios
CREATE VIEW u_tbarak.cell_scenarios AS
(
SELECT
      concat(id_cell
      , '_', s_rank
      , '_', pd_scenario_id) cell_rank_pd
      , concat(id_cell, '_', s_rank) cell_rank
      ,*
FROM
      (
      SELECT
            *
            , RANK(*) OVER (PARTITION BY pd_scenario_id, id_cell ORDER BY
lcoh_eur_kg) AS s_rank
            , pv_mw / pv_pd AS pv_km2
            , wind_mw / wind_pd AS wind_km2
      FROM
            (
            SELECT
                  pd.pd_scenario_id
                  , pd.pd_scenario_name
                  , pd.pv_pd
                  , pd.wind_pd
                  , m.id_cell
                  , m.id_region
                  , m.iso_a3
                  , m.country
                  , m.geom
                  , m.cell_area
                  , ci.configuration_scenario configuration_scenario_id
                  , ci.internal_id_name configuration_scenario_name
                  , sum(CASE WHEN ci.parameter = 'LCOH in eur/kg'
                                    THEN sum
                                    ELSE NULL END) AS lcoh_eur_kg
                  , sum(CASE WHEN ci.parameter = 'PV Installed Capacity in MW'
                                    THEN sum
                                    ELSE 0 END) AS pv_mw
                  , sum(CASE WHEN ci.parameter = 'Wind Installed Capacity in MW'
                                    THEN sum
                                    ELSE 0 END) wind_mw
            FROM
```

```
                u_tbarak.merra2_cells m
            LEFT JOIN u_tbarak.cell_inputs ci ON
                m.id_cell = ci.id_region
            CROSS JOIN u_tbarak.power_density pd
            GROUP BY
                pd.pd_scenario_id
                , pd.pd_scenario_name
                , pd.pv_pd
                , pd.wind_pd
                , m.id_cell
                , m.id_region
                , m.iso_a3
                , m.country
                , m.geom
                , m.cell_area
                , ci.configuration_scenario
                , ci.internal_id_name
        ) AS t
    WHERE
            lcoh_eur_kg>0
            AND (
             (configuration_scenario_id = 93 AND pv_mw > 0 AND wind_mw > 0)
            OR (configuration_scenario_id = 95 AND pv_mw > 0)
            OR (configuration_scenario_id = 96 AND wind_mw > 0)
        )
    ) AS t
);


-- create cell_scenario_1 (step 1)
CREATE VIEW u_tbarak.cell_scenario_1 AS
(
WITH input AS (
SELECT
        concat(m.id_cell
        , '_', m.s_rank
        , '_', s.le_scenario_id
        , '_', m.pd_scenario_id) primary_key
        , m.pd_scenario_id
        , m.pd_scenario_name
        , s.le_scenario_id
        , s.le_scenario_name
        , m.id_cell
        , m.cell_rank
        , m.id_region
        , m.iso_a3
        , m.country
        , m.geom
        , m.cell_area
        , s.el_pv_area
        , s.el_wind_area
        , m.configuration_scenario_id
        , m.configuration_scenario_name
        , m.lcoh_eur_kg
        , m.pv_mw
        , m.wind_mw
        , m.s_rank
        , m.pv_km2
        , m.wind_km2
```

```
	, CASE
		WHEN m.pv_km2 = 0
			THEN 0
		ELSE round(s.el_pv_area / m.pv_km2, 5)
	END pv_systems
	, CASE
		WHEN m.wind_km2 = 0
			THEN 0
		ELSE round(s.el_wind_area / m.wind_km2, 5)
	END wind_systems
	, pv_ec_count
	, wind_ec_count
	, hybrid_ec_count
	, el_pv_share
	, el_wind_share
	, el_hybrid_share
FROM
	u_tbarak.cell_scenarios m
LEFT JOIN u_tbarak.merra2_le s ON s.id_cell = m.id_cell
	AND s.le_scenario_id NOT IN (
	SELECT
		DISTINCT le_scenario_id
	FROM
		u_tbarak.merra2_h2)
WHERE
	m.s_rank = 1
)
SELECT
	*
FROM
	(
	SELECT
		*
		, CASE
			WHEN configuration_scenario_id = 95
				THEN pv_systems
			WHEN configuration_scenario_id = 96
				THEN wind_systems
			WHEN configuration_scenario_id = 93
			AND pv_systems >= wind_systems
				THEN wind_systems
			WHEN configuration_scenario_id = 93
			AND pv_systems < wind_systems
				THEN pv_systems
			END AS hourly_output
			, round(CASE
				WHEN configuration_scenario_id = 95
					THEN 8784 * pv_systems
				WHEN configuration_scenario_id = 96
					THEN 8784 * wind_systems
				WHEN configuration_scenario_id = 93
				AND pv_systems >= wind_systems
					THEN 8784 * wind_systems
				WHEN configuration_scenario_id = 93
				AND pv_systems < wind_systems
					THEN 8784 * pv_systems
				END, 5) AS yearly_output -- 8784 hours in 2020
			, CASE
				WHEN configuration_scenario_id = 95
```

```
                        THEN pv_systems * pv_km2
                  WHEN configuration_scenario_id = 96
                        THEN 0
                  WHEN configuration_scenario_id = 93
                  AND pv_systems >= wind_systems
                        THEN wind_systems * pv_km2
                  WHEN configuration_scenario_id = 93
                  AND pv_systems < wind_systems
                        THEN pv_systems * pv_km2
            END AS pv_allocated_area
            , CASE
                  WHEN configuration_scenario_id = 95
                        THEN 0
                  WHEN configuration_scenario_id = 96
                        THEN wind_systems * wind_km2
                  WHEN configuration_scenario_id = 93
                  AND pv_systems >= wind_systems
                        THEN wind_systems * wind_km2
                  WHEN configuration_scenario_id = 93
                  AND pv_systems < wind_systems
                        THEN pv_systems * wind_km2
            END AS wind_allocated_area
            , CASE
                  WHEN configuration_scenario_id = 95
                        THEN el_pv_area - pv_systems * pv_km2
                  WHEN configuration_scenario_id = 96
                        THEN el_pv_area
                  WHEN configuration_scenario_id = 93
                  AND pv_systems >= wind_systems
              THEN el_pv_area - wind_systems * pv_km2
                  WHEN configuration_scenario_id = 93
                  AND pv_systems < wind_systems
              THEN el_pv_area - pv_systems * pv_km2
            END AS remaining_el_pv_area
            , CASE
                  WHEN configuration_scenario_id = 95
                        THEN el_wind_area
                  WHEN configuration_scenario_id = 96
                        THEN el_wind_area - wind_systems * wind_km2
                  WHEN configuration_scenario_id = 93
                  AND pv_systems >= wind_systems
              THEN el_wind_area - wind_systems * wind_km2
                  WHEN configuration_scenario_id = 93
                  AND pv_systems < wind_systems
              THEN el_wind_area - pv_systems * wind_km2
            END AS remaining_el_wind_area
      FROM
            input) AS t
);

-- create cell_scenario_2 (step 2)
CREATE VIEW u_tbarak.cell_scenario_2 AS
(
WITH input AS (
SELECT
      concat(m.id_cell
      , '_', m.s_rank
      , '_', s.le_scenario_id
      , '_', m.pd_scenario_id) primary_key
```

```
        , m.pd_scenario_id
        , m.pd_scenario_name
        , s.le_scenario_id
        , s.le_scenario_name
        , m.id_cell
        , m.cell_rank
        , m.id_region
        , m.iso_a3
        , m.country
        , m.geom
        , m.cell_area
        , s.remaining_el_pv_area AS el_pv_area
        , s.remaining_el_wind_area AS el_wind_area
        , m.configuration_scenario_id
        , m.configuration_scenario_name
        , m.lcoh_eur_kg
        , m.pv_mw
        , m.wind_mw
        , m.s_rank
        , m.pv_km2
        , m.wind_km2
        , CASE
              WHEN m.pv_km2 = 0
                    THEN 0
              ELSE round(s.remaining_el_pv_area / m.pv_km2, 5)
        END pv_systems
        , CASE
              WHEN m.wind_km2 = 0
                    THEN 0
              ELSE round(s.remaining_el_wind_area / m.wind_km2, 5)
        END wind_systems
        , pv_ec_count
        , wind_ec_count
        , hybrid_ec_count
        , el_pv_share
        , el_wind_share
        , el_hybrid_share
FROM
        u_tbarak.cell_scenarios m
LEFT JOIN u_tbarak.cell_scenario_1 s ON
        s.id_cell = m.id_cell
        AND s.pd_scenario_id = m.pd_scenario_id
WHERE
        m.s_rank = 2
)
SELECT
        *
FROM
        (
        SELECT
              *
              , CASE
                    WHEN configuration_scenario_id = 95
                          THEN pv_systems
                    WHEN configuration_scenario_id = 96
                          THEN wind_systems
                    WHEN configuration_scenario_id = 93
                          AND pv_systems > wind_systems
                                THEN wind_systems
```

```
      WHEN configuration_scenario_id = 93
      AND pv_systems < wind_systems
            THEN pv_systems
END AS hourly_output
, round(CASE
      WHEN configuration_scenario_id = 95
            THEN 8784 * pv_systems
      WHEN configuration_scenario_id = 96
            THEN 8784 * wind_systems
      WHEN configuration_scenario_id = 93
      AND pv_systems >= wind_systems
            THEN 8784 * wind_systems
      WHEN configuration_scenario_id = 93
      AND pv_systems < wind_systems
            THEN 8784 * pv_systems
      END, 5) AS yearly_output -- 8784 hours in 2020
, CASE
      WHEN configuration_scenario_id = 95
            THEN pv_systems * pv_km2
      WHEN configuration_scenario_id = 96
            THEN 0
      WHEN configuration_scenario_id = 93
      AND pv_systems >= wind_systems
            THEN wind_systems * pv_km2
      WHEN configuration_scenario_id = 93
      AND pv_systems < wind_systems
            THEN pv_systems * pv_km2
END AS pv_allocated_area
, CASE
      WHEN configuration_scenario_id = 95
            THEN 0
      WHEN configuration_scenario_id = 96
            THEN wind_systems * wind_km2
      WHEN configuration_scenario_id = 93
      AND pv_systems >= wind_systems
            THEN wind_systems * wind_km2
      WHEN configuration_scenario_id = 93
      AND pv_systems < wind_systems
            THEN pv_systems * wind_km2
END AS wind_allocated_area
, CASE
      WHEN configuration_scenario_id = 95
            THEN el_pv_area - pv_systems * pv_km2
      WHEN configuration_scenario_id = 96
            THEN el_pv_area
      WHEN configuration_scenario_id = 93
      AND pv_systems >= wind_systems
  THEN el_pv_area - wind_systems * pv_km2
      WHEN configuration_scenario_id = 93
      AND pv_systems < wind_systems
  THEN el_pv_area - pv_systems * pv_km2
END AS remaining_el_pv_area
, CASE
      WHEN configuration_scenario_id = 95
            THEN el_wind_area
      WHEN configuration_scenario_id = 96
            THEN el_wind_area - wind_systems * wind_km2
      WHEN configuration_scenario_id = 93
      AND pv_systems >= wind_systems
```

```
                    THEN el_wind_area - wind_systems * wind_km2
                         WHEN configuration_scenario_id = 93
                         AND pv_systems < wind_systems
                    THEN el_wind_area - pv_systems * wind_km2
                END AS remaining_el_wind_area
            FROM
                INPUT) AS t
    );

-- create cell_scenario_3 (step 3)
CREATE VIEW u_tbarak.cell_scenario_3 AS
(
WITH INPUT AS (
SELECT
      concat(m.id_cell, '_', m.s_rank, '_', s.le_scenario_id, '_',
m.pd_scenario_id) primary_key
      , m.pd_scenario_id
      , m.pd_scenario_name
      , s.le_scenario_id
      , s.le_scenario_name
      , m.id_cell
      , m.cell_rank
      , m.id_region
      , m.iso_a3
      , m.country
      , m.geom
      , m.cell_area
      , s.remaining_el_pv_area AS el_pv_area
      , s.remaining_el_wind_area AS el_wind_area
      , m.configuration_scenario_id
      , m.configuration_scenario_name
      , m.lcoh_eur_kg
      , m.pv_mw
      , m.wind_mw
      , m.s_rank
      , m.pv_km2
      , m.wind_km2
      , CASE
            WHEN m.pv_km2 = 0
                  THEN 0
            ELSE round(s.remaining_el_pv_area / m.pv_km2, 5)
      END pv_systems
      , CASE
            WHEN m.wind_km2 = 0
                  THEN 0
            ELSE round(s.remaining_el_wind_area / m.wind_km2, 5)
      END wind_systems
      , pv_ec_count
      , wind_ec_count
      , hybrid_ec_count
      , el_pv_share
      , el_wind_share
      , el_hybrid_share
FROM
      u_tbarak.cell_scenarios m
LEFT JOIN u_tbarak.cell_scenario_2 s ON
      s.id_cell = m.id_cell
      AND s.pd_scenario_id = m.pd_scenario_id
WHERE
```

```
	m.s_rank = 3
)
SELECT
	*
FROM
	(
	SELECT
		*
		, CASE
			WHEN configuration_scenario_id = 95
				THEN pv_systems
			WHEN configuration_scenario_id = 96
				THEN wind_systems
			WHEN configuration_scenario_id = 93
				AND pv_systems > wind_systems
					THEN wind_systems
				WHEN configuration_scenario_id = 93
				AND pv_systems < wind_systems
					THEN pv_systems
			END AS hourly_output
			, round(CASE
				WHEN configuration_scenario_id = 95
					THEN 8784 * pv_systems
				WHEN configuration_scenario_id = 96
					THEN 8784 * wind_systems
				WHEN configuration_scenario_id = 93
					AND pv_systems >= wind_systems
						THEN 8784 * wind_systems
					WHEN configuration_scenario_id = 93
					AND pv_systems < wind_systems
						THEN 8784 * pv_systems
				END, 5) AS yearly_output -- 8784 hours in 2020
			, CASE
				WHEN configuration_scenario_id = 95
					THEN pv_systems * pv_km2
				WHEN configuration_scenario_id = 96
					THEN 0
				WHEN configuration_scenario_id = 93
				AND pv_systems >= wind_systems
					THEN wind_systems * pv_km2
				WHEN configuration_scenario_id = 93
				AND pv_systems < wind_systems
					THEN pv_systems * pv_km2
			END AS pv_allocated_area
			, CASE
				WHEN configuration_scenario_id = 95
					THEN 0
				WHEN configuration_scenario_id = 96
					THEN wind_systems * wind_km2
				WHEN configuration_scenario_id = 93
				AND pv_systems >= wind_systems
					THEN wind_systems * wind_km2
				WHEN configuration_scenario_id = 93
				AND pv_systems < wind_systems
					THEN pv_systems * wind_km2
			END AS wind_allocated_area
			, CASE
				WHEN configuration_scenario_id = 95
					THEN el_pv_area - pv_systems * pv_km2
```

```
                        WHEN configuration_scenario_id = 96
                              THEN el_pv_area
                        WHEN configuration_scenario_id = 93
                        AND pv_systems >= wind_systems
                    THEN el_pv_area - wind_systems * pv_km2
                        WHEN configuration_scenario_id = 93
                        AND pv_systems < wind_systems
                    THEN el_pv_area - pv_systems * pv_km2
                END AS remaining_el_pv_area
                , CASE
                        WHEN configuration_scenario_id = 95
                              THEN el_wind_area
                        WHEN configuration_scenario_id = 96
                              THEN el_wind_area - wind_systems * wind_km2
                        WHEN configuration_scenario_id = 93
                        AND pv_systems >= wind_systems
                    THEN el_wind_area - wind_systems * wind_km2
                        WHEN configuration_scenario_id = 93
                        AND pv_systems < wind_systems
                    THEN el_wind_area - pv_systems * wind_km2
                END AS remaining_el_wind_area
            FROM
                  INPUT) AS t
    );


-- create merra2_h2_le0
CREATE VIEW u_tbarak.merra2_h2_le0 AS
(
SELECT *
FROM u_tbarak.cell_scenario_1
WHERE le_scenario_id = 0
UNION
SELECT *
FROM u_tbarak.cell_scenario_2
WHERE le_scenario_id = 0
UNION
SELECT *
FROM u_tbarak.cell_scenario_3
WHERE le_scenario_id = 0
    );


-- input data for table merra2_h2
WITH INPUT AS (
SELECT * FROM u_tbarak.cell_scenario_1
UNION
SELECT * FROM u_tbarak.cell_scenario_2
UNION
SELECT * FROM u_tbarak.cell_scenario_3
        )
SELECT
      m.*
      , CASE
            WHEN p.iso_a3 IS NOT NULL
                  THEN TRUE
            ELSE FALSE
      END political_instability_countries
      , CASE
```

```
            WHEN n.iso_a3 IS NOT NULL
                  THEN TRUE
            ELSE FALSE
      END net_re_potential_countries
      , CASE
            WHEN p.iso_a3 IS NOT NULL
            AND n.iso_a3 IS NOT NULL
                  THEN 'Political instability & insufficient net RE potential'
            WHEN p.iso_a3 IS NOT NULL
            AND n.iso_a3 IS NULL
                  THEN 'Political instability'
            WHEN p.iso_a3 IS NULL
            AND n.iso_a3 IS NOT NULL
                  THEN 'Insufficient net RE potential'
            ELSE 'Requirements met'
      END minimum_requirements
      , l.yearly_output AS yearly_output_le0
      , l.hourly_output AS hourly_output_le0
      , m.pv_mw /(m.pv_mw + m.wind_mw) AS pv_share
      , m.wind_mw /(m.pv_mw + m.wind_mw) wind_share
      , m.yearly_output *(m.pv_mw /(m.pv_mw + m.wind_mw)) AS pv_yearly_output
      , m.yearly_output *(m.wind_mw /(m.pv_mw + m.wind_mw)) AS wind_yearly_output
FROM
      INPUT m
LEFT JOIN u_tbarak.political_instability_countries p ON
      p.iso_a3 = m.iso_a3
LEFT JOIN u_tbarak.net_re_potential_countries n ON
      n.iso_a3 = m.iso_a3
LEFT JOIN u_tbarak.merra2_h2_le0 l ON
      m.pd_scenario_id = l.pd_scenario_id
      AND m.id_cell = l.id_cell
      AND m.s_rank = l.s_rank;
```

Hydrogen potentials data structure in database object merra2_h2

Field name	Description
primary_key	Unique identifier for each LE scenario, PD scenario and cell (primary key)
pd_scenario_id	PD scenario unique identifier
pd_scenario_name	PD scenario description
le_scenario_id	LE scenario unique identifier
le_scenario_name	LE scenario description
id_cell	Cell unique identifier
cell_rank	Unique identifier of cell ID and rank of system configuration scenarios in cell by LCOH
iso_a3	Country ISO alpha-3 codes
country	Country name
geom	Cell geometry
cell_area	Total cell area (km²)
pv_available_area	Eligible area available for PV considering previous land allocation step (km²)
wind_available_area	Eligible area available for onshore wind considering previous land allocation step (km²)
configuration_scenario_id	System configuration scenario unique identifier

configuration_scenario_name	System configuration scenario description
lcoh_eur_kg	LCOH per cell and system configuration scenario
pv_mw	PV system required installed capacity (MW)
wind_mw	Onshore wind system required installed capacity (MW)
s_rank	Rank of system configuration scenarios in cell by LCOH
pv_km2	PV system land requirement (km²)
wind_km2	Onshore wind system land requirement (km²)
pv_systems	Maximal upscaling factor of PV system in cell
wind_systems	Maximal upscaling factor of PV system in cell
pv_ec_count	Number of EC that resulted of PV land exclusion in cell
wind_ec_count	Number of EC that resulted of onshore land exclusion in cell
hybrid_ec_count	Number of EC that resulted of PV or onshore wind land exclusion in cell
el_pv_share	Share of eligible area for PV from the total cell area (%)
el_wind_share	Share of eligible area for onshore wind from the total cell area (%)
el_hybrid_share	Share of eligible area for both PV and onshore wind from the total cell area (%)
hourly_output	Hourly hydrogen production potential
yearly_output	Yearly hydrogen production potential
pv_allocated_area	Area allocated for PV (km²)
wind_allocated_area	Area allocated for onshore wind (km²)
pv_remaining_area	Eligible area remaining for PV after land allocation in current step (km²)
wind_remaining_area	Eligible area remaining for onshore wind after land allocation in current step (km²)
political_instability_countries	True for cells in politically instable according to Breitschopf et al. (2022)
net_re_potential_countries	True for cells in countries with insufficient net RE potential according to Breitschopf et al. (2022)
minimum_requirements	Fulfillment status of minimal requirements for hydrogen exports according to Breitschopf et al. (2022)
yearly_output_le0	Yearly hydrogen production potential in a scenario where no LE is applied
hourly_output_le0	Hourly hydrogen production potential in a scenario where no LE is applied
pv_share	PV share from the system power generating hydrogen
wind_share	Onshore wind share from the system power generating hydrogen
pv_yearly_output	PV power from the system power generating hydrogen
wind_yearly_output	Onshore wind power from the system power generating hydrogen

7.2 Results and Discussion supplementary information

7.2.1 Systematic literature review

7.2.1.1 List of publications included in the systematic literature review

Publication	Project	Type	Regional Scope	Country/Region	RES	EC/AC	GIS
Agora Energiewende and AFRY Management Consulting (2021)	No-regret hydrogen	Gray literature	Europe		Solar/Wind	EC	Yes
Ali et al. (2022)		Peer-reviewed	Thailand	Southern Thailand	Solar	AC	Yes
Almutairi (2022)		Peer-reviewed	Saudi Arabia		Wind	AC	No
Ao Xuan et al. (2022)		Peer-reviewed	Uzbekistan		Solar	AC	No
Braun et al. (2022)	MENA-Fuels	Gray literature	MENA[32]		Solar/Wind	EC	Yes
Breitschopf et al. (2022)	HYPAT	Gray literature	Global		Solar/Wind	EC/AC	Yes
Franzmann et al. (2023)		Peer-reviewed	Global		Solar/Wind	EC	Yes
Gao et al. (2021)		Peer-reviewed	China	Inner Mongolia	Solar	AC	No
Heuser et al. (2020)		Gray literature	Global		Solar/Wind	EC	Yes
S. J. H. Dehshiri and Zanjirchi (2022)		Peer-reviewed	Iran	Hormozgan province	Wind	AC	No
S. S. H. Dehshiri and Dehshiri (2022)		Peer-reviewed	Iran	Yazd province	Wind	EC/AC	Yes
IRENA (2022)	Global Hydrogen Trade to Meet the 1.5°C Climate Goal	Gray literature	Global		Solar/Wind	EC	Yes
Jahangiri et al. (2020)		Peer-reviewed	Quatar		Solar/Wind	AC	No
Lux et al. (2021)		Peer-reviewed	MENA[33]		Solar/Wind	EC	Yes
Lux and Pfluger (2020)		Peer-reviewed	Europe		Solar/Wind	EC	Yes
Mah et al. (2022)		Peer-reviewed	Malaysia	Johor district	Solar	EC/AC	Yes
Messaoudi et al. (2019)		Peer-reviewed	Algeria		Solar	EC/AC	Yes

[32] While the cost-potential analysis concentrates on the MENA region, the energy supply analysis also considers generation potentials in European countries.
[33] Included Morocco, Algeria, Libya, Tunisia, Egypt, Saudi Arabia, Lebanon, Israel, Syria, and Turkey.

Publication	Project	Type	Regional Scope	Country/Region	RES	EC/AC	GIS
Mostafaeipour, Dehshiri, et al. (2020)		Peer-reviewed	Afghanistan		Wind	EC/AC	No
Mostafaeipour, Rezayat, and Rezaei (2020)		Peer-reviewed	Iran	12 cities of Isfahan in Iran	Solar	AC	No
Müller et al. (2023)		Peer-reviewed	Kenya[34]		Solar/Wind	AC	Yes
Okunlola et al. (2022)		Peer-reviewed	Canada		Solar/Wind	EC	Yes
Pfennig et al. (2023)	Fraunhofer IEE | Global PtX Atlas	Peer-reviewed	Global		Solar/Wind	EC/AC	Yes
Reed et al. (2022)		Peer-reviewed	USA	California	Solar/Wind	EC/AC	Yes
Rezaei et al. (2020)		Peer-reviewed	Iran	Capital cities of developing countries, case study of Iran	Solar/Wind	AC	No
Wang et al. (2019)		Peer-reviewed	Vietnam		Solar/Wind	AC	No
Y. Wu, Deng, et al. (2021)		Peer-reviewed	China	Zhangjiakou City, Hebei Province	Solar	AC	No
Y. Wu, He, et al. (2021)		Peer-reviewed	China	Hezhang County, Guizhou Province	Wind	EC/AC	Yes

[34] Focus on low- and middle-income countries.

7.2.1.2 *Water stress and drought risk categories*

Table 23: Water stress risk categories, source: Kuzma et al. (2023, p. 11)

Raw value	Risk category	Score
<10%	Low	0–1
10–20%	Low-medium	1–2
20–40%	Medium-high	2–3
40–80%	High	3–4
>80%	Extremely high	4–5
	Arid and low water use	5

Table 24: Water drought risk categories, source: Kuzma et al. (2023, p. 11)

Raw value	Risk category	Score
<10%	Low	0–1
10–20%	Low-medium	1–2
20–40%	Medium-high	2–3
40–80%	High	3–4
>80%	Extremely high	4–5
	Arid and low water use	5

7.2.2 Land eligibility analysis

7.2.2.1 *Assigned continent to countries*

Country	Continent
Azerbaijan, Republic of	Asia
Armenia, Republic of	Asia
Cyprus, Republic of	Europe
Georgia	Europe
Kazakhstan, Republic of	Asia
United States Minor Outlying Islands	North America
Russian Federation	Asia
Turkey, Republic of	Asia

7.2.2.2 *Countries with less than 0.1% post LE application*

Country	
American Samoa	Malta
Anguilla	Marshall Islands
Antigua and Barbuda	Mauritius
Armenia	Mayotte
Bahamas	Micronesia

Bahrain	Moldova
Barbados	Montserrat
Belarus	Nauru
Belgium	Nepal
Bermuda	Netherlands
Bhutan	Niue
British Territory in Indian Ocean	North Korea
British Virgin Islands	Palau
Brunei Darussalam	Panama
Bulgaria	Philippines
Cambodia	Pitcairn Islands
Cayman Islands	Poland
Comoros	Réunion
Cook Islands	Rwanda
Costa Rica	São Tomé and Príncipe
Czech Republic	Saint Kitts and Nevis
Denmark	Samoa
Dominica	Seychelles
East Timor (Timor-Leste)	Slovakia
El Salvador	Slovenia
Equatorial Guinea	Solomon Islands
Fiji	South Georgia and the South Sandwich Islands
Germany	South Korea
Grenada	Sri Lanka
Guernsey (Channel Island)	St. Helena
Hungary	St. Lucia
Jamaica	St. Vincent and the Grenadines
Japan	Taiwan
Jersey (Channel Island)	Tokelau
Kiribati	Tonga
Kosovo	Trinidad and Tobago
Liberia	Turks and Caicos Islands
Lithuania	Tuvalu
Macedonia	Ukraine
Malaysia	Valais and Futuna
Maldives	Vanuatu